AD-A086 683 ANALYTIC SCIENCES CORP READING MA F/G 17/7
DEVELOPMENT OF LORAN-C DATA COLLECTION AND ANALYSIS PROCEDURES.(U)
MAR 80 L M DEPALMA, E A SCHOEN, S F DONNELLY DOT-FA79WA-4271
UNCLASSIFIED TASC-TR-1021-1 FAA-RD-80-48 NL

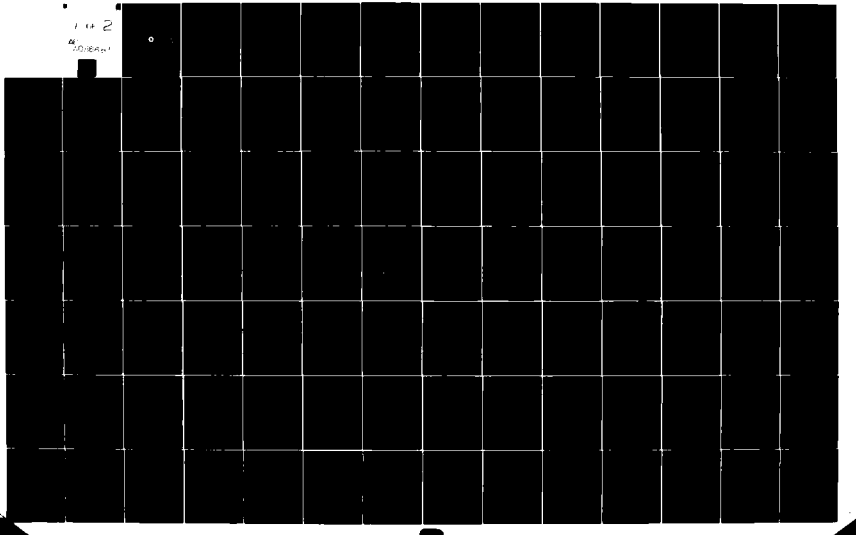

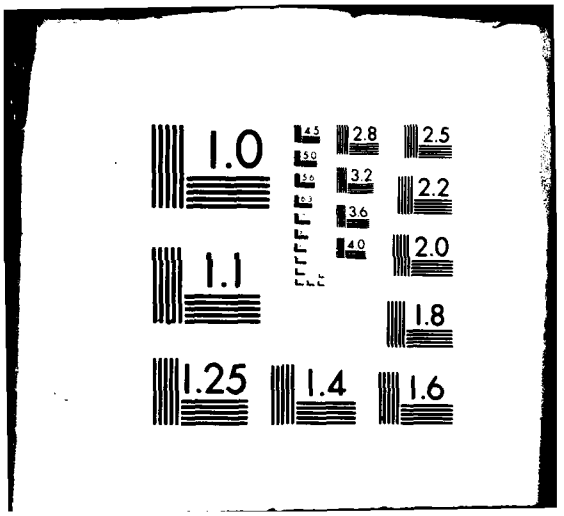
1.0
1.1
1.25
1.4
1.6
1.8
2.0
2.2
2.5
2.8
3.2
3.6
4.0
4.5
5.0

Report No. FAA-RD-80-48

LEVEL II

DEVELOPMENT OF LORAN-C DATA COLLECTION AND ANALYSIS PROCEDURES

Leon M. DePalma
Edward A. Schoen
Stephen F. Donnelly

THE ANALYTIC SCIENCES CORPORATION
Six Jacob Way
Reading, Massachusetts 01867

March 1980

FINAL REPORT, 175

Document is available to the U.S. public through the National Technical Information Service, Springfield, Virginia 22161

Prepared for

U.S. DEPARTMENT OF TRANSPORTATION

FEDERAL AVIATION ADMINISTRATION
Systems Research & Development Service
Washington, D.C. 20590

NOTICE

This document is disseminated under the sponsorship of the Department of Transportation in the interest of information exchange. The United States Government assumes no liability for its contents or use thereof.

Technical Report Documentation Page

1. Report No.	2. Government Accession No.	3. Recipient's Catalog No.
FAA-RD-80-48	AD-A086 683	

4. Title and Subtitle	5. Report Date
DEVELOPMENT OF LORAN-C DATA COLLECTION AND ANALYSIS PROCEDURES	March 1980
	6. Performing Organization Code
7. Author(s)	8. Performing Organization Report No.
L.M. DePalma, E.A. Schoen, and S.F. Donnelly	TR-1021-1
9. Performing Organization Name and Address	10. Work Unit No. (TRAIS)
The Analytic Sciences Corporation Six Jacob Way Reading, Massachusetts 01867	11. Contract or Grant No. DOT-FA79-WA-4271
12. Sponsoring Agency Name and Address	13. Type of Report and Period Covered
Federal Aviation Administration Systems Research and Development Service Washington, D.C. 20590	Final Report December 1979 to February 1980
	14. Sponsoring Agency Code

15. Supplementary Notes

16. Abstract

A unified data collection and analysis plan to support NAFEC and the FAA in the assessment of Loran-C as either a replacement for or supplement to the current network of VOR/DMEs is presented in this report. This effort focused on four specific areas:

- Developing mathematical models of temporal variations in Loran-C signal phase and amplitude;
- Developing data collection procedures to enable an assessment of the accuracy and adequacy of proposed models;
- Defining a data analysis plan that will enable maximum use of the data collected in identifying parameters of the proposed models and cause and effect relationships of Loran-C temporal variations; and
- Defining a plan for the design of a data management system for the storage and maintenance of collected data and an efficient interface for the data analysis programs.

The plans and models provide the necessary structure for the data collection and analysis effort anticipated to commence early in 1980. Subsequent analysis of the Loran-C data will validate the models and dictate any modifications of the plans.

17. Key Words	18. Distribution Statement
computer modeling Loran-C temporal and spatial variations Loran-C Data Base Management Plan	Document is available to the U.S. public through the National Technical Information Service, Springfield, Virginia 22161

19. Security Classif. (of this report)	20. Security Classif. (of this page)	21. No. of Pages	22. Price
Unclassified	Unclassified	184	

Form DOT F 1700.7 (8-72) Reproduction of completed page authorized

METRIC CONVERSION FACTORS

Approximate Conversions to Metric Measures

Symbol	When You Know	Multiply by	To Find	Symbol
	LENGTH			
in	inches	*2.5	centimeters	cm
ft	feet	30	centimeters	cm
yd	yards	0.9	meters	m
mi	miles	1.6	kilometers	km
	AREA			
in^2	square inches	6.5	square centimeters	cm^2
ft^2	square feet	0.09	square meters	m^2
yd^2	square yards	0.8	square meters	m^2
mi^2	square miles	2.6	square kilometers	km^2
	acres	0.4	hectares	ha
	MASS (weight)			
oz	ounces	28	grams	g
lb	pounds	0.45	kilograms	kg
	short tons (2000 lb)	0.9	tonnes	t
	VOLUME			
tsp	teaspoons	5	milliliters	ml
Tbsp	tablespoons	15	milliliters	ml
fl oz	fluid ounces	30	milliliters	ml
c	cups	0.24	liters	l
pt	pints	0.47	liters	l
qt	quarts	0.95	liters	l
gal	gallons	3.8	liters	l
ft^3	cubic feet	0.03	cubic meters	m^3
yd^3	cubic yards	0.76	cubic meters	m^3
	TEMPERATURE (exact)			
°F	Fahrenheit temperature	5/9 (after subtracting 32)	Celsius temperature	°C

*1 in = 2.54 (exactly). For other exact conversions and more detailed tables, see NBS Misc. Publ. 286, Units of Weights and Measures, Price $2.25, SD Catalog No. C13.10:286.

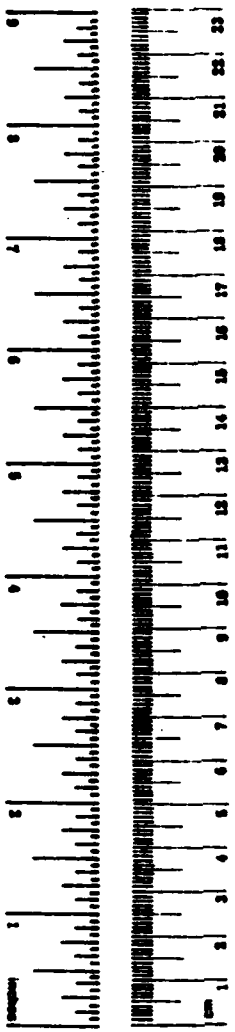

Approximate Conversions from Metric Measures

Symbol	When You Know	Multiply by	To Find	Symbol
	LENGTH			
mm	millimeters	0.04	inches	in
cm	centimeters	0.4	inches	in
m	meters	3.3	feet	ft
m	meters	1.1	yards	yd
km	kilometers	0.6	miles	mi
	AREA			
cm^2	square centimeters	0.16	square inches	in^2
m^2	square meters	1.2	square yards	yd^2
km^2	square kilometers	0.4	square miles	mi^2
ha	hectares (10,000 m^2)	2.5	acres	
	MASS (weight)			
g	grams	0.035	ounces	oz
kg	kilograms	2.2	pounds	lb
t	tonnes (1000 kg)	1.1	short tons	
	VOLUME			
ml	milliliters	0.03	fluid ounces	fl oz
l	liters	2.1	pints	pt
l	liters	1.06	quarts	qt
l	liters	0.26	gallons	gal
m^3	cubic meters	35	cubic feet	ft^3
m^3	cubic meters	1.3	cubic yards	yd^3
	TEMPERATURE (exact)			
°C	Celsius temperature	9/5 (then add 32)	Fahrenheit temperature	°F

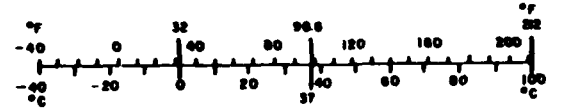

TABLE OF CONTENTS

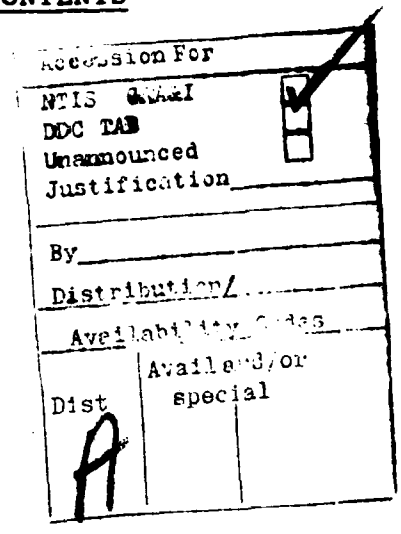

TABLE OF CONTENTS (Continued)

LIST OF FIGURES

LIST OF FIGURES (Continued)

LIST OF FIGURES (Continued)

LIST OF TABLES

LIST OF TABLES (Continued)

1. INTRODUCTION

1.1 BACKGROUND

The Federal Aviation Administration (FAA) is evaluating a number of candidate navigation systems as either replacements for the current network of VOR/DMEs, or as supplements to VOR/DMEs in areas not served by that system (Ref. 1). One candidate system being evaluated is the Loran-C system. For close to two decades, Loran-C has been utilized for high accuracy requirements of the Department of Defense, either as a relative navigation system or as part of modern avionic navigation systems. In more recent times due to technological advances and subsequent cost reductions, Loran-C has satisfied the requirements of a much larger user community; particularly, the maritime community. In fact, Loran-C has been selected as the national system to satisfy commercial marine requirements within the coastal confluence zone (Ref. 46).

Although employed in numerous applications, Loran-C has not been extensively tested in an operating environment as an Area Navigation System for use in the U.S. National Airspace System. General issues which must be addressed in assessing Loran-C in the context of the requirements of an Area Navigation System include:

- Accuracy
- Operational Adequacy
- Reliability

- Pilot Workload
- Cost.

Accuracy requirements placed on an Area Navigation System are defined in Ref. 2. The most stringent requirement is 0.3 nm (2σ) in crosstrack and downtrack directions during the non-precision approach phase. This requirement is for the navigation system contribution only and does not include Flight Technical Errors. Operational adequacy refers to the ability to maintain signal lock in various operating conditions such as thunderstorms, in the presence of radio frequency interference (RFI) in the Loran-C frequency band or near power lines. Reliability is a critical issue for Loran-C since loss of a transmitter affects numerous users over a wide geographic area. Pilot workload and cost must also be considered, if Loran-C receivers are to be installed in aircraft.

1.2 OBJECTIVES

A Loran-C development program (Ref. 1) under the auspices of the FAA is addressing these issues. One of the program activities is a ground-based data collection effort being conducted by the National Aviation Facilities Experimental Center (NAFEC). Data will be collected in order to provide a preliminary assessment of Loran-C for application to civil aircraft navigation. This effort is structured to address portions of the accuracy and operational adequacy issues. Two specific goals of the data collection effort (and the main issues discussed in this report) are to:

- Develop mathematical models to characterize the temporal and spatial variations in Loran-C signal propagation delay

- Evaluate the operational adequacy of Loran-C signals, in terms of susceptibility to noise and interference effects, in the ground environment of a number of airports.

Development of Loran-C signal propagation models is motivated by the following considerations:

- A convenient description of general propagation characteristics is required to aid in the planning of FAA ground and airborne Loran-C tests
- Reference models are required for use in certifying airborne equipment and conducting analytic system-level Loran-C studies, and for implementation in Loran-C system simulators.

Results of recent Loran-C tests in the airborne environment are very encouraging for the applicability of Loran-C to civil aircraft navigation (Refs. 18 and 48). However, these results are specific to the navigation equipment and operating regions selected for the tests, and are difficult to extrapolate to other test scenarios. By collecting Loran-C data at ground-based monitor sites, rather than in the context of aircraft navigation, it is anticipated that fundamental signal propagation characteristics can be identified. The information thus obtained will enable airborne test results to be extended more readily to other navigation equipment and operating regions.

TASC's role in the data collection effort is to insure, through analysis, that the data collection procedures, and consequently the collected data, offer maximum utility towards achieving the goals of the data collection effort. This is a cooperative effort with NAFEC personnel who are procuring the required equipment and providing operational inputs to the

data collection plan. In addition, TASC is defining procedures for analysis of the collected data for model development. In particular, four specific areas have been addressed:

- Computer Model Development
- Review of NAFEC Loran-C Data Collection Plan
- Development of Data Analysis Plan
- Design of Data Management System.

These efforts are obviously closely related, with results of any individual effort affecting the remaining. Taken as a group, these efforts represent the preliminary design of a Loran-C data collection and analysis program directed at assisting in the evaluation of the future utility of Loran-C in the U.S. National Airspace System. The term "preliminary design" is employed for two reasons. First, the NAFEC Loran-C data collection effort has not yet begun. Once data are collected, analyses will substantiate or refutiate initial assumptions concerning the characteristic of Loran-C signal propagation. These results may then require a modification of the models presented in this report. Second, the data collection procedures proposed in this study represent an initial assessment of the Loran-C system. The primary goal of the current program (Ref. 1) is to utilize collected data to enhance the proposed models and define long-term data collection procedures needed to increase confidence in the models.

1.3 REPORT ORGANIZATION

Mathematical development of computer models is discussed in Chapter 2. Prior to detailed discussion of these

models, a brief overview of the Loran-C system and Loran-C groundwave propagation theory are outlined in order to relate the structure of proposed models to physical characteristics of Loran-C signal propagation. A short discussion of modeling in general, also for background purposes, is included prior to discussion of specific computer models. Review of the NAFEC Loran-C Data Collection Plan is outlined in Chapter 3. This material is discussed in detail in Ref. 3 and only portions of this material, required to maintain report continuity, are included. The interaction between recommended data collection procedures and how specific data will be utilized to identify parameters of the proposed computer models is included in Chapter 3. A separate issue not directly related to the data collection plan, but more closely to data collection equipment, is also addressed in Chapter 3. This item is the examination of the effect of notch filters, which are commonly employed with Loran-C receivers to reduce RFI, on the quality of collected data.

Recommended data analysis procedures, the subset of data each procedure will utilize and the anticipated results of this analysis are outlined in Chapter 4. Definition of the data analysis plan essentially "closes the loop" between proposed computer models and collected data as illustrated in Fig. 1.3-1. Results of the data analyses enable verification, enhancement, or modification of existing models. The block diagram representation is utilized to enforce the point that the model development procedure is a dynamic process requiring a number of iterations before achieving program goals. Figure 1.3-1 indicates the data analysis portion of the program requires the structure of the computer models as well as the actual collected data. Because of uncertainties in the initial model structures, non-parametric data analysis techniques will initially be utilized because they require no a priori

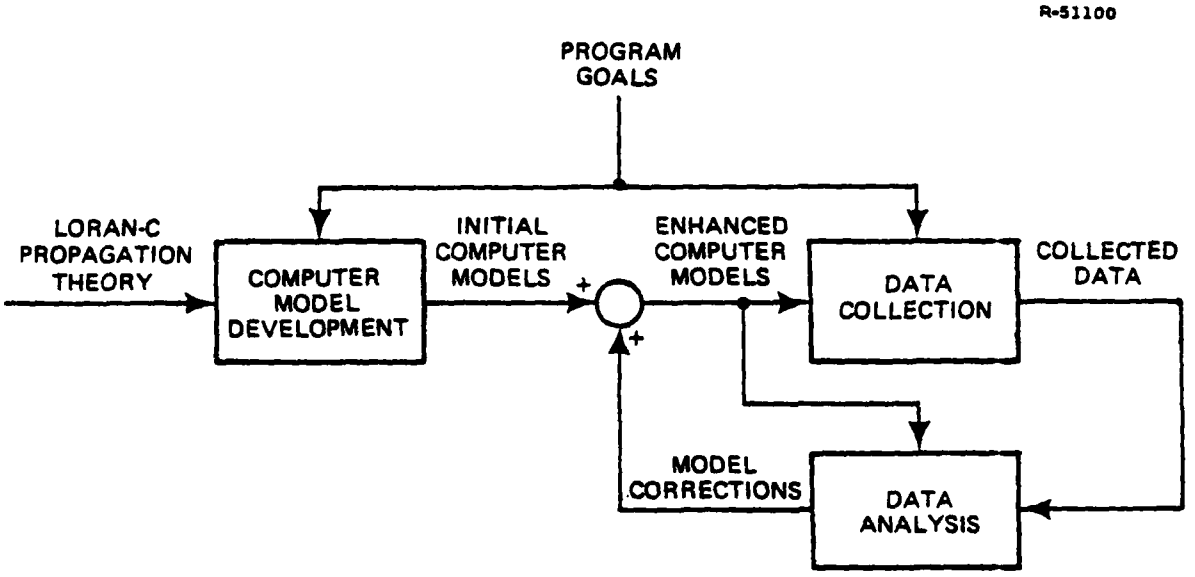

Figure 1.3-1 Computer Model Development Block Diagram

information conerning model structure. These techniques, such as Fourier analysis, relay on statistical and time and frequency domain characteristics of the data, independent of the model. Identification of model parameters is based on parametric data analysis techniques which rely on a model structure for the basis of their analysis. Maximum likelihood estimation is an example of a parametric technique.

An interface between the data analysis program and collected Loran-C data is required. This interface is provided by the data management system described in Chapter 5. The data management system provides a general and flexible framework for simple and efficient storage, management and processing of all data. This includes not only the Loran-C data, but weather data and anomalous event data. A summary of the efforts is contained in Chapter 6.

2. LORAN-C MODEL DEVELOPMENT

2.1 OVERVIEW OF THE LORAN-C SYSTEM

The Loran-C radionavigation system consists of transmitting stations which are grouped into chains, each chain serving a particular coverage area. Four Loran-C chains -- the Northeast U.S., Southeast U.S., Great Lakes,* and U.S. West Coast chains -- currently provide coverage for most of the 48 contiguous states of the United States. The coverage areas for these chains are shown in Fig. 2.1-1, and the transmitter

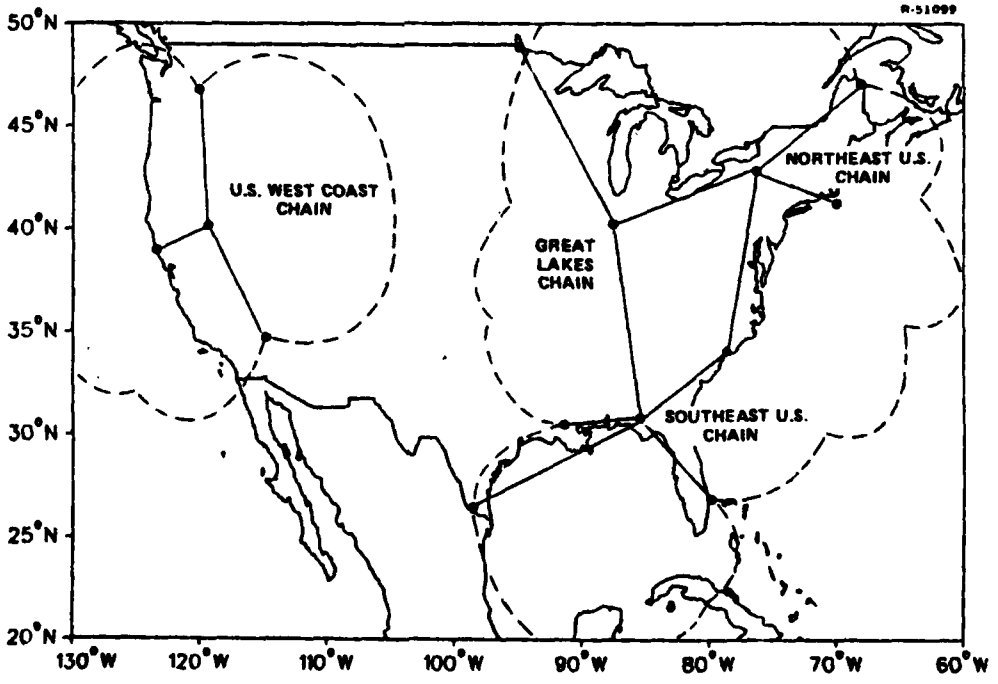

Figure 2.1-1 Approximate Loran-C Chain Coverage Areas in the United States (Ref. 4)

*The Great Lakes chain is scheduled to become operational in February 1980.

locations are listed in Table 2.1-1. The Loran-C system, in its present configuration, does not provide complete coverage for the central and southwestern United States. A fifth Loran-C chain, the Gulf of Alaska chain, provides coverage for the Alaskan Coastal Confluence Zone, but only a small portion of the Alaskan mainland. The models developed herein are general enough to be applied to any Loran-C chain. However,

TABLE 2.1-1

LORAN-C CHAINS PROVIDING COVERAGE FOR THE UNITED STATES*

T-3467

LORAN-C CHAIN AND RATE	TRANSMITTER	LOCATION	NORTH LATITUDE (deg-min-sec)	WEST LONGITUDE (deg-min-sec)
NORTHEAST U.S. (9960)	Master†	Seneca, NY	42 42 50.603	76 49 33.862
	W	Caribou, ME	46 48 27.199	67 55 37.713
	X	Nantucket, MA	41 15 11.930	69 58 39.090
	Y†	Carolina Beach, NC	34 03 46.040	77 54 46.760
	Z†	Dana, IN	39 51 07.540	87 29 12.140
SOUTHEAST U.S. (7980)	Master†	Malone, FL	30 59 38.740	85 10 09.305
	W	Grangeville, LA	30 43 33.018	90 49 43.600
	X	Raymondville, TX	26 31 55.006	97 50 00.093
	Y	Jupiter, FL	27 01 58.490	80 06 53.520
	Z†	Carolina Beach, NC	34 03 46.040	77 54 46.760
GREAT LAKES (9930)	Master†	Dana, IN	39 51 07.540	87 29 12.140
	W†	Malone, FL	30 59 38.740	85 10 09.305
	X†	Seneca, NY	42 42 50.603	76 49 33.862
	Y	Baudette, MN	48 36 49.826	94 33 18.434
U.S. WEST COAST (9940)	Master	Fallon, NV	39 33 06.620	118 49 56.370
	W	George, WA	47 03 47.990	119 44 39.530
	X	Middletown, CA	38 46 56.990	122 29 44.530
	Y	Searchlight, NV	35 19 18.180	114 48 17.430

*From Ref. 4.

†Dual-rated transmitter.

the Northeast U.S. chain (shown in detail in Fig. 2.1-2) is focused upon, because the initial NAFEC data collection effort is planned to take place in the northeast region (within a one-day drive from NAFEC).

Each Loran-C chain indicated in Table 2.1-1 is comprised of one master transmitter and three or four secondary transmitters (designated W, X, Y. and Z). The most common form of Loran-C navigation is the hyperbolic mode, in which the Loran-C user is equipped with a receiver which measures the Time Difference (TD) between the arrival times of the secondary and master signals. The TD measurement defines a hyperbolic Line-of-Position (LOP), along which the difference between secondary-to-user and master-to-user ranges is a constant. Two TD measurements, corresponding to two different

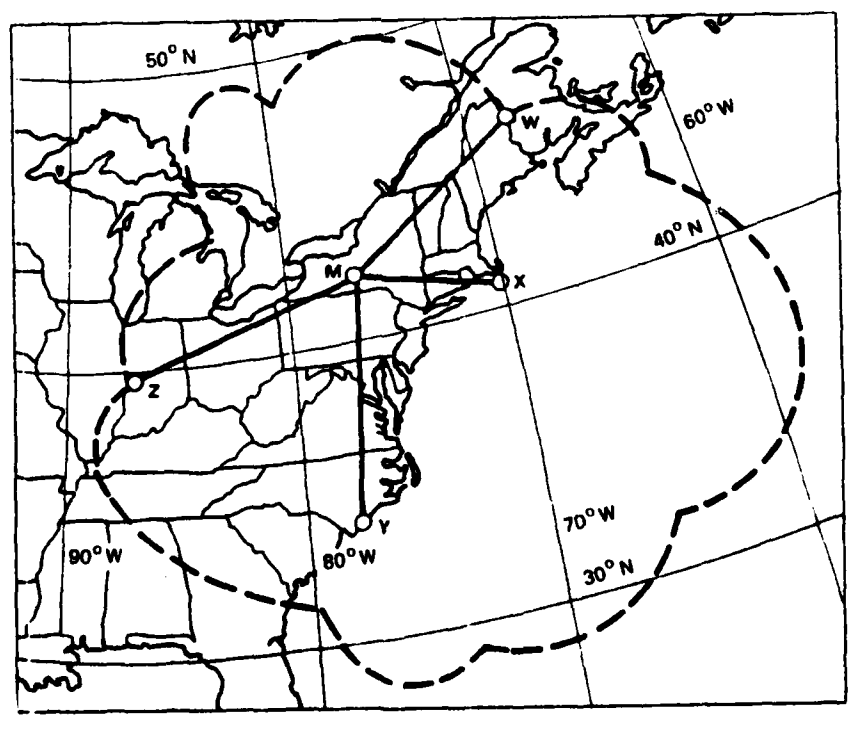

Figure 2.1-2 Northeast U.S. Loran-C Chain Coverage Area

secondary/master pairs, define a hyperbolic Loran-C position fix, as illustrated in Fig. 2.1-3. Other possible modes of Loran-C navigation include:

- Master-independent hyperbolic mode, whereby each TD is formed from two secondary signal arrival times
- Direct-ranging mode, whereby a precision clock is interfaced with a Loran-C receiver or additional Loran-C signals are processed, to estimate signal Time-of-Arrival (TOA)

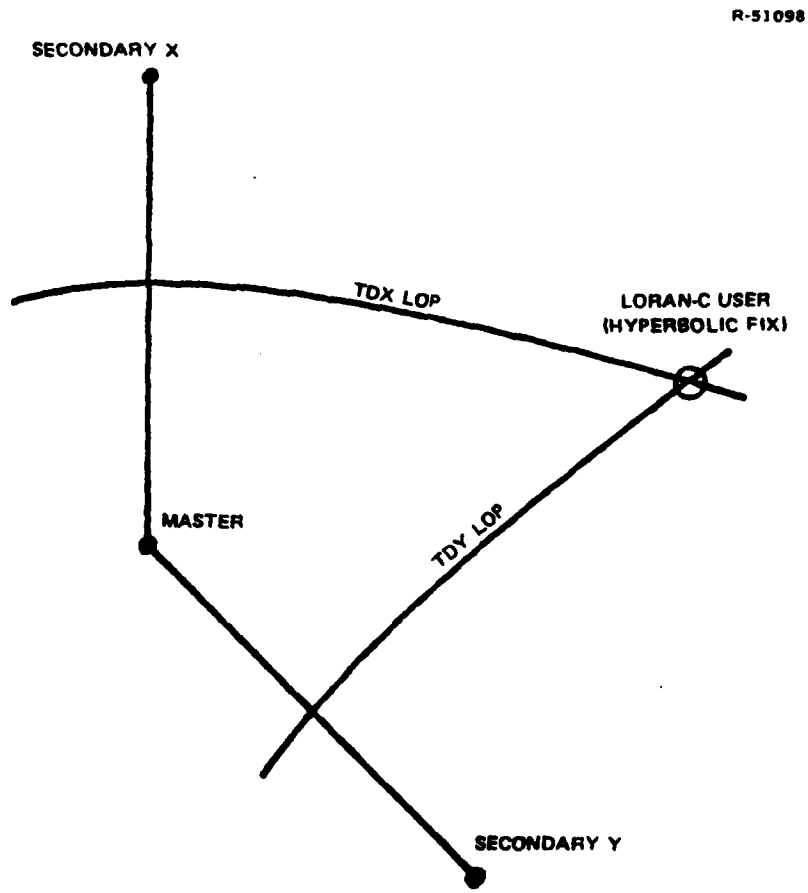

Figure 2.1-3 Hyperbolic Loran-C Position Fix

- Dual-chain hyperbolic or direct-ranging mode, whereby signals from two Loran-C chains are employed simultaneously.

The mathematical models presented in this report are applicable to all Loran-C navigation modes. However, depending on the type of data available for model calibration (e.g., TDs vs. TOAs), it may only be possible to estimate certain combinations of model parameters and apply the models to certain navigation modes. The data collection plan recommended by TASC to support an initial assessment of Loran-C emphasizes the single-chain hyperbolic mode, which is anticipated to be the primary navigation mode implemented in low-cost airborne Loran-C receivers. However, the calibrated models will be applicable to other navigation modes to the extent detailed herein.

The actual LOPs associated with a Loran-C position fix differ from the ideal hyperbolic LOPs due to spatial anomalies in the Loran-C signal propagation medium (see Fig. 2.1-4a). Furthermore, the spatial anomalies vary with time due to temporal variations in the propagation medium (see Fig. 2.1-4b). In order to account for spatial and temporal variations in the propagation medium, it is necessary to employ a Loran-C signal propagation model -- i.e., a mathematical relationship between signal propagation path length (and possibly other path characteristics) and signal propagation time delay. Candidate models range from a simple model, utilizing only the signal propagation velocity for free space, to a highly complex model, which relies on a detailed physiographic description of the chain coverage area.

In this chapter, Loran-C signal propagation models are proposed, which will be calibrated and updated using data collected by NAFEC. These models are referred to as operational models and could be employed for airborne equipment

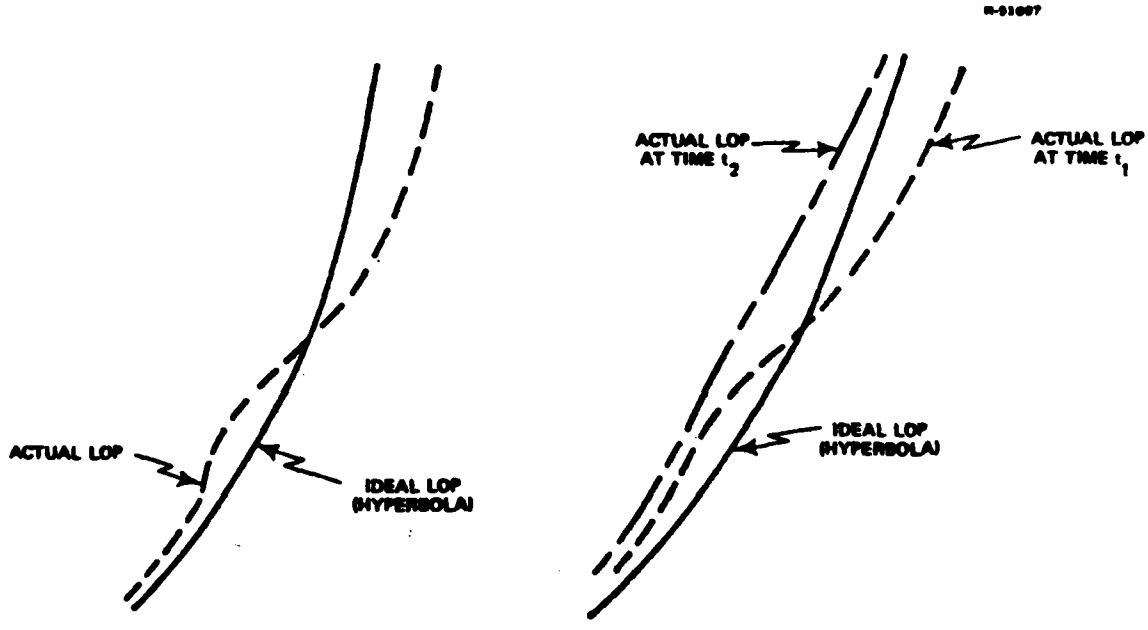

a) Spatial Variation b) Temporal Variation

Figure 2.1-4 LOP Distortion Induced by Spatial and Temporal Variations in the Signal Propagation Medium

certification and in analytic system-level studies. Development of the operational models leads naturally to sensitivity models, which can be used to indicate there spatial and temporal variations in Loran-C TDs are largest. The sensitivity models are employed in Chapter 3 to identify appropriate data collection sites for the NAFEC tests.

A review of Loran-C groundwave propagation theory is provided in Section 2.2 to establish terminology and nomenclature. In Section 2.3, the differences between deterministic and stochastic models, and between theoretical and empirical models, are addressed in the context of Loran-C operational

and sensitivity models. Sections 2.4 and 2.5 present descriptions of the proposed operational and sensitivity models, respectively. In addition to models of Loran-C signal propagation delay, models are developed for Loran-C signal amplitude. The signal amplitude model is presented in Section 2.6, together with a discussion of how the model can be utilized with existing atmospheric noise data to predict Signal-to-Noise Ratio (SNR). The modeling efforts are summarized in Section 2.7.

2.2 REVIEW OF LORAN-C GROUNDWAVE PROPAGATION THEORY

Conceptually, the Low Frequency (LF) Loran-C signal is comprised of skywave and groundwave components, as illustrated in Fig. 2.2-1. Due to ionospheric fluctuations, the skywave component of a Loran-C pulse does not contain the

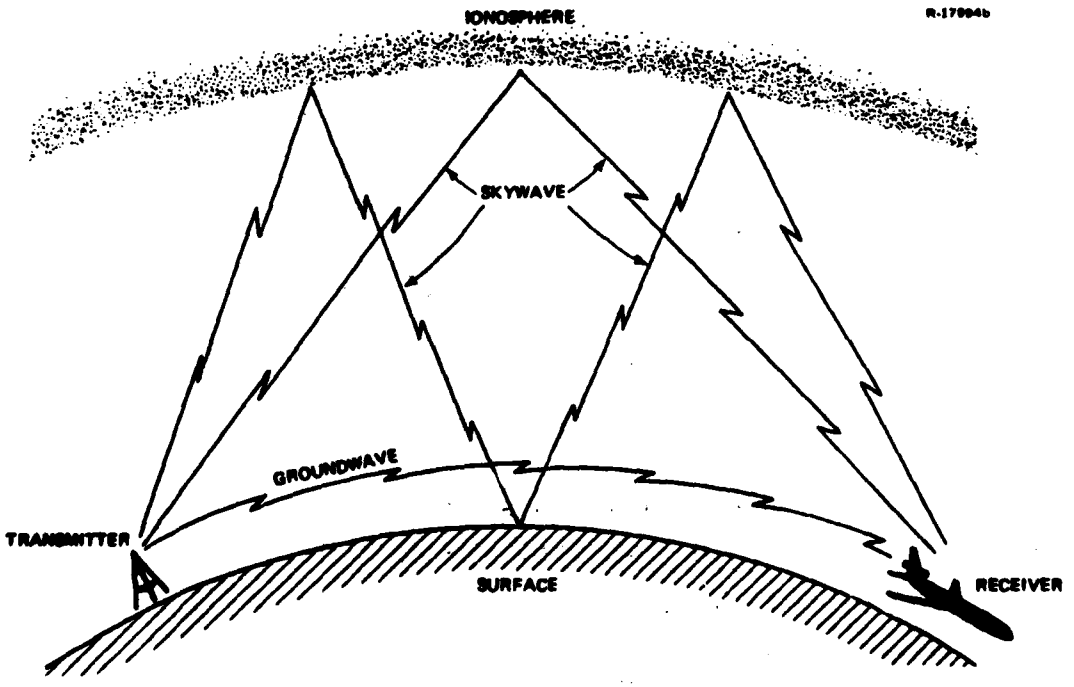

Figure 2.2-1 Skywave and Groundwave Components of the Loran-C Signal

precise timing information which the groundwave component con-tains. However, the skywave component is received at a point in time delayed from the groundwave component, and does not interfere with its utility in the chain coverage areas indicated in Fig. 2.1-1. It is assumed in the development of the models discussed herein that the Loran-C receiver is able to track the groundwave component of the Loran-C pulse without skywave contamination.

2.2.1 Time Difference Equation

Each measured TD is a function of signal propagation delays, the secondary station emission delay,* and measurement noise. The TD measured at a Loran-C user location (designated by u) at time t is denoted by $TD_i(u,t)$, for a transmitter pair consisting of a secondary station (i) and the master station (m). $TD_i(u,t)$ is expressed by:

$$TD_i(u,t) = \phi_i(u,t) - \phi_m(u,t) + ED_i(t) + v_i(u,t) \quad (2.2\text{-}1)$$

where

$\phi_i(u,t)$ = propagation delay from i to u

$\phi_m(u,t)$ = propagation delay from m to u

$ED_i(t)$ = emission delay for secondary i

$v_i(u,t)$ = measurement noise

Propagation delays and measurement noise depend on the user location and measurement time, whereas the emission delay is

*Emission delay is the time delay between transmission of the secondary and master signals.

the same for all user locations, at any particular measurement time.

2.2.2 Signal Propagation Delay

Loran-C signal propagation delay depends on the following characteristics of the propagation path:

- Transmitter-to-receiver geodetic range
- Atmospheric refractive index at the Earth's surface
- Vertical lapse rate (gradient) of the atmospheric refractive index
- Conductivity of the surface soil or water and the underlying rock strata
- Terrain topography
- Manmade structures, such as bridges and power lines.

In principle, the propagation delay can be expressed as the solution to an electromagnetic wave equation, regardless of the complexity of the propagation path. However, inclusion of the effects of topography and manmade structures results in a significant computational burden, which is not justified in practical applications of Loran-C propagation theory. A tractable solution to the wave equation exists for a propagation path which is homogeneous in surface refractive index and vertical lapse rate, and which consists of smooth path segments, each homogeneous in conductivity.

In this case, the solution is given by the equation

$$\phi_i = \frac{n_i}{c} R_i + SF(\sigma_i, \sigma_{i1}, \ldots, \sigma_{iJ}, R_{i1}, \ldots, R_{iJ}) \quad (2.2\text{-}2)$$

where

ϕ_i = propagation delay* from transmitter i to user

c = speed of light in free space

n_i = surface refractive index

R_i = transmitter-to-user range

α_i = parameter related to vertical lapse rate

J = number of path segments

σ_{ij} = path segment conductivities (j=1,...,J)

R_{ij} = path segment lengths (j=1,...,J)

$SF(\ )$ = secondary phase delay† function

The first term in Eq. 2.2-2 is the primary phase delay and is typically a factor of 100 larger than the second term, the secondary phase delay. Although the primary delay is the dominant propagation delay component, the secondary delay is more difficult to compute and, therefore, receives greater attention in modeling efforts.

The secondary phase delay can be computed using classical propagation theory (Ref. 5), in the case of a single path segment with homogeneous conductivity. The classical theory results are presented in Fig. 2.2-2 for a vertical lapse rate parameter (α) equal to 0.75 and for various values of conductivity. The secondary phase delay is a minimum for sea water paths, and differs only slightly for values of sea

*Propagation delay, phase delay, and time delay are used synonymously, and are expressed in units of μsec.

†In this report, SF is defined to include the combined delay due to land and sea water paths, not just the delay due to an assumed all sea water path.

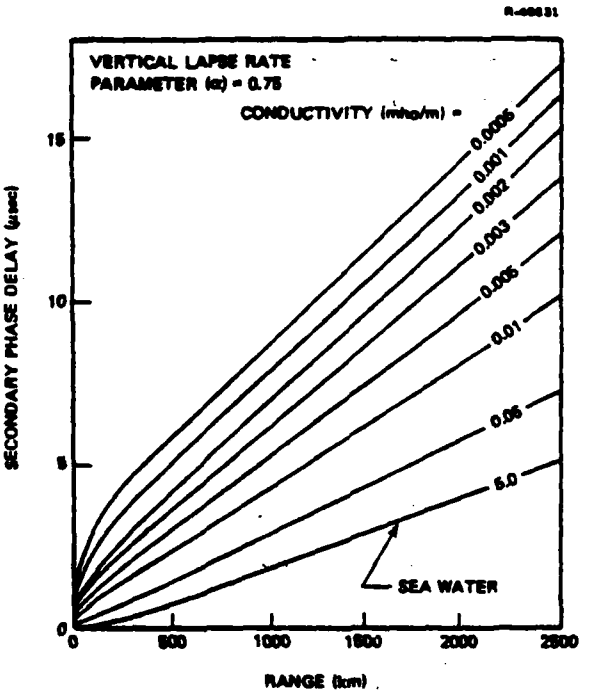

Figure 2.2-2 Classical Theory Solution to Secondary Phase Delay for a Homogeneous Propagation Path (Ref. 5)

water conductivity between 4.0 mho/m and 6.0 mho/m. On the other hand, the secondary phase delay is very sensitive to the value of land conductivity, which ranges from 0.0005 mho/m to 0.01 mho/m, depending on the composition of the land (see Ref. 6). The dependence of secondary phase delay on the vertical lapse rate parameter differs for different conductivities. This dependence is shown in Fig. 2.2-3 for a conductivity of 0.005 mho/m.

Classical propagation theory for a mixed conductivity path is cumbersome and poorly suited for practical application (Ref. 7). However, a convenient approximation to the classical mixed-path theory is provided by Millington's method (Ref. 8). In Millington's method, secondary phase delay is computed by

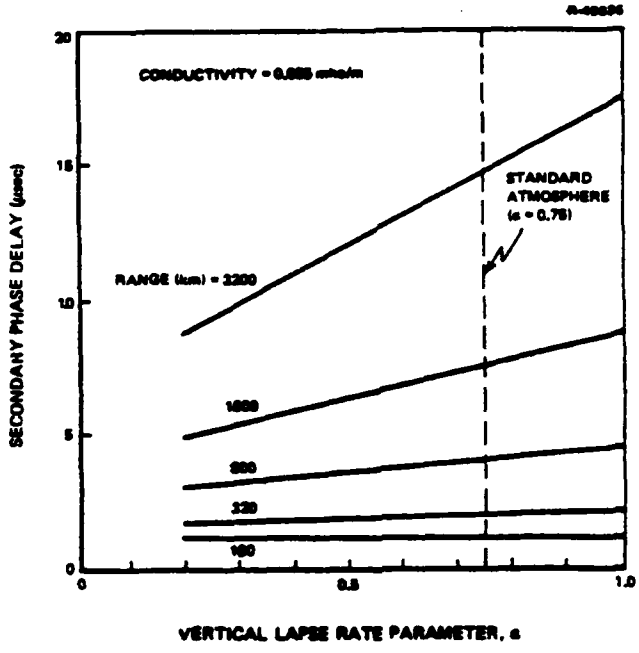

Figure 2.2-3 Effect of Vertical Lapse Rate Parameter On Secondary Phase Delay (Ref. 5)

combining a number of terms, each term corresponding to the delay for a homogeneous path segment. For example, Millington's method for the mixed land and sea water path shown in Fig. 2.2-4 involves six terms:

$$SF = \tfrac{1}{2}[SF(\sigma_L,R_L) + SF(\sigma_S,R_L+R_S) - SF(\sigma_S,R_L) + SF(\sigma_S,R_S) + SF(\sigma_L,R_L+R_S) - SF(\sigma_L,R_S)] \quad (2.2\text{-}3)$$

where σ_L and σ_S are the conductivities of the land and sea water path segments, respectively, and R_L and R_S are the associated path segment lengths. Each term in Eq. 2.2-3 is computed using classical propagation theory for a homogeneous path (Fig. 2.2-2).

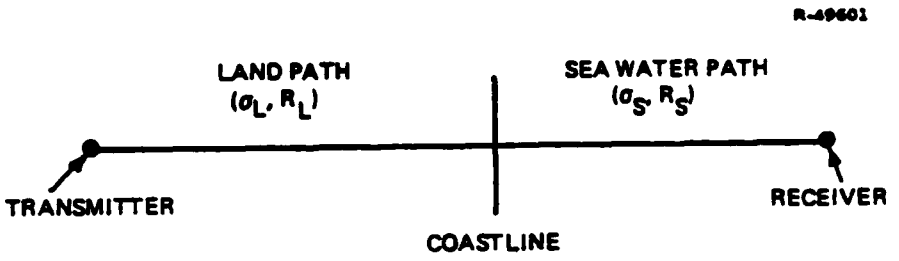

Figure 2.2-4 Mixed Land and Sea Water Path

Secondary phase delay for a mixed land and sea water path is plotted in Fig. 2.2-5 for four values of land conductivity and various land path segment lengths. Secondary phase delay decreases upon crossing the coastline, with the extent of the decrease depending on the value of land conductivity. Beyond a range of approximately 200 km from the coastline, the slopes of the secondary phase delay curves approach the slope indicated for an all sea water path.

Secondary phase delay for a propagation path consisting of sea water followed by land can be determined from Eq. 2.2-3 with the subscripts "S" and "L" interchanged. (Such a sea water/land path may be representative if the transmitter is close to the coast.) Secondary phase delay for a sea water/land path is plotted in Fig. 2.2-6 for four values of land conductivity and various sea water path lengths. In contrast to a land/sea water path, secondary phase delay increases upon crossing the coastline and approaches the slope for an all land path. The effect of land/sea water and sea water/land conductivity interfaces is an important issue which should be addressed in the development of Loran-C models.

Secondary phase delay is also influenced by receiver altitude, increasing at the rate of approximately 0.1 μsec per km increase in altitude, over the first 15 km (Ref. 5). This

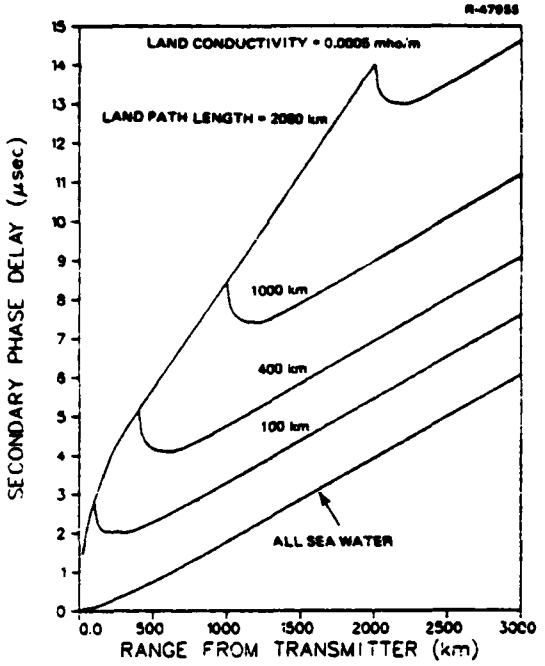

a) Land Conductivity = 0.0005 mho/m

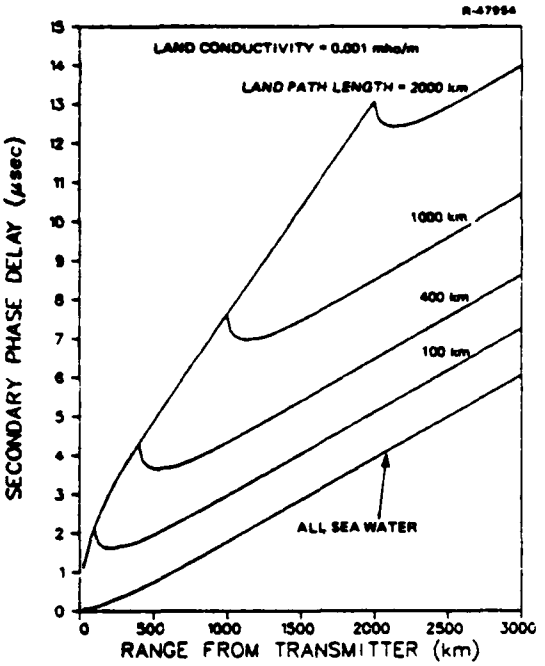

b) Land Conductivity = 0.001 mho/m

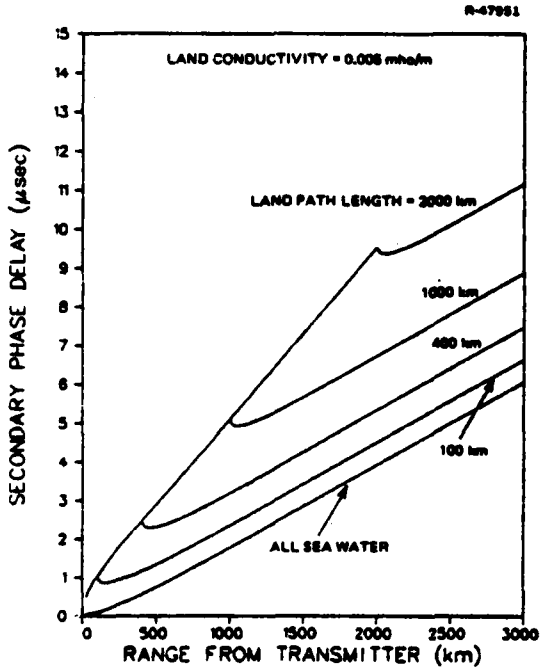

c) Land Conductivity = 0.005 mho/m

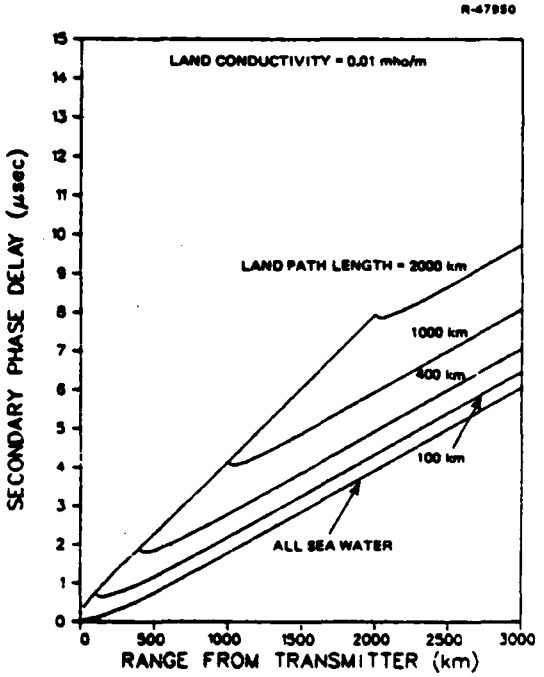

d) Land Conductivity = 0.01 mho/m

Figure 2.2-5 Millington's Method Solution to Secondary Phase Delay for a Mixed Land and Sea Water Propagation Path

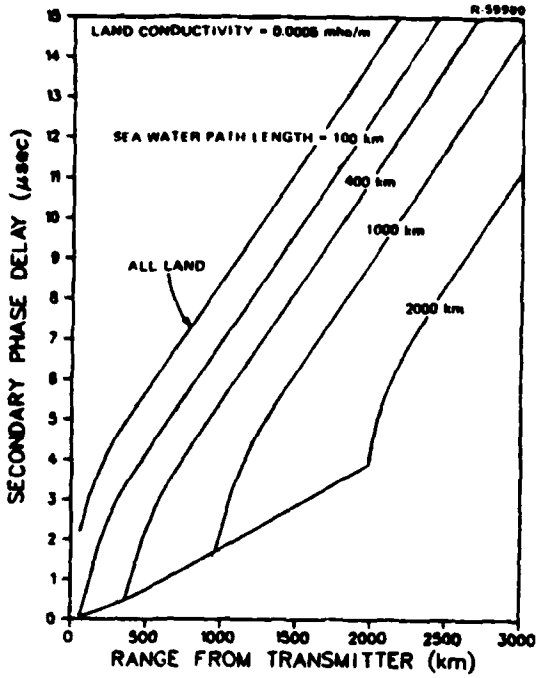

a) Land Conductivity = 0.0005 mho/m

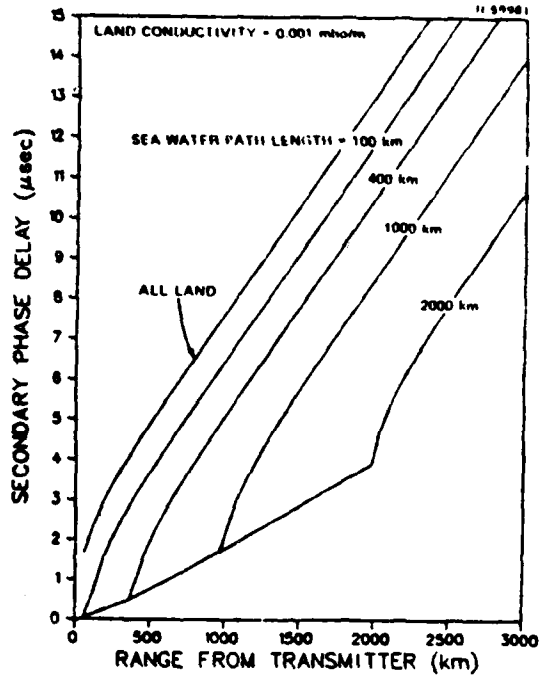

b) Land Conductivity = 0.001 mho/m

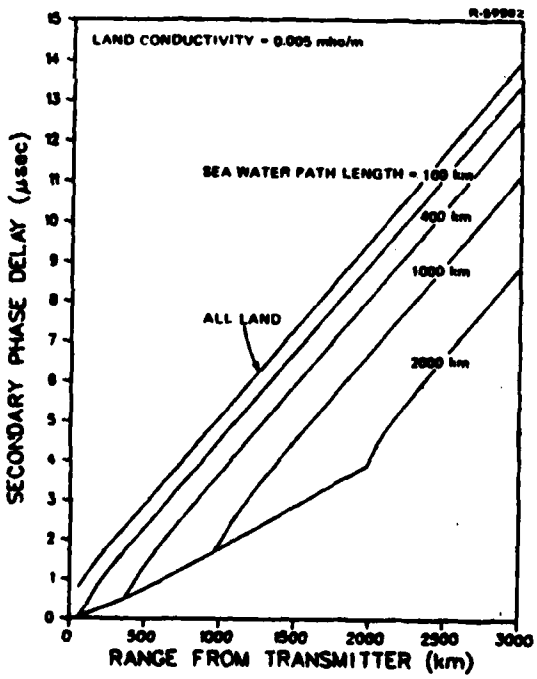

c) Land Conductivity = 0.005 mho/m

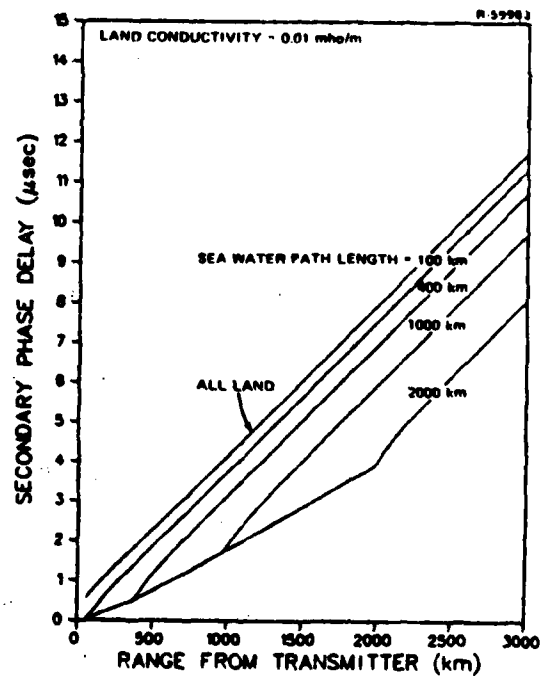

d) Land Conductivity = 0.01 mho/m

Figure 2.2-6 Millington's Method Solution to Secondary Phase Delay for a Mixed Sea Water and Land Propagation Path

effect results in a TD bias for aircraft flying at the same altitude.

2.2.3 Emission Delay

The emission delay is the time delay between transmission of the secondary and master Loran-C signals (see Eq. 2.2-1). Although the emission delay for each secondary station is published as a constant (e.g., see Ref. 4), it is important to recognize that temporal variations in the emission delay may be comparable to variations in the transmitter-to-user propagation delays. Emission delay variations are related to Loran-C signal timing, which is based on time standards (i.e., clocks) located at the transmitters and controlled by a System Area Monitor (SAM) located in the chain coverage area. The method employed to time the secondary and master signals has been changed from a "slaved" to a "free-running" method, since the advent of the Loran-C system.

In the original timing method, the secondary signal transmission time is slaved to reception of the master signal, which is itself timed with a cesium beam clock. The master signal is received at the secondary station and, after a fixed delay (the coding delay), the secondary signal is transmitted. Therefore, the emission delay is the summation of the coding delay and the master-to-secondary (i.e., base-line) propagation delay. In this method, emission delay variations are caused primarily by weather-induced variations in the base-line propagation delay, and to a less extent by the long-term frequency variations of the quartz-crystal oscillator which establishes the coding delay. The emission delay variations are controlled by a feedback mechanism involving the SAM (described below).

In the present timing method, the secondary station is not slaved to the master station. Rather, the secondary signal transmissions are timed with a free-running cesium beam clock, in the same manner as the master signal transmissions. In this scheme, emission delay variations are caused by the difference between the frequencies of the secondary and master clocks, both of which are highly-stable. The frequency difference is manifested in an emission delay drift, which is controlled by the SAM.

Although emission delay variations are influenced by different factors in the slaved and free-running timing methods, the approach used to control the variations is the same in the two methods. Loran-C chain control involves the following procedure, which is applied essentially continuously:

- Each TD is measured at a System Area Monitor (SAM) located in the chain coverage area
- The difference between the measured SAM TD and a reference TD (the Controlling Standard Time Difference or CSTD) is computed
- If the difference exceeds an established tolerance of 50 nsec, the secondary station is instructed to apply a Local Phase Adjustment (LPA) to the emission delay to re-establish tolerance.

The LPAs are based on TDs measured at the SAM, and therefore are influenced by temporal variations in the transmitter-to-SAM propagation delays.

In particular, consider the TD equation presented in Section 2.2.1 (Eq. 2.2-1), with the Loran-C user location u replaced by the SAM location s. This equation expresses the

TD measured at the SAM, in terms of propagation delays, the emission delay, and measurement noise:

$$TD_i(s,t) = \phi_i(s,t) - \phi_m(s,t) + ED_i(t) + v_i(s,t) \quad (2.2\text{-}4)$$

Denoting the difference between the measured SAM TD and the reference TD by

$$\tau_i(s,t) = TD_i(s,t) - CSTD_i \quad (2.2\text{-}5)$$

and combining Eqs. 2.2-4 and 2.2-5, yields the following equation for emission delay:

$$ED_i(t) = CSTD_i - \phi_i(s,t) + \phi_m(s,t) - v_i(s,t) + \tau_i(s,t) \quad (2.2\text{-}6)$$

Equation 2.2-6 shows that the emission delay varies with time, due to transmitter-to-SAM propagation delay variations. The emission delay also varies with time due to clock drift, but these variations are bounded by the 50 nsec control tolerance.

Under ideal conditions of no SAM or user measurement noise ($v_i = 0$), and continuous, precise chain control ($\tau_i = 0$), Eq. 2.2-6 can be combined with Eq. 2.2-1 to yield:

$$TD_i(u,t) = [\phi_i(u,t) - \phi_m(u,t)] - [\phi_i(s,t) - \phi_m(s,t)] + CSTD_i \quad (2.2\text{-}7)$$

Equation 2.2-7 is employed in the formulation of models for temporal TD variations.

2.3 MODELING CONCEPTS

It is useful to consider the relationship between the Loran-C models presented herein, and models previously reported in the literature. For this purpose, Loran-C models are classified according to their utility and data requirements.

Loran-C models are classified according to their utility, in the following manner:

- Deterministic Model - Used to express TD values in terms of specific values of propagation path parameters (e.g., refractive index)
- Stochastic Model - Used to characterize the ensemble or statistical properties (e.g., standard deviation) of TD variations or TD residuals.*

The operational models are initially developed as deterministic models based on characteristics of the Loran-C propagation medium. Stochastic models, if required, will be developed when sufficient data are collected to enable a statistically-based evaluation of TD residuals. It is important to note that since TD residuals are a function of the deterministic model, the resulting stochastic model is also a function of the deterministic model structure, and therefore cannot be developed independent of deterministic models. A stochastic model could be employed to process TD residuals in conjunction with other navigation information in a statistically-based procedure (e.g., Kalman filter; Ref. 17) in an airborne Loran-C navigation system.

*TD residuals are the differences between deterministic model predictions and measurements.

Loran-C models can also be classified according to the data required for model development, in the following manner:

- Theoretical Model - Structure and coefficients based solely on Loran-C propagation theory; not calibrated using TD data
- Semi-Empirical Model - Structure based on theory, but coefficients calibrated using TD data
- Empirical Model - Structure and coefficients based solely on TD data.

The operational models are based partly on Loran-C propagation theory, since they are intended to be applicable in large geographic areas where only sparse data may be collected. However, the models are formulated as semi-empirical models which can be calibrated and updated using Loran-C data.

Specific examples of the types of Loran-C models defined above are indicated in Table 2.3-1, including models developed by TASC for the U.S. Coast Guard and Transportation Systems Center. Of particular interest in the present study are the semi-empirical range- and bearing-dependent models developed for the St. Marys River and U.S. West Coast Loran-C chains (Refs. 11 and 12).

2.4 LORAN-C OPERATIONAL MODELS FOR CIVIL AIRCRAFT NAVIGATION

The Loran-C operational models must be consistent with the navigation system accuracy requirements established by the FAA Area Navigation Systems Specification (Ref. 2), as presented in Table 2.4-1. The accuracy requirements for non-precision

TABLE 2.3-1

EXAMPLES OF LORAN-C MODELS

T-3468

	DETERMINISTIC	STOCHASTIC
THEORETICAL	Integral Equation for Terrain Effect (Ref. 9); Prediction Technique for Vertical Lapse Rate Effect (Ref. 10)	Differential Loran-C Error Model Emphasizing Land/ Sea Water Interface Effect (Ref. 14)
SEMI-EMPIRICAL	Range- and Bearing-Dependent Models for St. Marys River and U.S. West Coast Loran-C TD Grids (Refs. 11 and 12)	Vertical Lapse Rate Model, Characterized by a Temporal Markov Process With Variance Computed From Weather Data (Ref. 15)*
EMPIRICAL	Orthogonal Polynomial Representation of TD Grid Warpage (Ref. 13)	Error Model for Grid Warpage, Characterized by a Spatial Markov Process (Ref. 16)

*A semi-empirical stochastic model based on TD data was not encountered during the literature survey.

TABLE 2.4-1

AREA NAVIGATION SPECIFICATION FOR U.S. NATIONAL AIRSPACE SYSTEM (AIRBORNE EQUIPMENT ERROR CONTRIBUTION)*

FLIGHT PHASE	CROSSTRACK OR DOWNTRACK ERROR SPECIFICATION, 2σ
Enroute	1.5 nm (2.8 km)
Terminal	1.1 nm (2.0 km)
Non-Precision Approach	0.3 nm (0.6 km)

*From Ref. 2.

approach are significantly more stringent than accuracy requirements for the enroute and terminal flight phases. Since the accuracy specified for non-precision approach is only required in limited geographic regions near airports, the following two-tier operational model is proposed:

- Global Operational Model - Valid throughout the Loran-C chain coverage area, but meeting only the enroute and terminal accuracy requirements
- Local Operational Model - Valid only in the airport approach area*, and meeting non-precision approach accuracy requirements.

A global model is required for each Loran-C chain, and a local model is required for each airport. However, it is advantageous to select general global and local model structures, which -- upon assignment of appropriate values to model coefficients and/or propagation path parameters -- can accommodate any particular Loran-C chain or airport.

2.4.1 Global Operational Model

The accuracy requirements for enroute and terminal flight are expected to be achievable with existing models, in a large portion of the published Loran-C chain coverage areas (see test data in Ref. 18). The U.S. Coast Guard presently employs Millington's method (see Section 2.2) and a map of

*The airport approach area encompasses flight operations between the "final approach waypoint" and the airport (Ref. 2). Although the final approach waypoint is typically less than 10 km from the airport, the approach area is conservatively defined to be a circle with a 20-km radius centered at the airport, for the purpose of this study.

effective ground conductivity*, in the generation of Loran-C TD grid (LOP) charts. The effective ground conductivity map (comparable to the map shown in Fig. 2.4-1) is initially developed from physiographic data, and subsequently calibrated using Loran-C TD data. The conductivity map is adjusted until the residual error between predicted and measured TDs approaches 0.2 μsec (2σ), thereby resulting in position errors less than 0.5 km (2σ) for much of the chain coverage area. In regions affected by large conductivity gradients, however, the TD

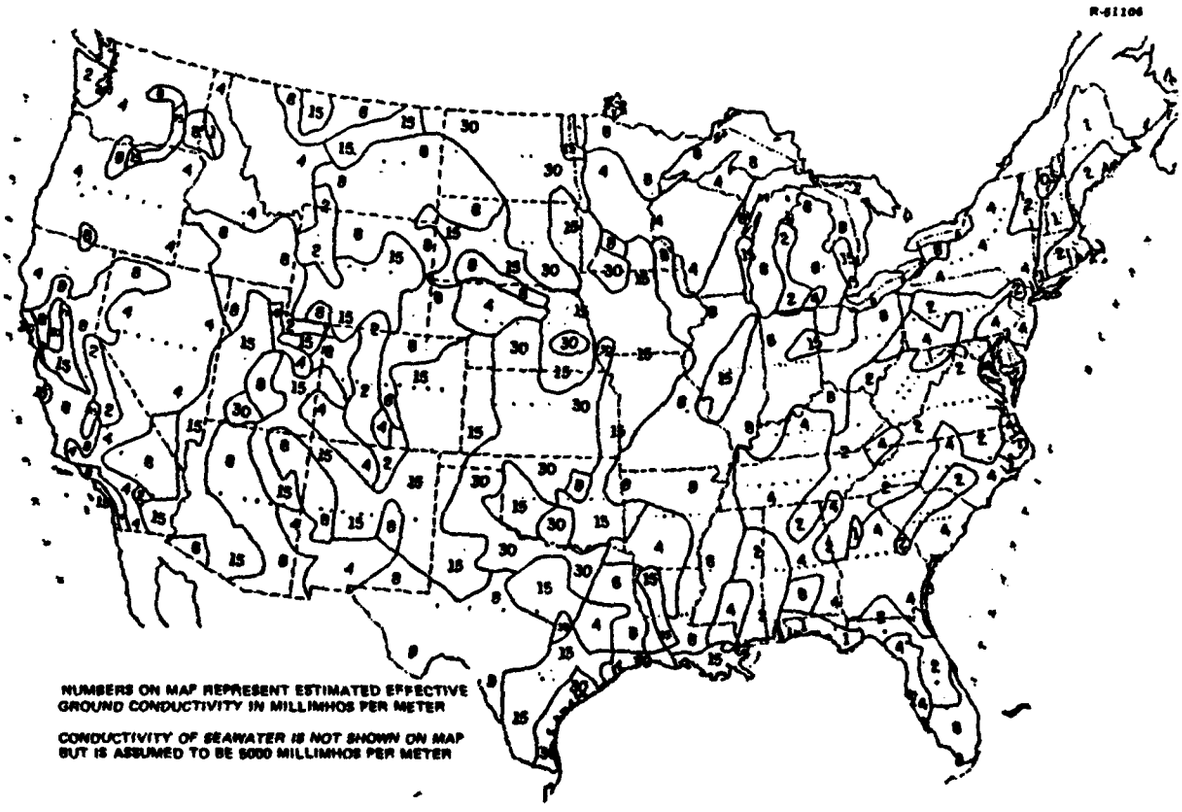

Figure 2.4-1 Effective Ground Conductivity Map for the United States (Ref. 6)

*Effective ground conductivity accounts for the effects of surface soild and water, as well as terrain topography and subterranean rock strata.

residuals may exceed 1.0 μsec (e.g., the Southern California Coastal Confluence Zone; see Ref. 10). In these regions, the TD grid is adjusted, by using force-fit techniques (Ref. 20) and additional TD data. Note that the U.S. Coast Guard approach does not account for temporal variations in signal propagation parameters. The surface refractive index and vertical lapse rate are chosen to equal the values for a standard atmosphere ($n = 1.000338$ and $\alpha = 0.75$). The conductivity map is calibrated using data collected at various times of the year and, therefore, is considered to represent the "average" conductivity characteristic. The U.S. Coast Guard approach also does not account for altitude effects.

An alternative to the U.S. Coast Guard approach is given by semi-empirical range- and bearing-dependent models. An example of a range- and bearing-dependent model is provided by the TASC TD grid prediction model, designed for the Southern California Coastal Confluence Zone (Ref. 12). This model is calibrated with TD data collected at the land and sea sites shown in Fig. 2.4-2. The secondary phase delay for the land segment of the transmitter (i)-to-receiver signal propagation path is modeled by

$$SF_i = a + b\,R_i + f(c_i, d_i, \beta_i) \qquad (2.4\text{-}1)$$

where

a, b, c_i, d_i = calibrated model coefficients

$f(\,)$ = bearing-dependent function (harmonic series)

R_i = path segment range

β_i = path bearing angle

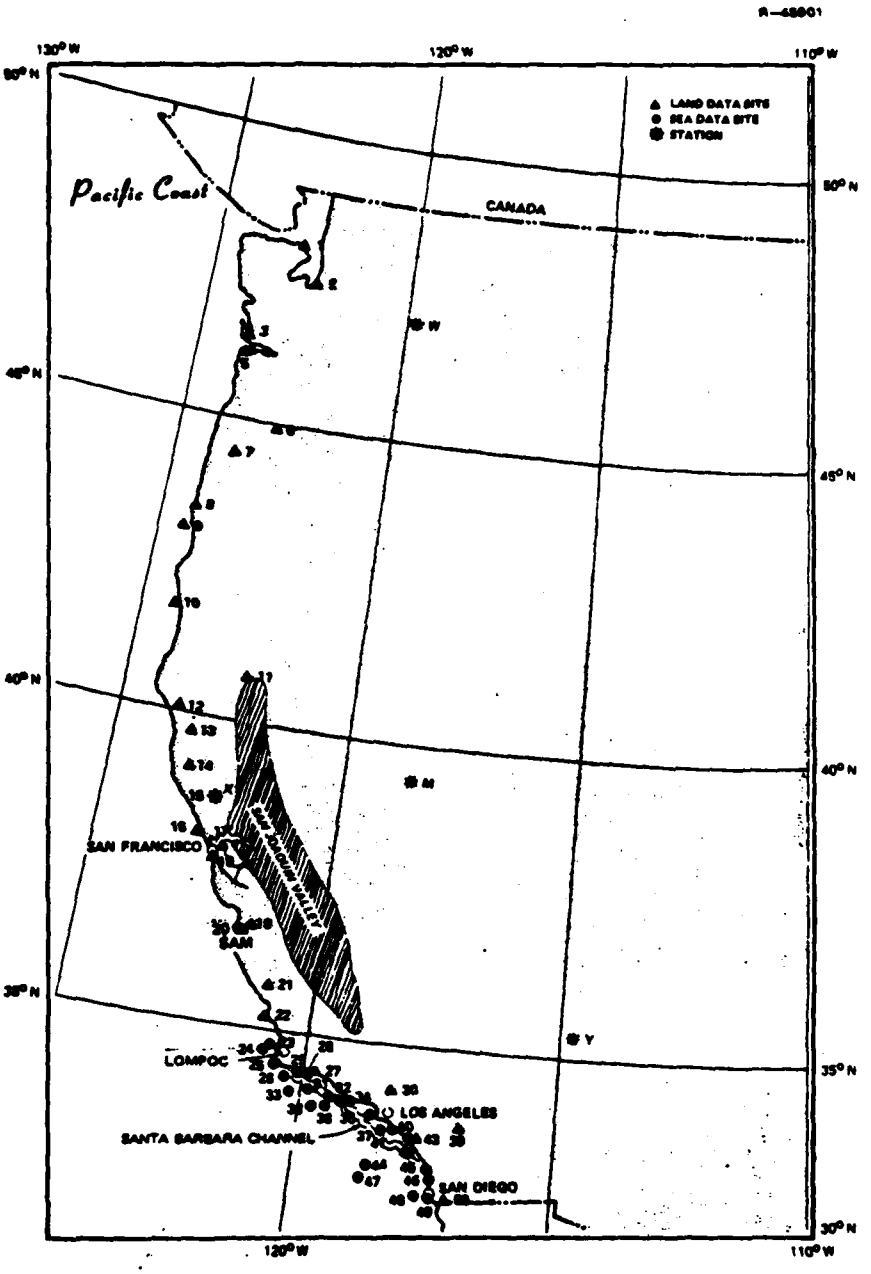

Figure 2.4-2 Data Collection Sites for U.S. West Coast Loran-C Chain Calibration

The secondary phase delay for the sea water path segment is modeled by classical theory, and the total delay is based on Millington's method.

The range/bearing concept is well-suited to marine applications, since it is only necessary to model the land-path SF along the coastline. This results because the Loran-C receiver is on the sea water path segment of a mixed land and sea water propagation path. If the land-path SF is known (i.e., at the coastline), it is straightforward to extrapolate SF to the receiver, using classical theory for the sea-path SF and Millington's method to estimate the total SF. Complex variations in the land-path SF (such as those associated with the San Joaquin Valley; see Fig. 2.4-2) can be modeled by a bearing-dependent function, permitting the range-dependence to be decoupled and kept simple (see Eq. 2.4-1). In applications of Loran-C over land, however, it is necessary to model land-path SF in the entire chain coverage area. Therefore, the model would include a complex function in which range and bearing are strongly coupled, likely imposing significant data collection requirements and model calibration problems. For these reasons, a global operational model, based on the range/bearing concept, is not considered to be a viable alternative to the U.S. Coast Guard model.

It is recommended that the global operational model be based on the U.S. Coast Guard TD grid. If the Loran-C system is selected as a replacement for the VOR/DME system, specific techniques should be developed to compress the U.S. Coast Guard TD grid for efficient storage and to interpolate between the points of the compressed grid for enroute/terminal navigation. Since the U.S. Coast Guard approach is based on a conductivity map, TOA grids can be computed and stored in the same manner as TD grids. Therefore, the approach is applicable to all modes of Loran-C navigation, not just single-chain hyperbolic mode. It is expected that the approach can meet the enroute and terminal accuracy requirements, without the need for a model of temporal and altitude effects. If data

from NAFEC ground and airborne tests indicate that temporal and altitude effects are larger than expected, it may be necessary to appropriately modify the U.S. Coast Guard TD grid.

2.4.2 Local Operational Model

The global operational model discussed in Section 2.4.1 is not expected to meet the accuracy requirements for non-precision approach (0.6 km, 2σ), with the possible exception of airports which exhibit good Loran-C geometry. To obtain the specified accuracy, it may be necessary to design a local operational model for the approach area of each airport. It is considered to be impractical and unnecessary for the local model TD grid to be coincident with the global model TD grid, in the approach area.

The local model can be formulated with a less complex spatial structure than the global model, because it applies to a limited geographic region (i.e., a circle with a 20 km radius). However, in contrast to the global model, the local model should include the effect of temporal TD variations. (Based on data in Refs. 21, 22, and 23, temporal TD variations may exceed 1.0 μsec at certain locations in the chain coverage area.) The recommended local model is characterized by independent temporal and spatial components, as illustrated in Fig. 2.4-3 and defined below:

- A model of temporal TD variations at the airport itself
- A model of spatial TD variations for the airport approach area; the modeled quantity is the difference (assumed constant) between the TDs in the approach area and at the airport.

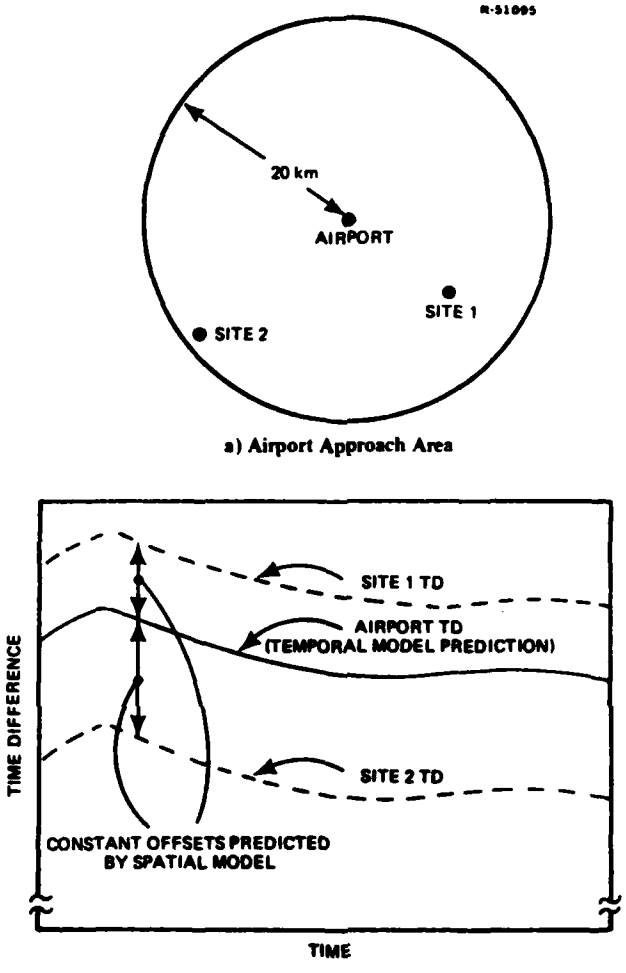

Figure 2.4-3 Definition of Temporal and Spatial Compoments of Local Model

It is possible that the character of spatial TD variations may vary with time, thus requiring a coupling between the temporal and spatial model components.

Local Temporal Model - It is advantageous to choose a local temporal model structure, which is applicable to all airports, and to determine specific model coefficient values for each airport. The amount of TD data required to calibrate the model coefficients can be minimized by employing the

relationship between TDs and physical parameters (e.g., temperature). In particular, if historical data are available for the physical parameters these data can supplement the TD data. Alternatively, the physical parameters can be interpreted as independent variables and updated in real time via physical measurements. However, this is less desirable from an operational viewpoint. The local temporal model described below can be utilized with either historical or real-time data.

The required Loran-C signal propagation parameters (i.e., refractive index, vertical lapse rate, and conductivity) can be expressed in terms of physical parameters. Refractive index (n) is related to surface meteorological parameters in Ref. 25 by

$$n = 1.0 + \left[77.6 \frac{p}{T} + 3730.0 \frac{e_s RH}{T^2} \right] \times 10^{-6} \qquad (2.4\text{-}2)$$

where

p = atmospheric pressure (mbar)
T = absolute temperature (°Kelvin)

RH = relative humidity (percent)

e_s = saturation water vapor pressure (mbar), at temperature T

Historical refractive index data are summarized in Ref. 26, based on National Weather Service meteorological data and Eq. 2.4-2. Available data summaries include seasonal refractive index cycles for certain National Weather Service stations (e.g., see Fig. 2.4-4), and refractive index contour maps for the United States (e.g., see Fig. 2.4-5).

The vertical lapse rate parameter (α) is normally defined in terms of the change in refractive index between the surface and 1.0 km altitude (i.e., the vertical lapse rate or Δn), by the equation

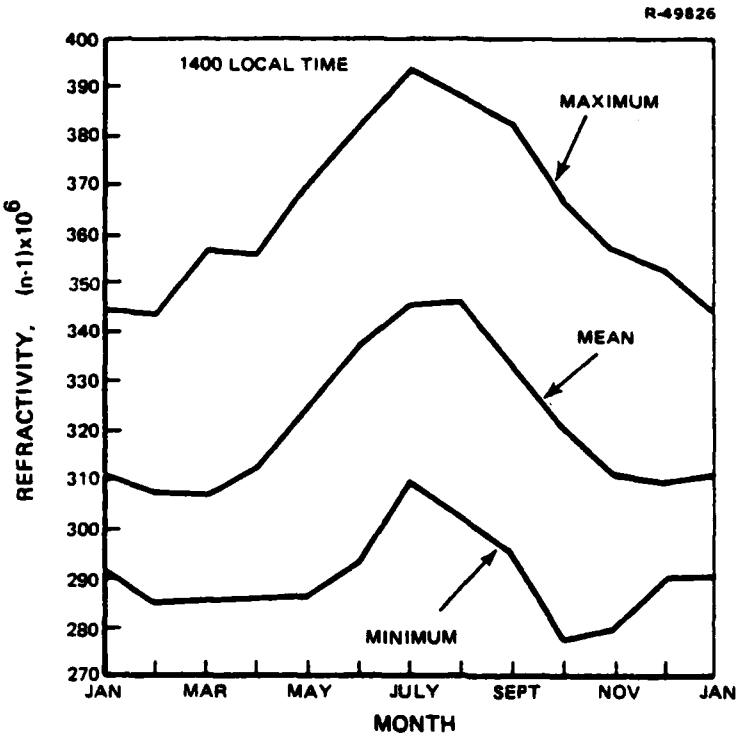

Figure 2.4-4 Seasonal Refractive Index Cycle for Washington, D.C. (Ref. 26)

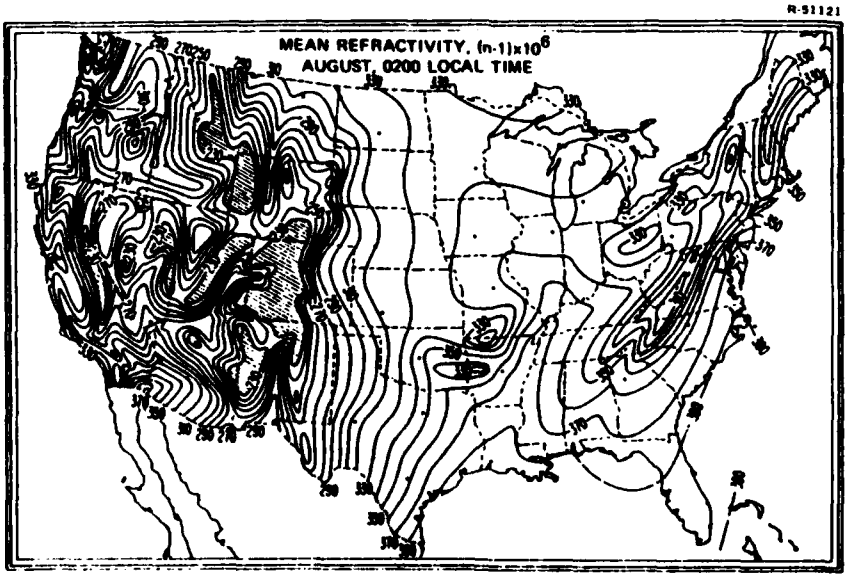

Figure 2.4-5 Refractive Index Contour Map for the United States (Ref. 26)

$$\alpha = 1 + 6378\,\Delta n \qquad (2.4\text{-}3)$$

A radiosonde profile of pressure, temperature, and humidity can be employed in the computation of Δn, using Eq. 2.4-2. Historical vertical lapse rate data, based on National Weather Service radiosonde data, are summarized in Ref. 26. (Examples of vertical lapse rate contour maps for the United States are presented in Fig. 2.4-6.) Although it is preferable to compute

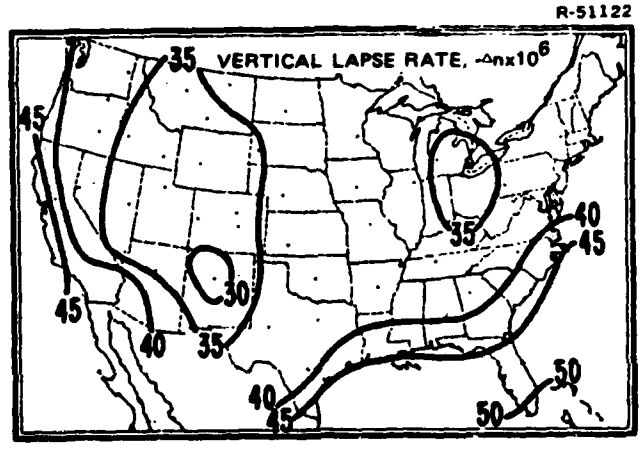

a) January, 0300 Greenwich Mean Time

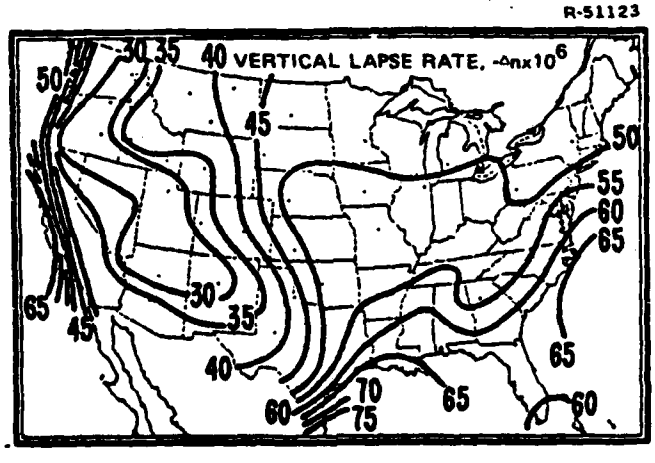

b) July, 0300 Greenwich Mean Time

Figure 2.4-6 Vertical Lapse Rate Contour Maps for the United States (Ref. 26)

the vertical lapse rate from radiosonde data, these data are collected less frequently and at fewer locations than surface meteorological data. However, for most meteorological conditions, the vertical lapse rate is highly correlated with surface refractive index (n). In Ref. 27, the following regression equation is fit to 888 pairs of data from 45 National Weather Service stations:

$$\Delta r = -7.32 \times 10^{-6} \, e^{5577 \, (n-1)} \qquad (2.4\text{-}4)$$

The resulting correlation coefficient (0.93) makes Eq. 2.4-4 very attractive for practical computation of vertical lapse rate.

Ground conductivity, unlike refractive index and vertical lapse rate, can not be related to routinely-measured physical parameters. (Conductivity maps, such as presented in Fig. 2.4-1, are based on physiographic considerations and LF data.) In Ref. 28, the conductivity of soil, σ (mho/m), is expressed in terms of the soil moisture content W (percent by volume) and the soil temperature T (°C) by

$$\sigma = 7.7 \times 10^{-5} \, (0.73 \, W^2 + 1) \, (1 + 0.03 \, T) \qquad (2.4\text{-}5)$$

However, application of Eq. 2.4-5 is complicated by variability in rainwater absorption and by the necessity to account for soil and rock strata as deep as the skin depth (20 m to 200 m; Ref. 29).

Based on the above discussion, it is suggested that the local temporal model include theoretical terms for refractive index and vertical lapse rate, but an empirical term for conductivity. The hypothesized model incorporates the following functional form for propagation delay:

$$\phi_i(t) = \frac{n_i(t)}{c} R_i + 0.00373 \, [\alpha_i(t) - 0.75] \, R_i$$

$$+ [a_i \, R_i \, \sin(2\pi f t + \theta_i) + b_i] \qquad (2.4\text{-}6)$$

where

t = time of year (days)

$\phi_i(t)$ = propagation delay from transmitter i to the airport (μsec)

R_i = transmitter-to-airport path range (km)

c = speed of light in free space (0.30 km/μsec)

$n_i(t)$ = average refractive index along path

$\alpha_i(t)$ = average vertical lapse rate parameter along path

a_i, θ_i, b_i = uncertain coefficients characterizing the effect of conductivity (μsec/km, rad, μsec)

f = seasonal frequency = 1/(365 days)

The refractive index term in Eq. 2.4-6 is simply the primary phase delay (see Eq. 2.2-2); the vertical lapse rate term is based on a linearization of the classical theory secondary phase delay (see Fig. 2.2-3); and the conductivity term is empirical with a sinusoidal time dependence. The following remarks apply to the calibration and utility of the model:

- The time functions $n_i(t)$ and $\alpha_i(t)$ are computed from historical or real-time meteorological data (e.g., see Figs. 2.4-3, 2.4-4, and 2.4-5)
- The coefficient (0.00373) in the vertical lapse rate term is based on a nominal conductivity of 0.005 mho/m, and may alternatively be replaced by an uncertain coefficient

- The uncertain model coefficients are calibrated using seasonal TD data collected at the airport
- The sinusoidal structure for the conductivity term is subject to modification based on data
- The coefficient values are generally transmitter- and airport-dependent
- The TD model consists of Eq. 2.2-7, with Eq. 2.4-6 substituted for propagation delays; propagation delay models are required for the secondary and master transmitters, for both the airport and the SAM
- Only certain aggregates of model parameters can be calibrated with TD data; specifically, the parameters for master and secondary paths can not be isolated (see Section 4.3.5)
- The model is only applicable to single-chain hyperbolic mode when calibrated with TD data from the chain; models for two TDs (e.g., TDX and TDY) can be subtracted to obtain a model for the master-independent mode.

Techniques for calibrating the model coefficients are discussed in Chapter 4.

Local Spatial Model - The local spatial model, as indicated in Fig. 2.4-3, is employed to extrapolate from the airport TD (given by the local temporal model) to the TD at each location in the airport approach area. The extrapolation is assumed to be constant in time, a simplification which is expected to be compatible with non-precision approach accuracy requirements, but must be verified with collected data.

The proposed local spatial model is a semi-empirical model, and is based on the coordinate system shown in Fig. 2.4-7.

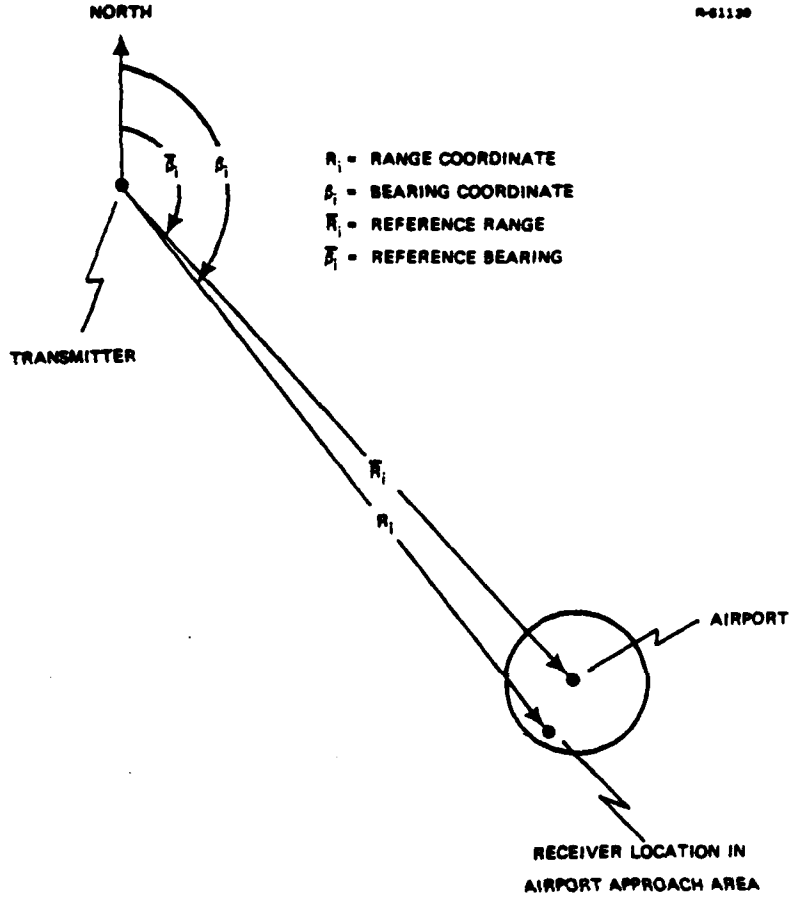

Figure 2.4-7 Range/Bearing Coordinate System for Local Spatial Model

The coordinates are the <u>transmitter-to-receiver</u> range (R_i) and bearing (β_i), where the reference range (R_i) and bearing (β_i) are those associated with the airport itself. This coordinate system is selected because Loran-C signal propagation paths are radials from the transmitter to the receivers. Signal propagation theory can be used to greater advantage in a transmitter-oriented coordinate system, than it can in an airport-oriented coordinate system (e.g., where the coordinates

are the airport-to-receiver range and bearing). If an airport-oriented coordinate system were employed, an empirical model would be more appropriate.

The local spatial model incorporates the following functional form for propagation delay:

$$\Delta\phi_i = \left\{ \frac{n_i}{c} + 0.00373\ (\alpha_i - 0.75) + \xi_i + d_i\ (\beta_i - \beta_i) \right\} [R_i - R_i] \qquad (2.4\text{-}7)$$

where

$\Delta\phi_i$ = difference between propagation delays from transmitter i to the receiver, and to the airport (μsec)

R_i, $\bar{R}_i$ = ranges defined in Fig. 2.4-7 (km)

β_i, $\bar{\beta}_i$ = bearings defined in Fig. 2.4-7 (rad)

c = speed of light in free space (0.30 km/μsec)

n_i = average refractive index along path

$\bar{\alpha}_i$ = average vertical lapse rate parameter along path

ξ_i, d_i = uncertain coefficients characterizing the effect of conductivity (μsec/km, μsec/km/rad)

The following remarks apply to the calibration and utility of the model:

- The values of n_i and α_i are selected as the annual mean values of $n_i(t)$ and $\alpha_i(t)$, from historical meteorological data
- The uncertain model coefficients are calibrated using spatial TD data collected in the airport approach area

- The linear structure for the conductivity term is subject to modification based on data
- The coefficient values are generally transmitter- and airport-dependent
- It may be necessary to augment the model to include a term which is linear in altitude, depending on the results of airborne tests
- The TD at a receiver location in the airport approach area is predicted by adding the quantity $\Delta\phi_i - \Delta\phi_m$ (for secondary i and master m) to the TD predicted by the local temporal model.
- All model parameters can be calibrated with TD data, due to the observability afforded by collecting TD data at various ranges and bearings (Refs. 11 and 12); if bias parameters are included in the model, only the difference between secondary and master biases can be calibrated
- The model is applicable to any Loran-C navigation mode, even though it is calibrated with TD data; the only terms of the model which are needed are those associated with the relevant Loran-C stations.

For most airport locations, the sector of bearing angles subtended by the airport approach area is very narrow. For example, if the airport is greater than 200 km from the transmitter, the sector is less than 0.2 rad (12 deg) wide. It is likely that the bearing dependence included in Eq. 2.4-7 is negligible for narrow sectors -- i.e., d_i is relatively small. In this case, the effect of conductivity is characterized by ξ_i, which is termed the "Loran-C scale factor."

The Loran-C scale factor depends on the slope of the secondary phase delay curve over the range interval relevant to the particular transmitter and airport approach area. For example, if the propagation paths from the transmitter to the airport approach area are all-land paths with homogeneous conductivity, the scale factor is given by the slope of the appropriate secondary phase delay curve in Fig. 2.2-2. The propagation paths for other airports may be mixed land/sea water or sea water/land. In these cases, the scale factor is given by the slope of the appropriate secondary phase delay curve in Fig. 2.2-5 or 2.2-6. The slope depends primarily on the conductivity of the land path segment and on the range from the airport to the coastline (in the transmitter direction). This dependence is illustrated in Fig. 2.4-8, where secondary phase delay is plotted relative to its value at the coastline for a land/sea water path. The slopes of the curves depend on land conductivity for coastline-to-airport ranges less than 200 km. However, for ranges greater than 200 km, the curves approach a common slope -- the slope for an all sea water path.

2.5 LORAN-C SENSITIVITY MODELS FOR SELECTION OF DATA COLLECTION SITES

A plan is proposed in Chapter 3, whereby NAFEC can collect Loran-C data to calibrate and refine the local operational models presented in Section 2.4.2. Specifically, Loran-C receivers are to be placed at certain fixed sites, to monitor temporal TD variations for a year, and on a mobile test van, to monitor spatial TD variations in the approach areas of several airports. The fixed-site and mobile-site data will be employed in analyses of local temporal models and local spatial models, respectively.

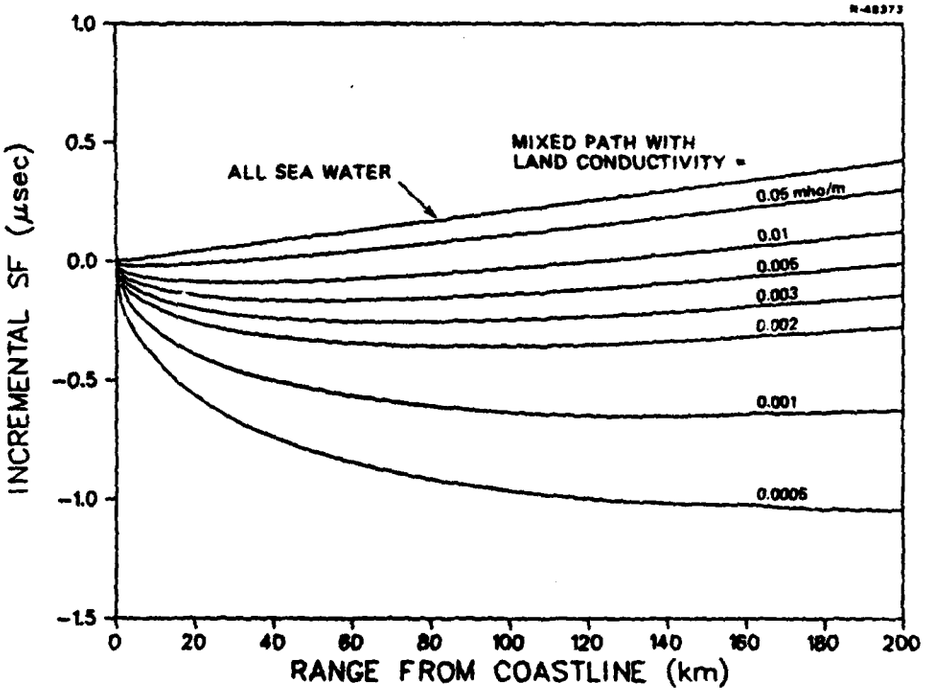

Figure 2.4-8 Secondary Phase Delay (Relative to the Value at the Coastline) on the Sea Water Path Segment of a Mixed Propagation Path

Sensitivity models have been developed to aid NAFEC in selecting fixed and mobile data collection sites. The models are intended to characterize TD variations (temporal or spatial) in terms of propagation parameter variations. Data collection sites should be selected in regions where the predicted TD variations are largest, so as to maximize the observability of model coefficients.

2.5.1 Temporal Sensitivity Model

The purpose of the temporal sensitivity model is to indicate those regions of the Loran-C chain coverage area which exhibit the largest temporal TD variations. The intent

is to predict the sensitivity of temporal TD variations to signal propagation parameter variations, rather than to predict the temporal variations themselves. To meet this objective with a simple model, the following assumptions are made:

- The Loran-C chain coverage area is homogeneous in refractive index, vertical lapse rate, and conductivity
- The nominal value of conductivity is 0.005 mho/m and variations about the nominal are less than ±0.002 mho/m
- The model is only employed to compare temporal TD variations at locations greater than 200 km from the Loran-C transmitters.

Under these assumptions, the temporal variation in propagation delay, induced by temporal variations in propagation parameters, is

$$\delta\phi_i(u) = [3.33\ \delta n + 0.00373\ \delta\alpha - 0.173\ \delta\sigma]\ R_i(u) \qquad (2.5\text{-}1)$$

where

$\delta\phi_i(u)$ = temporal variation in the propagation delay from transmitter i to the user location u

$R_i(u)$ = transmitter-to-user range

δn, $\delta\alpha$, $\delta\sigma$ = temporal variations in n, α, and σ; $\delta\sigma$ is in units of mho/m

Equation 2.5-1 is derived by linearizing Eq. 2.2-2 about nominal values of vertical lapse rate (α = 0.75) and conductivity (σ = 0.005 mho/m). The coefficients for the vertical lapse rate and conductivity terms differ from those in Eq. 2.5-1, if different nominal parameter values are selected.

By employing Eqs. 2.2-7 and 2.5-1, the TD variation may be expressed by

$$\delta TD_i(u) = [\delta\phi_i(u) - \delta\phi_m(u)] - [\delta\phi_i(s) - \delta\phi_m(s)]$$

$$= [3.33\ \delta n + 0.00373\ \delta\alpha - 0.173\ \delta\sigma] \times [R_i(u) - R_m(u)] - [R_i(s) - R_m(s)] \quad (2.5\text{-}2)$$

where i and m denote the secondary and master transmitters, respectively, and u and s denote the user and SAM locations, respectively. Knowledge of the statistics of propagation parameter variations is not required to apply Eq. 2.5-2. The equation defines the sensitivity of TD variations to arbitrary propagation parameter variations. TD sensitivity is zero along the hyperbolic LOP which passes through the SAM, and increases with increasing "double range difference," the quantity in braces in Eq. 2.5-2.

TD sensitivity predictions are illustrated for TDW for the Northeast U.S. Loran-C chain, in Fig. 2.5-1. The hyperbolic LOPs are labeled with the associated double range difference. Temporal sensitivity is zero along the hyperbolic LOP which passes through Cape Elizabeth, Maine -- the controlling SAM for TDW. Temporal sensitivity curves for TDX, TDY, and TDZ, for the Northeast U.S. chain, are presented in Chapter 3.

2.5.2 Spatial Sensitivity Model

The purpose of the spatial sensitivity model is to indicate those directions in the airport approach area which exhibit the greatest TD sensitivity to uncertainty in the Loran-C scale factor (defined in Section 2.4.2). The model is based on the following assumptions:

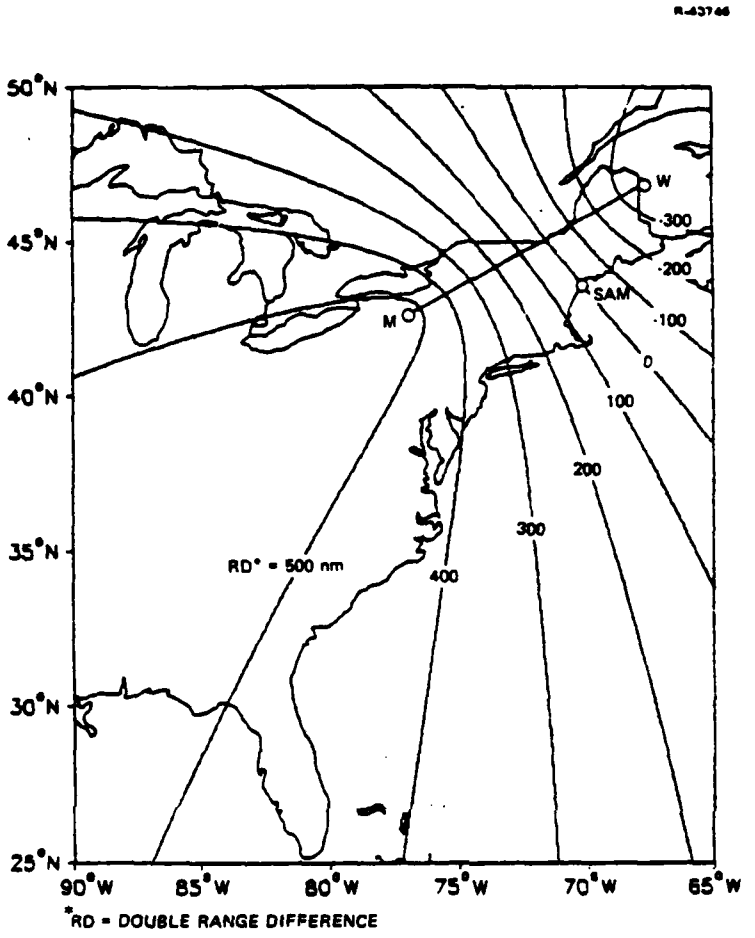

Figure 2.5-1 Temporal Variation Sensitivity for the Northeast U.S. Loran-C Chain (TDW)

- The scale factors for the secondary and master paths may be different, but their variances (uncertainties) are equal; i.e., var ξ_i = var ξ_m
- The secondary and master scale factors are correlated with correlation coefficient ρ.

It can be shown that the corresponding TD variance is expressed by the equation

$$\text{var } TD_i = [(1 + \rho)(1 - \cos\theta)\, x^2 + (1 - \rho)(1 + \cos\theta)\, y^2]\ \text{var } \xi_i \qquad (2.5\text{-}3)$$

where

x, y = coordinates indicating the Loran-C user location in the airport approach area (see Fig. 2.5-2)

θ = angle subtended by the secondary and master paths at the airport (see Fig. 2.5-2).

Equation 2.5-3 indicates that the sensitivity of the TD variance to the scale factor variance (i.e., var TD_i/var ξ_i) is constant on ellipses centered at the airport.

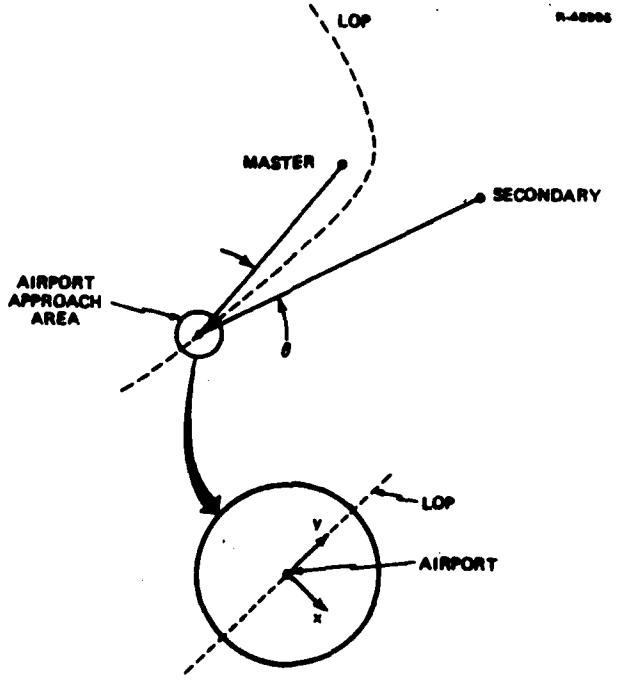

Figure 2.5-2 Coordinate System for Spatial Sensitivity Model

The orientation of the elipses depends on the correlation coefficient ρ and the secondary/master subtended angle θ, in the manner indicated in Fig. 2.5-3. The "switching curve," defined by the equation $\rho = \cos \theta$, partitions the p-θ plane into two regions. Above the switching curve, the major axis of the ellipse is aligned with the hyperbolic LOP which passes through the airport, while below the switching curve, the major axis is perpendicular to the LOP. The major axis of the ellipse does not switch discontinuously; rather, the ellipses degenerate to circles for p-θ pairs on the switching

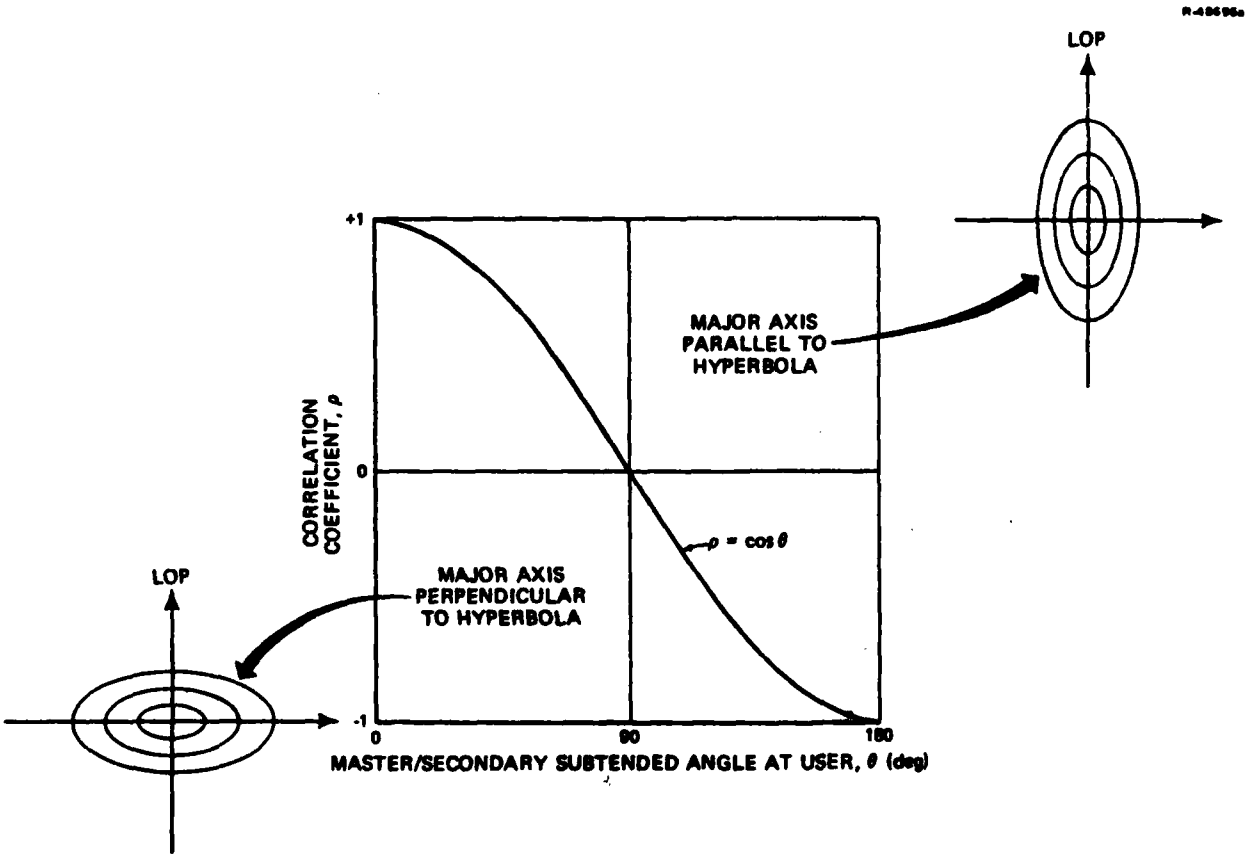

Figure 2.5-3 Orientation of Elliptical Contours Predicted by Spatial Sensitivity Model

curve. Generally, ρ is positive and increases with decreasing θ (secondary and master paths overlap for θ = 0 deg), thereby resulting in elliptical contours with major axes aligned with the LOP. In this case, it is advantageous to cluster the mobile data collection sites along the perpendicular to the LOP, since this is the direction of maximum TD sensitivity. The utility of the spatial sensitivity model in the selection of data collection sites is discussed further in Chapter 3.

2.6 LORAN-C SIGNAL AMPLITUDE MODEL

As with the phase of the LF groundwave, signal amplitude is also a complex function of the propagation medium. The most common procedure for evaluating these effects is through use of classical theory which assumes a homogeneous propagation medium. Based on this approach, the Loran-C signal amplitude can be calculated as a function of range from the transmitter (assumed to be a vertical electric dipole) for various values of ground conductivity and vertical lapse rate.

The signal amplitude model is based on classical theory curves of amplitude versus range, which are parametric in conductivity and peak transmitter power. Vertical lapse rate is not a critical factor for the range of parameters considered (Ref. 5). The classical theory signal amplitude predictions (Ref. 5) are depicted in Fig. 2.6-1 as a function of range from the transmitter. These curves are for a vertical dipole of 1.0 amp-meter and correspond to an assumed vertical lapse rate parameter (α) of 0.75. Over a range of one to 900 nm, the set of curves depicted in Fig. 2.6-1 can be least-squares fit to the expression:

$$S = 106.6 - 20 \log_{10} R - \alpha R^{\beta} + 10 \log_{10} P \qquad (2.6\text{-}1)$$

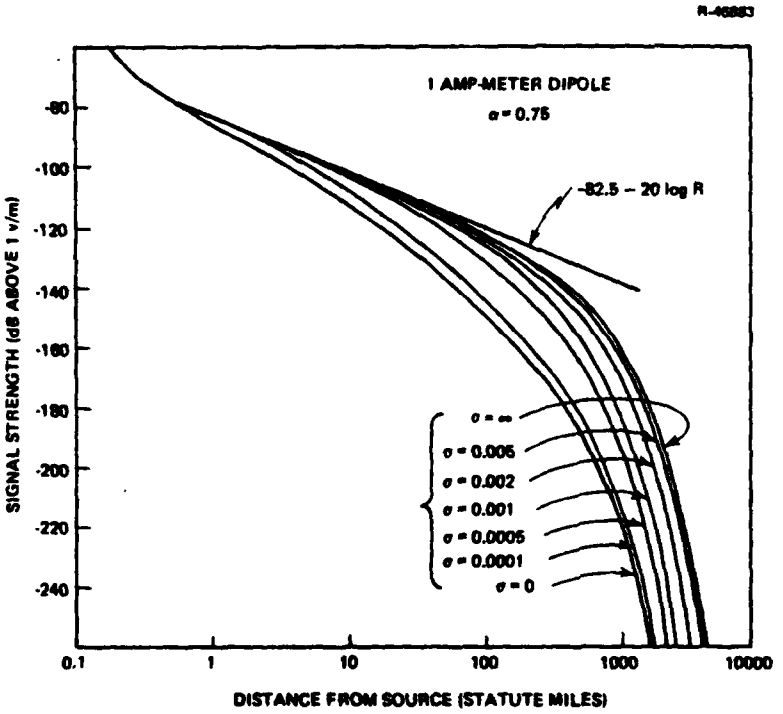

Figure 2.6-1 Amplitude of Loran-C Groundwave (Classical Theory; Ref. 5)

where

S = signal strength (dB relative to 1μv/m)

R = distance from transmitter (nm)

P = peak transmitter power (kw)

σ = ground conductivity (mho/m)

The parameters α and β are defined as a function of ground conductivity in Table 2.6-1. Over the range of parameters defined in Fig. 2.6-1, the model has a 1.6 dB rms error and a 5.8 dB maximum error. The maximum error occurs at long range and low conductivity, which would be representative of a long propagation path consisting of glacial ice and is, in general, not critical for the current study. In addition, based on measurements of the variation in actual signal strength for

TABLE 2.6-1

PARAMETER VALUES FOR LORAN-C SIGNAL AMPLITUDE MODEL

T-3469

GROUND CONDUCTIVITY RANGE	a	β
Glacial Ice: $\sigma < 6 \times 10^{-5}$	3.11	0.465
Land: $6 \times 10^{-5} \leq \sigma \leq 2 \times 10^{-2}$	$1.69 \times 10^{-6}\ \sigma^{-1.475}$	$0.398 \log_{10}\sigma + 2.156$
Seawater: $\sigma > 2 \times 10^{-2}$	-7.580×10^{-4}	1.466

the St. Marys River chain (Ref. 11), this modeling error is not significant. For mixed conductivity paths, Millington's method is applicable with amplitude dependence (in dB units) replacing phase dependence in Eq. 2.2-3.

In general, Loran-C receiving equipment does not generate an estimate of signal strength, but rather an estimate of signal-to-noise ratio. To supply data consistent with this output, CCIR noise tables (Ref. 30) can be used to give averages of expected noise for various seasons. Noise in the Loran-C frequency band, primarily due to local thunderstorms, has significant high-frequency content and cannot, in general, be predicted except for these average values. Signal-to-noise ratios are desired for two sites (see Chapter 3) where data will be continually collected. These are London, KY and Buffalo, NY. Based on the signal amplitude model previously presented, Table 2.6-2 lists the estimated signal strength at these two locations for each transmitter in the Northeast chain, assuming a ground conductivity of 0.005 mho/m. A 24-hour average of the seasonal median noise at the two sites is listed in Table 2.6-3. These data are from Ref. 30 and assume a 45 kHz bandwidth for the Loran-C receivers. Based on the data in Tables 2.6-2 and 2.6-3, adequate signal-to-noise ratio should be available at both sites (see Table 2.6-4). A

TABLE 2.6-2

ESTIMATED SIGNAL STRENGTH

TRANSMITTER	SIGNAL STRENGTH (dB relative to 1 μv/m)	
	LONDON, KY	BUFFALO, NY
Seneca, NY (Master)	74.0	98.5
Caribou, ME (W)	52.5	67.5
Nantucket, MA (X)	60.0	72.5
Carolina Beach, NC (Y)	78.0	71.0
Dana, IN (Z)	81.5	71.5

TABLE 2.6-3

SEASONAL MEDIAN NOISE (24-HR AVERAGE)

SEASON	NOISE LEVEL* (dB relative to 1 μv/m)	
	LONDON, KY	BUFFALO, NY
Winter (Dec-Feb)	25.5	24.5
Spring (Mar-May)	37.5	34.5
Summer (June-Aug)	43.5	40.5
Fall (Sept-Nov)	33.5	31.5

*For a 45 kHz receiver bandwidth.

TABLE 2.6-4a

ESTIMATED SIGNAL-TO-NOISE RATIO
FOR SENECA TRANSMITTER

SEASON	SIGNAL-TO-NOISE RATIO (dB relative to 1 μv/m)	
	LONDON, KY	BUFFALO, NY
Winter	48.5	74.0
Spring	36.5	64.0
Summer	30.5	58.0
Fall	40.5	67.0

TABLE 2.6-4b

ESTIMATED SIGNAL-TO-NOISE RATIO
FOR CARIBOU TRANSMITTER

SEASON	SIGNAL-TO-NOISE RATIO (dB relative to 1 μv/m)	
	LONDON, KY	BUFFALO, NY
Winter	27.0	43.0
Spring	15.0	33.0
Summer	9.0	27.0
Fall	19.0	36.0

TABLE 2.6-4c

ESTIMATED SIGNAL-TO-NOISE RATIO
FOR NANTUCKET TRANSMITTER

SEASON	SIGNAL-TO-NOISE RATIO (dB relative to 1 μv/m)	
	LONDON, KY	BUFFALO, NY
Winter	34.5	48.0
Spring	22.5	38.0
Summer	16.5	32.0
Fall	26.5	41.0

TABLE 2.6-4d

ESTIMATED SIGNAL-TO-NOISE RATIO
FOR CAROLINA BEACH TRANSMITTER

SEASON	SIGNAL-TO-NOISE RATIO (dB relative to 1 μv/m)	
	LONDON, KY	BUFFALO, NY
Winter	52.5	46.5
Spring	40.5	36.5
Summer	34.5	30.5
Fall	44.5	39.5

TABLE 2.6-4e

ESTIMATED SIGNAL-TO-NOISE RATIO
FOR DANA TRANSMITTER

SEASON	SIGNAL-TO-NOISE RATIO (dB relative to 1 μv/m)	
	LONDON, KY	BUFFALO, NY
Winter	56.0	47.0
Spring	44.0	37.0
Summer	38.0	31.0
Fall	48.0	40.0

comparison of predicted signal-to-noise ratio to measured signal-to-noise ratio will be made as part of the data analysis.

2.7 SUMMARY OF LORAN-C MODELS

The features of the Loran-C models discussed in this chapter are:

Global Operational Model - Employed for navigation in enroute and terminal flight phases; recommended to be based on the U.S. Coast Guard model predictions

Local Operational Model (Temporal) - Employed for navigation in non-precision approach flight phase; characterizes temporal TD variations at the airport itself (see Eq. 2.4-6)

Local Operational Model (Spatial) - Employed for navigation in non-precision approach

flight phase; characterizes spatial TD variations within 20 km of the airport (see Eq. 2.4-7)

Temporal Sensitivity Model - Employed to identify candidate locations for fixed-site monitors, for collection of temporal Loran-C data; approximates temporal TD variations as being constant on hyperbolas (see Eq. 2.5-2 and Fig. 2.5-1)

Spatial Sensitivity Model - Employed to identify candidate locations for test van sites, for collection of spatial Loran-C data near airports; approximates spatial TD uncertainty as being constant on ellipses (see Eq. 2.5-3 and Fig. 2.5-3)

Signal Amplitude Model - Employed with an atmospheric noise model to predict signal-to-noise ratio; characterizes the classical theory signal amplitude predictions by a simple equation (see Eq. 2.6-1).

These models provide a framework, which the FAA can use to plan Loran-C data collection efforts and specify airborne receiver capabilities.

3. LORAN-C DATA COLLECTION PLAN

3.1 INTRODUCTION

To properly assess the validity of proposed computer models, data must be collected which will allow subsequent identification of key parameters of proposed models. This requires a strong interaction between the model development and data collection plan. In addition, it is necessary to recognize the intended scope of the data collection effort and objectives of the overall project. As a result, the data collection plan is structured to support achievement of the following goals:

- Development of mathematical models to characterize the temporal variation in Loran-C signal phase and amplitude
- Evaluation of the operational adequacy of Loran-C signals, in terms of susceptibility to noise and interference effects, in the ground environment of a number of airports.

The data collection plan has evolved as a two step process. An initial data collection plan (Ref. 31) proposed data collection procedures to enable NAFEC to collect data to provide an assessment of Loran-C. After the computer models discussed in Chapter 2 were developed, the initial data collection plan was revised and expanded to better support computer model validation and long-term assessment of Loran-C signal propagation variation. A summary of the original data collection plan and the modifications recommended by TASC are documented in Ref. 3. Implementation of the modified data collection

plan, will result in a set of data to provide an initial quantitative assessment of Loran-C for application to civil aircraft navigation. The modified data collection plan is summarized in this chapter.

3.2 DATA COLLECTION PROCEDURES

Model development is supported by two specific data collection procedures:

- TD data collection at various sites within 20 km of the NAFEC airport and four additional airports
- Data collection at two fixed-site monitors to continually collect Loran-C TD information.

High density data near airports are required because the accuracy requirement in this region is the most stringent. In particular, this is the region where the non-precision approach accuracy requirements of the AC-90-45A specification apply. The intent of this portion of the data collection plan is to be able to determine if local spatial models will be required as part of the local operational model for the approach region of each airport and, if so, to utilize collected data to support development of these models. To assess seasonal temporal variations in these models, data will be collected at each airport four times a year. This will determine if the parameters of the local spatial model have a temporal dependence which cannot be accounted for in the local temporal model. Assessment of temporal dependence is important for future data collection efforts. If results indicate minimal temporal variation in spatial model parameters, spatial models (if required at all) could be formulated by collecting data once at each airport.

It is desirable to minimize the effects of diurnal variations in the collected data. This is accomplished by placing a second receiver at the airport itself to monitor temporal TD variations during the data collection period. The measured temporal variation from the stationary receiver can be applied as a correction to data measured at sites surrounding the airport. This correction is valid if temporal and spatial variations can be decoupled, as assumed in development of the local model. A second benefit of the stationary receiver is that a data base is established to assess the accuracy of differential Loran-C for the non-precision approach phase. The correction from the stationary receiver is equivalent to the correction that would be provided by a differential Loran-C pattern monitor.

The intermittent nature of the data collection procedures limits the utility of collected data in the assessment of possible seasonal variations in the Loran-C grid and therefore has limited utility in developing local temporal models. The data required to assess long-term seasonal variations due to changes in the Loran-C signal propagation medium is acquired from two fixed-site monitors. Time difference data are automatically recorded once every 15 min at each site. This high-frequency data record provides a clear history of Loran-C TDs and possibly allows TD variations due to atmospheric noise and chain and receiver malfunctions to be separated from variations due to changes in the propagation medium.

The primary purpose of the fixed-site monitor data is to establish the required complexity of the temporal portion of the local operational model. Calibration of the local temporal model involves establishment of cause and effect relationships for secondary phase delay variations. Additional purposes of this data are to determine if a non-temporal global

operational model is adequate and to assess the validity of the homogeneous and linear assumptions utilized in the development of the sensitivity model. Table 3.2-1 summarizes the utility of the different data to be collected.

The data collection procedures described above are directed at TD measurements for the following reasons:

- The data collection procedures are designed to support an initial assessment of the utility of Loran-C in the U.S. National Airspace System
- Single-chain hyperbolic mode is expected to be the primary navigation mode implemented in most low-cost airborne Loran-C receivers
- The additional information provided by TOAs in the initial assessment of Loran-C does not warrant the increase in experimental cost and complexity associated with proper TOA data collection (Ref. 47).

The applicability of the calibrated propagation models to master-independent, ranging, and dual-chain Loran-C navigation modes is discussed in Section 2.4. Although it is not recommended that TOA data be collected for analysis purposes, it is suggested that the Austron 5000 be interfaced with a cesium beam oscillator when not being used for tests at NAFEC. Time series plots of TOAs can be observed by NAFEC personnel to gain experience with TOA data, in the event that such data are collected for analysis purposes in the future.

The second portion of the data collection plan addresses the operational adequacy of Loran-C signals. For this aspect of the data collection plan, operational adequacy is defined in terms of receiver susceptibility to atmospheric

TABLE 3.2-1

UTILITY OF LORAN-C DATA FOR MODEL CALIBRATION AND VALIDATION

T-3482

TYPE OF DATA	APPLICATION	UTILIZATION
Fixed-Site Monitor Data	Global Operational Model	Determine if a non-temporal model is adequate.
	Local Operational Model (Temporal)	Calibrate temporal portion of the local model.
	Temporal Sensitivity Model	Assess the validity of homogeneous and linear assumptions.
	Cross-Correlation Analyses	Establish cause and effect relationship in Loran-C temporal variations. Examine correlations between variations in different TD.
Mobile-Site (Test-Van) Data	Local Operational Model (Spatial)	Calibrate the spatial portion of the local model. Determine if spatial portion of model has a temporal dependence.
	Differential Loran-C Analyses	Data from second local-site receiver will minimize temporal variations over data collection period, and enable an assessment of differential Loran-C concepts.

noise and RFI. A high-quality receiver (Austron 5000) and an average-quality receiver (Micrologic ML-220) are tested in this regard, with the understanding that atmospheric noise and RFI may influence other types of receivers differently. To assess operational adequacy, RFI and noise measurements will be made at NAFEC and four additional airports. The effects of RFI and noise are ascertained through use of a spectrum analyzer and associated support equipment and receiver-generated estimates of signal-to-noise ratio. Details of these tests are presented in Ref. 31.

The RFI and noise measurements are intended to validate that Loran-C signal quality is adequate to enable tracking of Loran-C signals while on the ground in preparation for flight. This assumes that the ground-based operations will encounter the most significant signal interference. One goal of this portion of the test is to determine the susceptibility of the Loran-C receiver to airport-related emissions. To accomplish this, measurements will be made with Loran-C receiver equipment located at or near the following items in the vicinity of the five test-site airports:

- VORTAC
- Glideslope (ILS)
- Localizer (ILS)
- Marker Beacons
- Compass Locater
- Airport Surveillance Radars
- UHF/VHF Communications
- Metal Hangers and Other Structures
- Airport Ground Traffic
- Local Power Lines.

There is a dichotomy between the RFI and local data collection requirements. For the former, the presence of RFI is "desirable" in order to ascertain its effect on Loran-C receivers, while for the latter, since propagation effects are of interest, a minimum amount of RFI is desired. To resolve this difference, RFI measurements should be initially made without any receiver filtering of RFI. Then RFI filtering should be employed to determine if the effects of RFI can be minimized. If the latter cannot be accomplished, data for

local model validation should not be collected in the immediate vicinity of the airport in question.

3.3 LORAN-C DATA COLLECTION AREAS

In addition to the data collection procedures defined in the previous section, specific data collection areas for the fixed-site monitor locations and the four airports for the spatial variation study have been identified. The data collection areas are critical because different locations display different sensitivity to variations in Loran-C related parameters. The primary factor in site selection is the relative position of the test site to individual transmitters and SAMs for the Northeast chain. Location relative to the transmitters and SAMs is important because, if the propagation medium is homogeneous, Loran-C TD sensitivity is proportional to the double range difference at the test site. TD data collected at a test site on the hyperbolic LOP which passes through the SAM is expected to display minimal seasonal variations.

Since the purpose of data collected from the fixed-site monitors is to identify Loran-C seasonal variations, it is desirable to choose fixed-site monitor locations which display a high TD sensitivity to propagation parameter variations. This is accomplished by selecting a monitor site that has a large double range difference between the monitor site and SAM (see Section 2.5.1). Based on the temporal sensitivity model, TD sensitivities for the four TDs of the Northeast chain are illustrated in Figs. 3.3-1 to 3.3-4. Table 3.3-1 summarizes TD sensitivities for six regions. Based on these results, the two fixed-site monitors are recommended to be located at Flight Service Stations in Buffalo, NY and London, KY. Before any fixed-site monitor is established, the NAFEC test van will

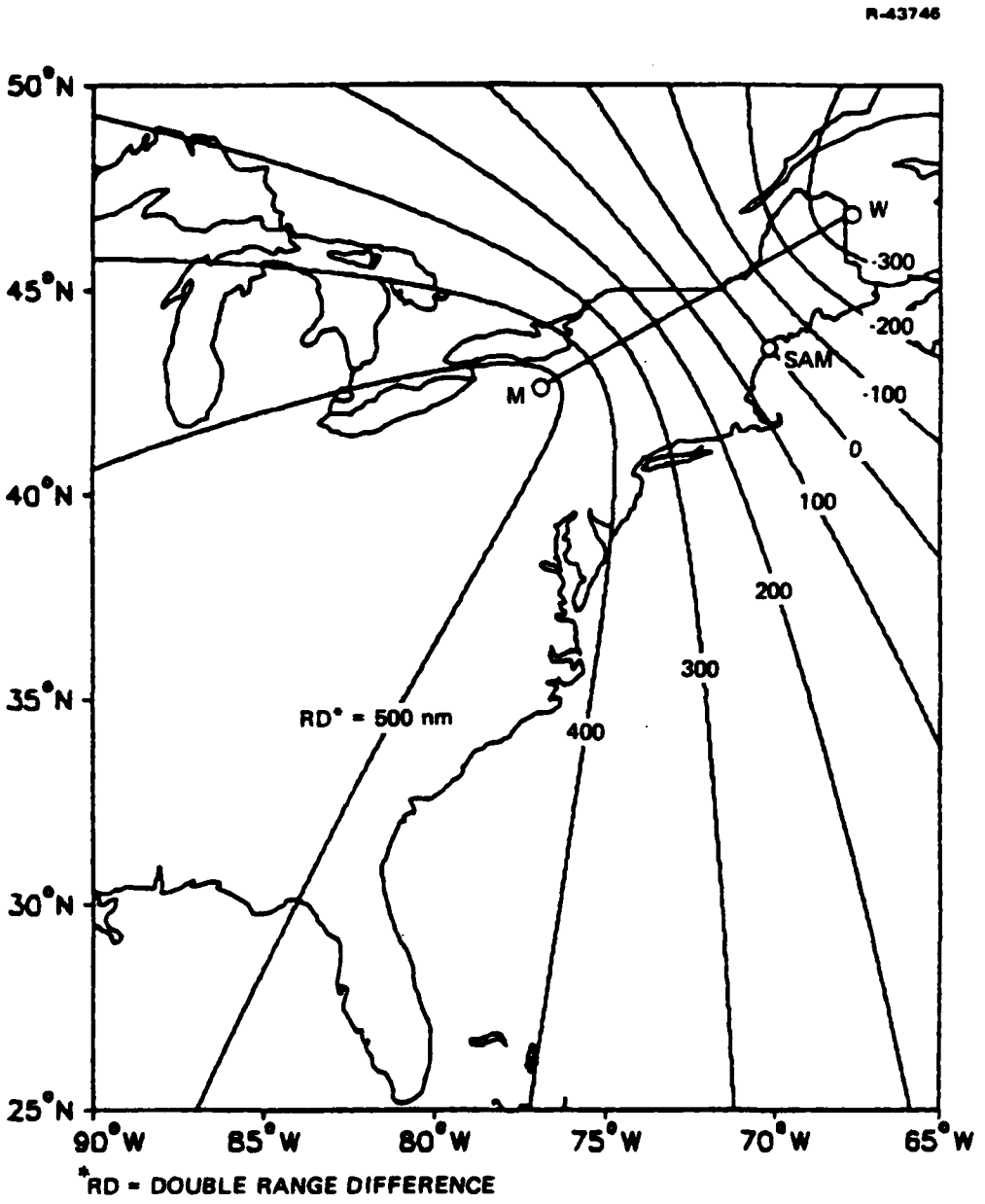

Figure 3.3-1 Temporal Variation Sensitivity for Northeast Chain (TDW)

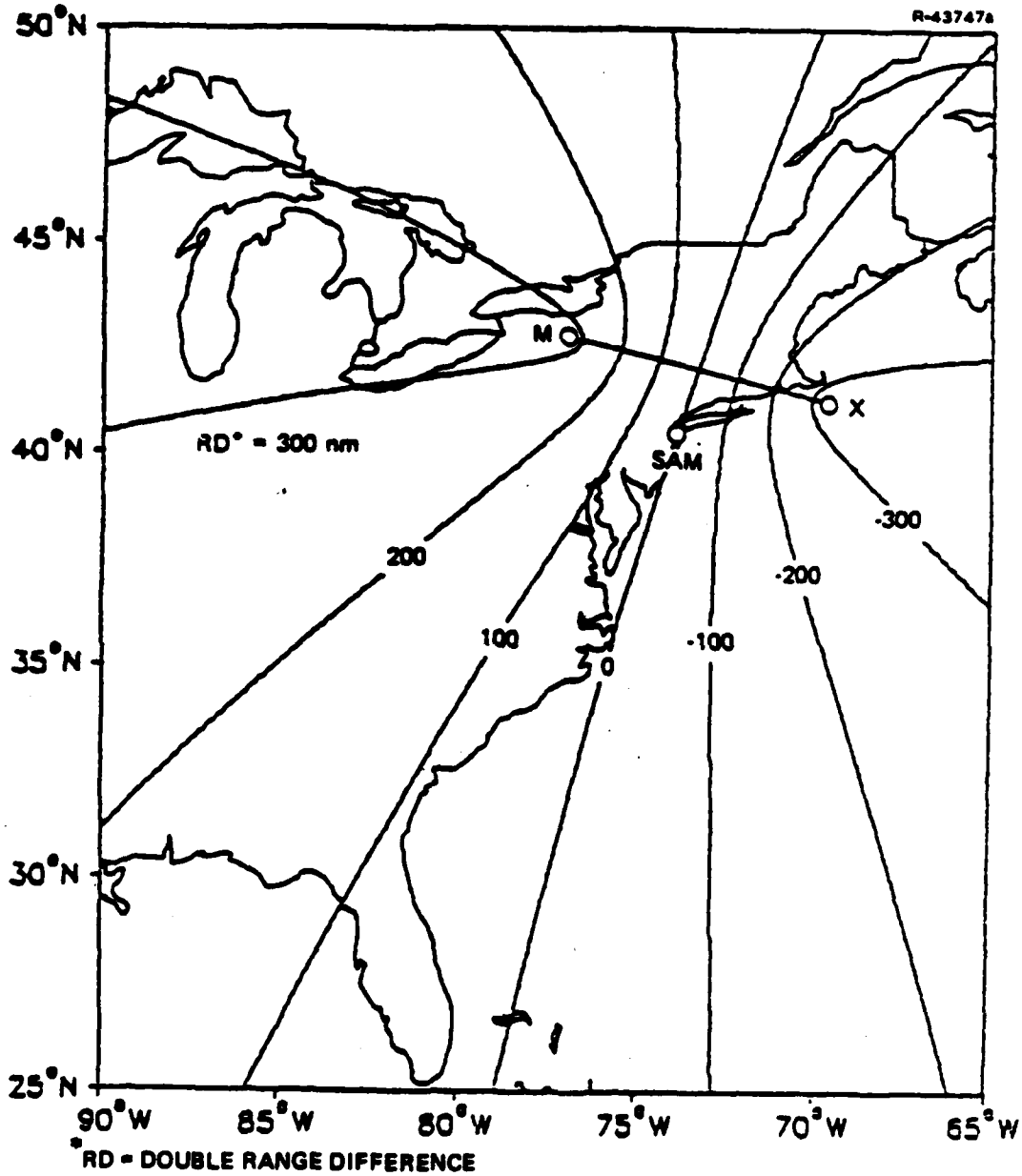

Figure 3.3-2 Temporal Variation Sensitivity for Northeast Chain (TDX)

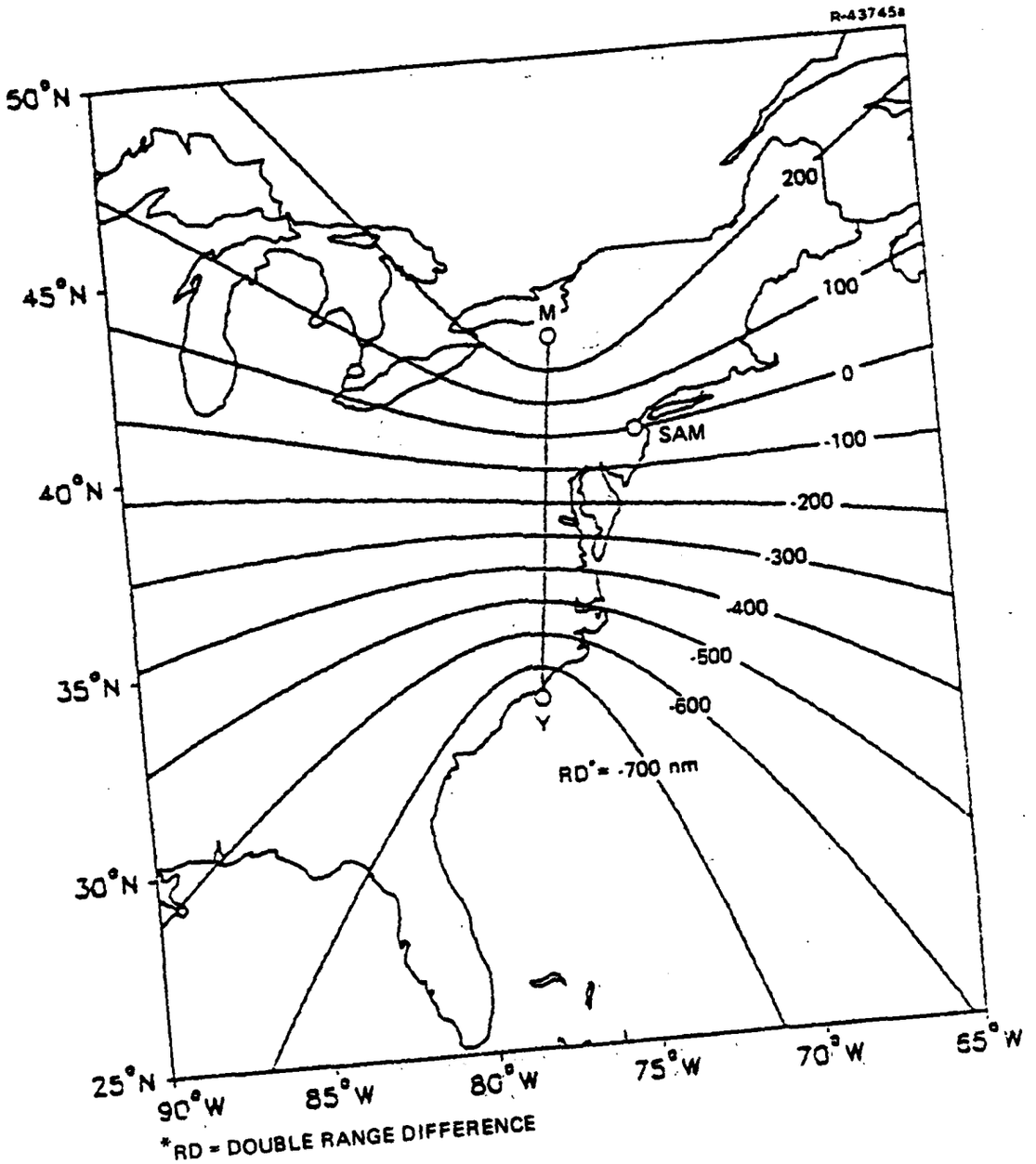

Figure 3.3-3 Temporal Variation Sensitivity for Northeast Chain (TDY)

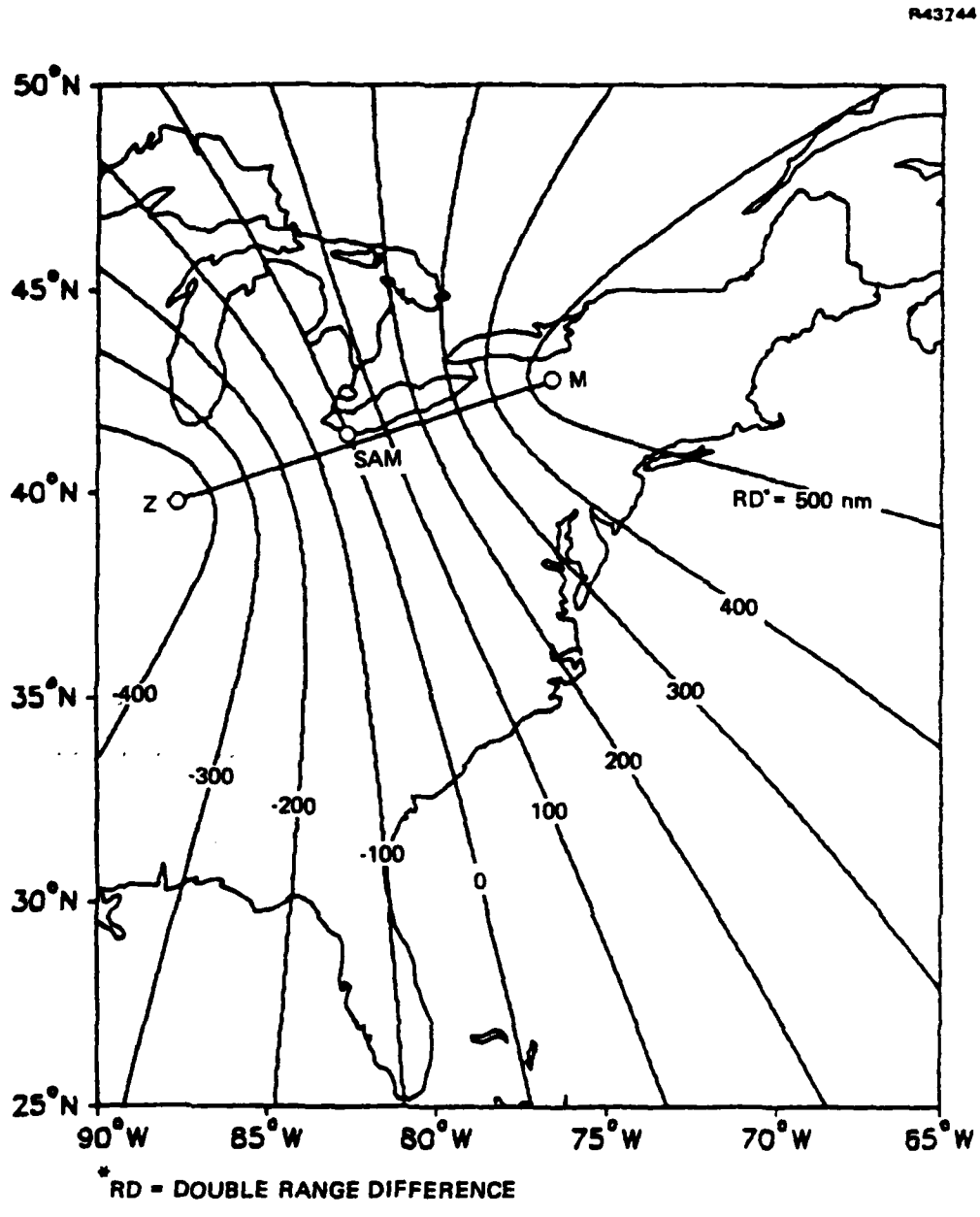

Figure 3.3-4 Temporal Variation Sensitivity for Northeast Chain (TDZ)

TABLE 3.3-1
TD SENSITIVITY TO PROPAGATION PARAMETER VARIATIONS

T-3470

MONITOR LOCATION	DOUBLE RANGE DIFFERENCE (nm)			
	W	X	Y	Z
Western New York (e.g., Dunkirk)	>500	>300	100-200	300-400
Central Kentucky (e.g., Lexington)	>500	200-300	300	200-300
Northern Maine (e.g., Houlton)	200-300	100	200	>500
Southern Virginia (e.g., Blacksburg)	>500	100-200	300-400	0-100
New Jersey (e.g., NAFEC)	350-400	0-50	0-100	400-450
Vermont (e.g., Rutland)	0-100	0-100	150-200	>500

collect data at the proposed sites to assure that adequate signal-to-noise ratio and minimum RFI conditions exists. If signal reception is a problem at either of the two recommended sites, Flight Service Stations in Southern Virginia represent an acceptable alternative.

Site selection for each airport visited by the test van also requires sufficient temporal variation in spatial models. In addition, sites should be chosen in diverse areas (e.g., mountaineous areas, urban areas, etc) to determine if any local phenomena introduce significant spatial variations. To meet these requirements, four airports are selected where the double range differences for at least two TDs exceed 200

nm and where one of the following geophysical feature is predominate:

- Mountainous Terrain
- Flat Terrain
- Major Metropolitan Area
- Land/Sea Path.

The last feature is to include a propagation path where significant portions are over land and sea and does not refer to a location that is at a land/sea boundary. Based on these criteria, the following sites are recommended: Rutland, VT (mountainous), Columbus, OH (flat terrain), Philadelphia, PA (metropolitan) and Worcester, MA (land/sea). As with the fixed-site monitor locations, test data will be collected at the recommended sites to assure that adequate signal-to-noise ratio and minimum RFI conditions exist before local airport locations are finalized.

For each airport, data will be collected at 10 to 20 different sites surrounding the airport. It is desired to collect data at surrounding sites such that the data will display a spatial sensitivity. The directions from the airport to the data collection sites are selected based on the spatial sensitivity model developed in Section 2.5.2. The desired data-collection radials for each TD, for each of the five airports, are shown in Figs. 3.3-5 to 3.3-9.

Because of time limitations for test data collection, only 10 to 20 sites can be visited at each airport. To accomplish this, data should be collected on three radials that coincide with the preferred directions defined in Figs. 3.3-5 to 3.3-9 and are approximately equal in angular separation. The recommended directions are summarized in Table 3.3-2.

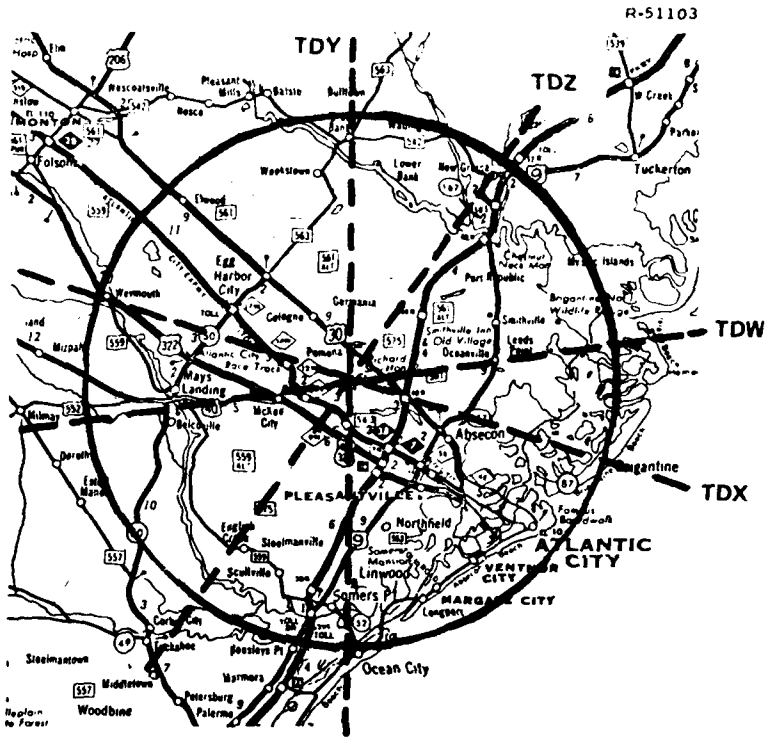

Figure 3.3-5 Preferred Data Collection for NAFEC (Pomona, NJ)

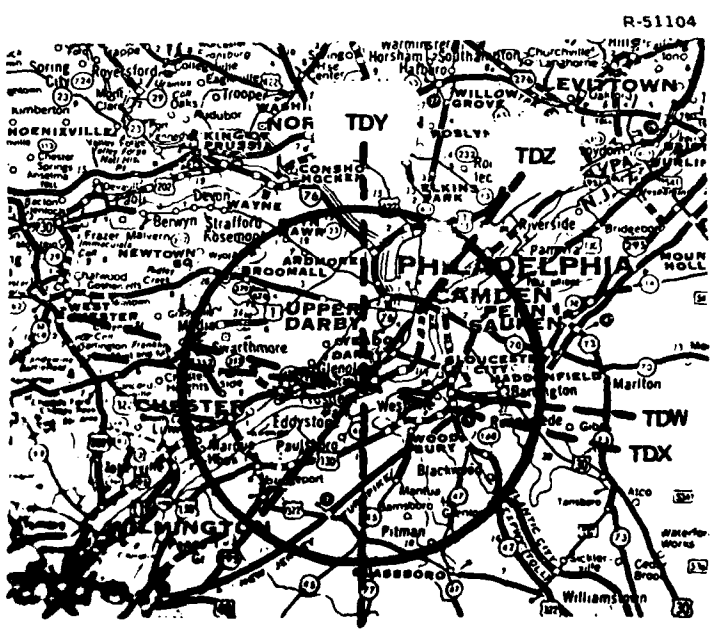

Preferred Data Collection Radials for Philadelphia, PA

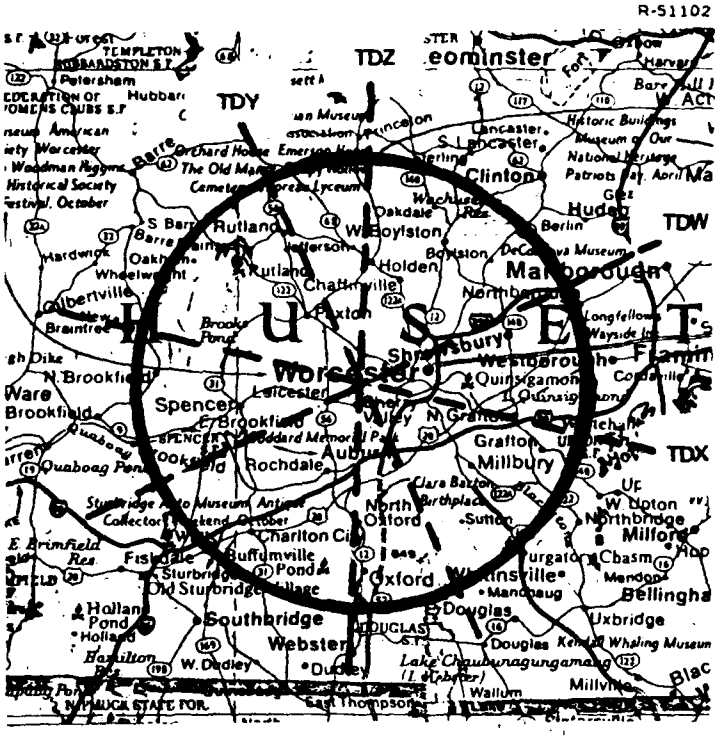

Figure 3.3-7 Preferred Data Collection Radials for Worcester, MA

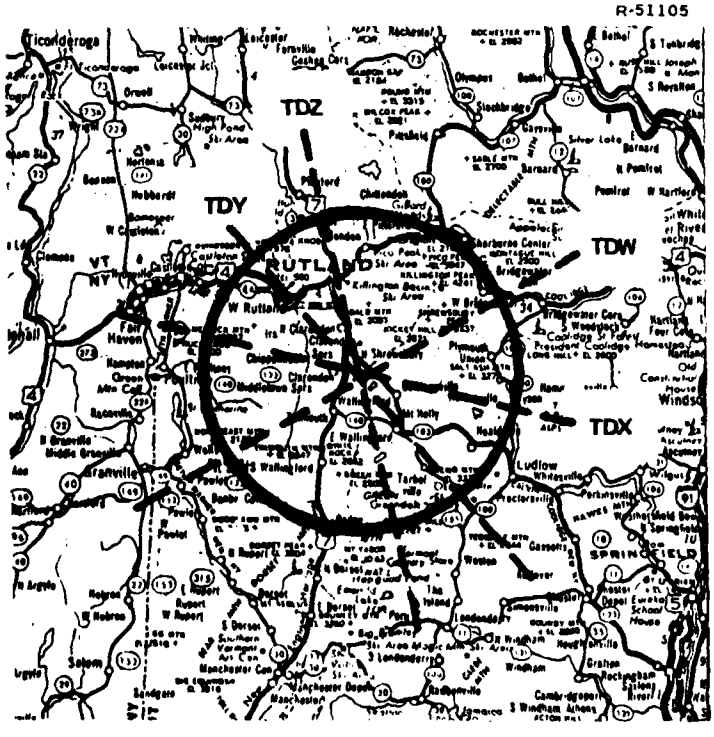

Figure 3.3-8 Preferred Data Collection Radials for Rutland, VT

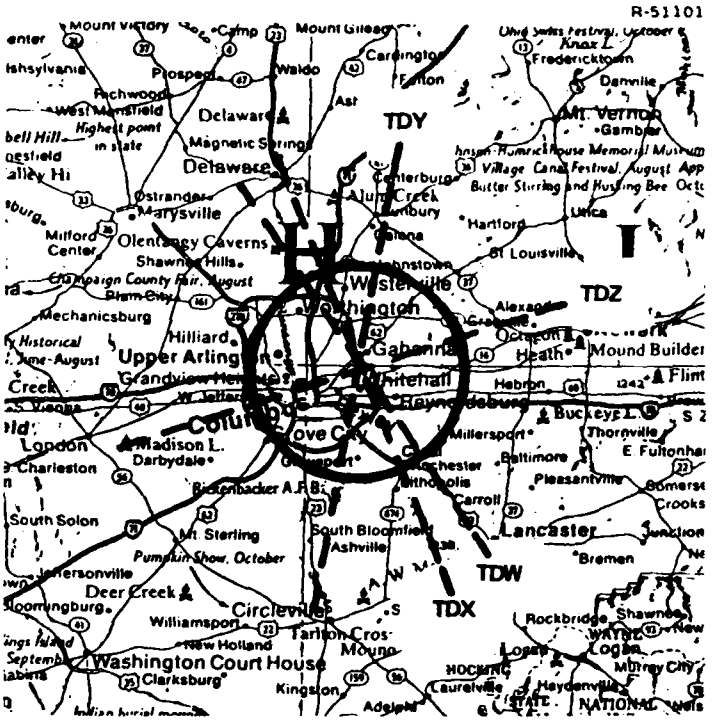

Figure 3.3-9 Preferred Data Collection Radials for Columbus, OH

TABLE 3.3-2

PREFERRED DATA COLLECTION RADIALS

T-3471

AIRPORT	PREFERRED RADIAL DIRECTIONS		
NAFEC	North	East	Southwest
Philadelphia	North	East	Southwest
Worcester	North	East-Southeast	Southwest
Rutland	North-Northwest	East-Southeast	Southwest
Columbus	North-Northwest	East-Northeast	South-Southeast

Final selection of sites are based on the preferred radial directions defined in Table 3.3-2, with sites selected at distances of approximately 5, 10, 15, and 20 km from the airport, if accessible by the test van. Other considerations in the selection of local sites are: the sites must be accessible at all times of the year and must be surveyed prior to, or during, the data collection period. NAFEC personnel anticipate that the data collection sites will be surveyed by either conventional geodetic survey or by translocation with the Transit Navigation Satellite System. In either case, the airport itself can be referenced to the World Geodetic System (WGS-72) via existing benchmarks. The sites should be surveyed relative to the airport to a precision of 10 m rms or better, to be compatible with data analysis objectives.

3.4 LORAN-C DATA COLLECTION EQUIPMENT

3.4.1 General Equipment Suite

The Loran-C data collection plan (Ref. 3) requires four receivers (two for fixed site data collection and two for local airport data collection), a van for transportation to the various local airport sites, and a spectrum analyzer to evaluate the presence of RFI. Based on the original Loran-C test plan (Ref. 31), a majority of the required components had been selected prior to TASC's involvement in the program. These original equipment recommendations focused on van-related items since the original test plan did not recommend fixed-site monitors. Items that had been ordered or made available to the FAA include the Austron 5000 Monitor Receiver System, a Hewlett-Packard 8565A Spectrum Analyzer and the van itself. Following revision of the original test plan, the utility of these pieces of equipment were reviewed and, with the exception

of minor modifications to the van, they were found to be adequate to accomplish the goals of the test plan. Three Micrologic ML-220 Loran-C receivers were subsequently purchased by NAFEC. Selection of these particular receivers was based on a review of off-the-shelf low-cost Loran-C receivers. In deciding which receiver to purchase, a number of general requirements had to be satisfied. These included:

- Ability to track the master and four secondaries
- Automatic acquisition and re-acquisition in case of temporary signal loss
- At least two adjustable notch filters
- Measure of signal-to-noise ratio
- Tracking loop characteristics consistent with fixed-site monitor operation
- Standard digital serial output interface
- Output software program.

The first four requirements, particularly the ability to track four secondaries, combined with cost constraints, dictate that the receivers be microprocesser-based. Although there are a number of microprocesser-based Loran-C receivers currently-manufactured and commercially-available, these are designed for maritime applications rather than for the automatic fixed-site monitor application. The capabilities of the Micrologic receiver that make it best suited for the current application are:

- Existing output software program, developed for the Department of Transportation, which automatically interfaces the required internal data (i.e., time difference measurements, signal-to-noise ratio, etc) to the output device

- Industry-wide standard RS-232C serial data output interface which allows direct interface of the receiver with a tape recorder
- "Back-panel" access, via a 25 pin DB-connector, to modify automatic operation record output rate and data transfer band rate.

Each ML-220 receiver purchased by NAFEC was modified by Micro-logic for the fixed-site monitor application, to provide increased smoothing of the reported 40-nsec TD jitter. Smoothing is accomplished by a low-pass filter which is independent of the phase-locked loops and characterized by a 2-min time constant.

3.4.2 Notch Filters

Another aspect of Loran-C test equipment, which has been evaluated by TASC, is the effect of Austron 5000 receiver notch filters on measured TDs and TOAs.* Although the NAFEC Loran-C data collection plan includes an assessment of the effect of RFI on Loran-C performance, it is desirable to minimize the effect of RFI during collection of the TD data specified in the plan, so as to isolate Loran-C signal propagation effects. RFI is minimized by attenuating the interfering frequencies with notch filters.

The Austron 5000 Loran-C receiver carried in the NAFEC test van is inherently capable of providing the precise data

*The Austron 5000 receiver has the capability to measure TOAs, when interfaced with a precision clock. Although TOA measurements are not included in the initial data collection effort, the effect of notch filters on TOAs is considered in the event that such measurements are made in future data collection efforts.

necessary for assessment of local grid warpage in airport approach areas. To take full advantage of the precision of the Austron 5000 receiver, it is operated with the following combination of notch filters:

- Three filters with tunable center frequencies designed by Austron and included in the Austron 5000 receiver
- A filter bank with fixed filter center frequencies designed by the U.S. Coast Guard and not included in the receiver.

The fixed notch filter bank is based on experience obtained by the U.S. Coast Guard during calibration of the Northeast U.S. Loran-C chain. The bank includes notch filters at interfering frequencies generated by broadcast facilities (e.g., Annapolis Naval communications channel NSS at 88.0 kHz) and radionavigation aids (e.g., Canadian Decca transmitter at 114.3 kHz). The tunable notch filters can be employed to attenuate additional interfering frequencies encountered in the local areas visited by the NAFEC test van. Potential sources of local RFI are airport navigation and communication facilities, industrial facilities, and power lines (Ref. 32).

The Micrologic ML-220 Loran-C receivers, employed as fixed-site monitors during the data collection effort, are less accurate than the Austron 5000 receiver and serve primarily to monitor large-scale temporal TD variations. Each Micrologic receiver is equipped with two notch filters which can be tuned to attenuate the dominant interfering frequencies identified at the receiver location. It is unlikely that the additional reduction in RFI provided by U.S. Coast Guard notch filter banks would contribute significantly to the utility of the fixed-site monitor data.

Notch filters distort part of the Loran-C frequency spectrum. Distortion of the spectrum may be accompanied by distortion of the Loran-C pulse envelope and by phase shifts in the 100 kHz Loran-C carrier. Loran-C receivers can normally be calibrated to compensate for the effect of the notch filters. In particular, the Austron receiver can be calibrated prior to the data collection effort to compensate for the fixed U.S. Coast Guard notch filter bank. However, because the center frequencies of the tunable notch filters in the Micrologic and Austron receivers are selected at the data collection sites, in-field receiver calibration may be required. In-field calibration of the Micrologic receivers is practical, since they will remain at fixed locations for an extended period of time (three days at each airport visited by the test van; one year at London, Kentucky and Buffalo, New York). However, in-field calibration of the Austron receiver may be impractical, because the test van only remains at a local data collection site for one to two hours. A computer simulation has been developed to predict the effect of the tunable Austron notch filters on the Loran-C signal, for the case where no in-field receiver calibration is performed. The simulation model and results are discussed in the following sections.

3.4.3 Notch Filter Simulation Model

The effect of an Austron notch filter on a Loran-C pulse is simulated by passing an ideal Loran-C current pulse through a second-order approximation to the Austron notch filter. The ideal Loran-C current pulse is taken to be the Loran-C transmitter antenna base current (Ref. 4), which is described by the equation

$$i(t) = A\,(t/\Delta)^2\, e^{2\,(1\,-\,t/\Delta)}\, \sin(2\pi ft) \qquad (3.4\text{-}1)$$

where

A = peak envelope current = 1 unit

Δ = peak envelope time = 65 μsec

f = 0.1 cycle/μsec = 100 kHz

t = time (μsec) referenced to start of envelope

The Loran-C pulse is an amplitude modulation of the 100 kHz Loran-C carrier, rising to a peak value in 65 μsec and decaying to one percent of peak value in approximately 300 μsec (see Fig. 3.4-1). The frequency spectrum of the Loran-C pulse is concentrated between 90 and 110 kHz (see Fig. 3.4-2). The spectrum magnitude peaks at 100 kHz and is down approximately 20 dB at 90 and 110 kHz. The spectrum of a train of Loran-C pulses from a particular transmitter consists of discrete frequency lines separated by 10 to 25 kHz, corresponding to pulse group repetition intervals of 0.04 to 0.10 sec. The lines are arranged in "bundles" which are separated by 1 kHz, corresponding to the 0.001 sec pulse spacing within a pulse group. The Loran-C pulse spectrum is the envelope of the discrete frequency lines.

To obtain the precise data necessary to identify Loran-C grid warpage in airport approach areas, it is necessary to track the third-cycle positive-going zero crossing of the Loran-C carrier (see Fig. 3.4-1). The third cycle is identified in the Austron 5000 receiver by searching for the pair of adjacent positive carrier peaks, whose ratio is nearest to the ideal ratio of the third and fourth positive peaks (indicated in Fig. 3.4-1). One objective of the notch filter simulations is to predict the effect of Austron notch filters on third-cycle

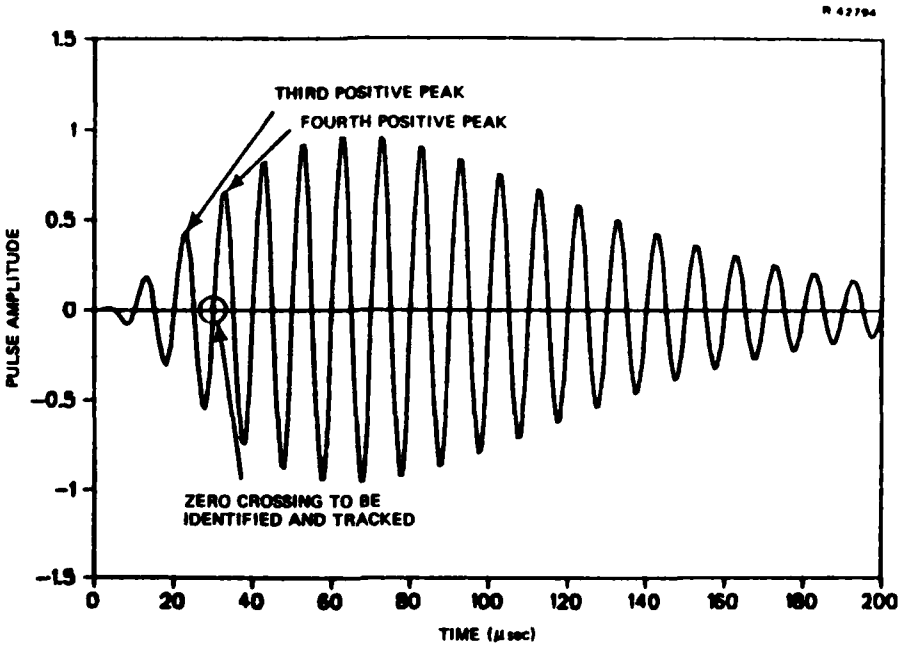

Figure 3.4-1 Ideal Loran-C Pulse Employed in Notch Filter Simulation

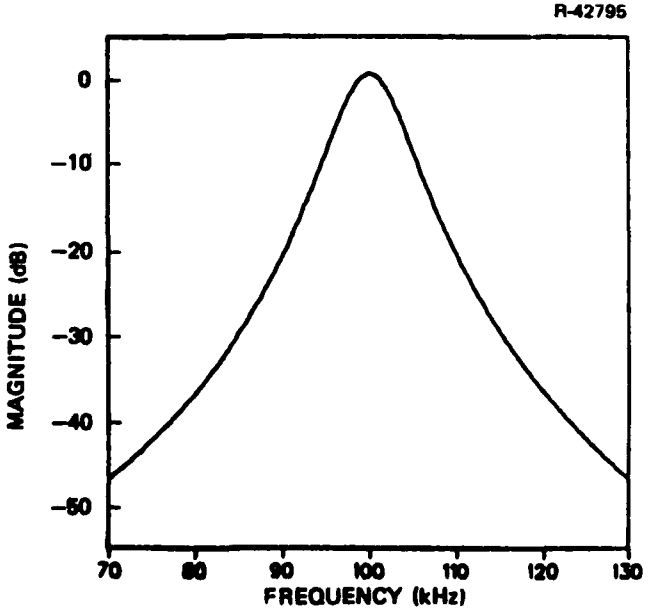

Figure 3.4-2 Magnitude of Loran-C Pulse Spectrum

identification. An additional objective is to predict the shift in the third-cycle positive-going zero crossing (i.e., Envelope-to-Cycle Difference or ECD) induced by the notch filters.

To meet these objectives, it is assumed that the notch filters eliminate the RFI for which they are designed and, in so doing, delete part of the Loran-C spectrum. Each Austron notch filter is approximated by a second-order Butterworth filter with a particular center frequency, a -3 dB bandwidth of 3.76 kHz, and a maximum attenuation of -40.5 kB (Ref.33). The frequency spectrum for the assumed notch filter is plotted in Fig. 3.4-3, for a center frequency of 100 kHz. Since the time constant of the notch filter is 85 μsec and the time between adjacent Loran-C pulses exceeds 700 μsec (for an effective pulse duration of 300 μsec), it is sufficient to examine the effect of the notch filter on a single pulse. In the frequency domain, this implies that a notch filter with a 3.76 kHz bandwidth is too "wide" to fit between the Loran-C spectral lines, which are separated by 1.0 kHz or less. That is, the actual Loran-C line spectrum may be approximated by a continuous spectrum (the pulse spectrum shown in Fig. 3.4-2), without affecting the results of the notch filter study.

The notch filter simulation is actually conducted in the time domain by implementing the notch filter with a second-order differential equation. The pulse at the output of the notch filter (or a series of notch filters) is examined to determine the ECD and the ratio of each adjacent pair of positive carrier peaks.

3.4.4 Notch Filter Simulation Results Pertaining to Third-Cycle Identification

Notch filter simulations are performed for a single notch filter over the range of center frequencies from 70 to 130 kHz,

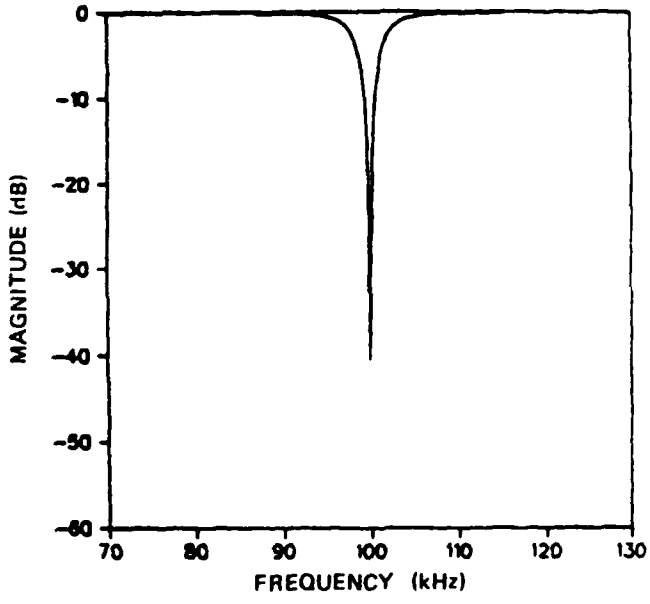

a) Magnitude

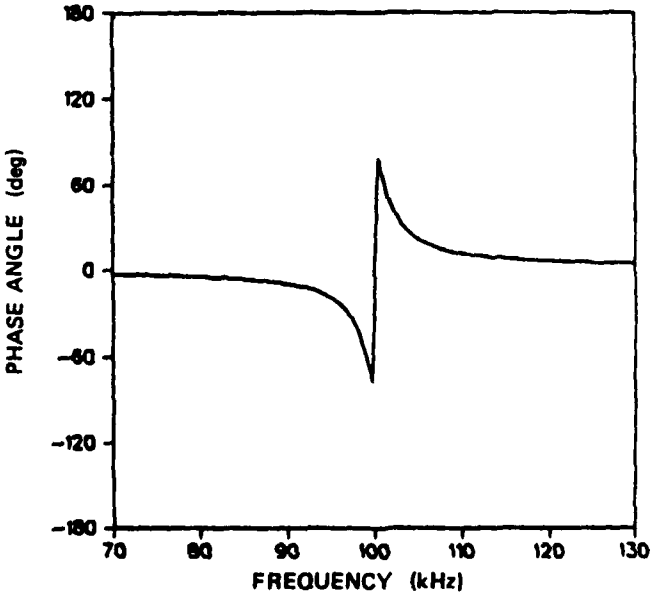

b) Phase Angle

Figure 3.4-3 Spectrum of Simulated Austron Notch Filter

and for selected combinations of two or three notch filters. The ratio of the fourth and third positive peaks of the filtered pulse is presented in Fig. 3.4-4 for a single notch filter. This ratio ranges from 1.44 to 1.57 for notch filter center frequencies ranging from 70 kHz to 130 kHz, compared to a ratio of 1.53 for the ideal Loran-C pulse. Corresponding ratios of the third and second peaks exceed 2.23 for all center frequencies, and the ratios of the fifth and fourth peaks are less than 1.29 for all center frequencies. Because the ratio of the fourth and third peaks is closer to the ideal ratio of 1.53 than are the ratios of other pairs of peaks,

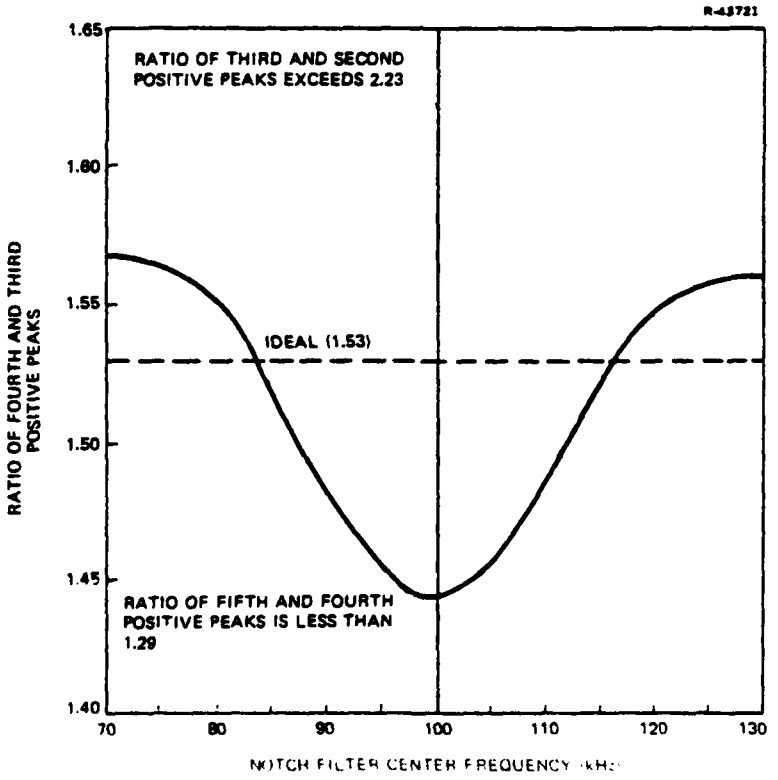

Figure 3.4-4 Effect of a Single Notch Filter on Ratio of Fourth and Third Positive Peaks

it is expected that the Austron 5000 receiver can identify the Loran-C third cycle correctly when using a single notch filter.

If two or three notch filters are employed in the simulation, the ratio of the fourth and third positive peaks can differ significantly from the ideal ratio of 1.53. For example, notch filters at 90, 100, and 110 kHz result in a ratio of 1.30. However, even in this extreme case, the ratio is closer to the ideal ratio than are the ratios of other pairs of peaks. It is expected that each of the three Austron notch filters can be tuned to any frequency without affecting third-cycle identification. Nevertheless, it is prudent to avoid placing notch filters in the 90 to 110 kHz frequency band unless such placement is accompanied by a receiver calibration.

3.4.5 Notch Filter Simulation Results Pertaining to ECD

ECD for a filtered pulse is presented in Fig. 3.4-5 for a single notch filter. The largest ECD is associated with notch filter center frequencies near 80 and 120 kHz, while negligible ECD is introduced for notch filter center frequencies near 100 kHz. This is in contrast to the effect of a notch filter on third-cycle identification, where the largest effect is realized for notch filter center frequencies near 100 kHz. Since the ECD introduced by a notch filter is theoretically the same for pulses received from all Loran-C transmitters* it is expected to cancel out in the measurement of a TD. However, if a cesium beam clock is interfaced with the

*The ECD resulting from other sources (e.g., the finite conductivity of the earth's surface) may be transmitter-dependent.

AD-A086 683 ANALYTIC SCIENCES CORP READING MA F/G 17/7
DEVELOPMENT OF LORAN-C DATA COLLECTION AND ANALYSIS PROCEDURES.(U)
MAR 80 L M DEPALMA, E A SCHOEN, S F DONNELLY DOT-FA79WA-4271
UNCLASSIFIED TASC-TR-1021-1 FAA-RD-80-48 NL

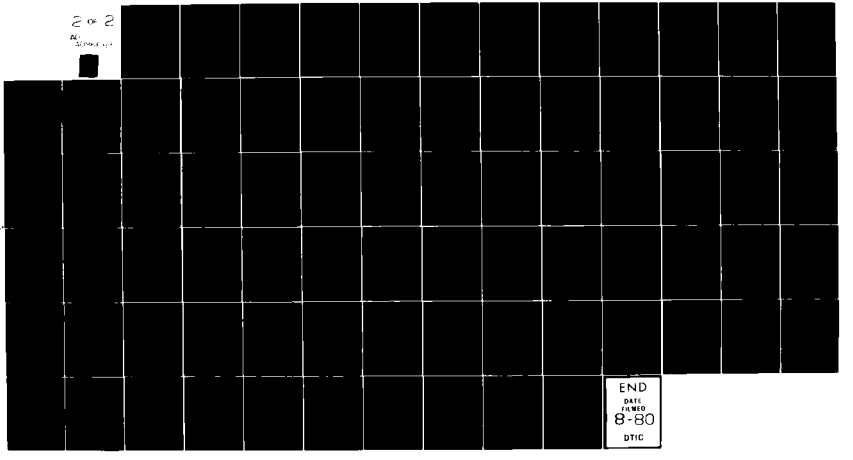

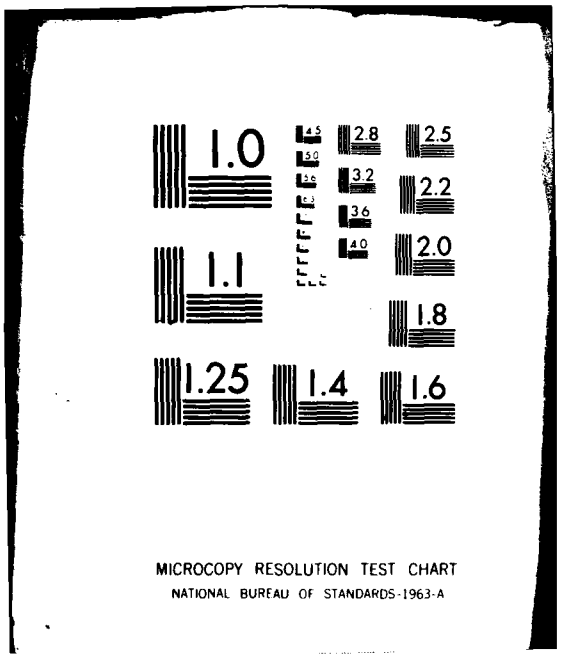
1.0
1.1
1.25
1.4
1.6
1.8
2.0
2.2
2.5
2.8
3.2
3.6
4.0
4.5
5.0
MICROCOPY RESOLUTION TEST CHART
NATIONAL BUREAU OF STANDARDS-1963-A

Austron 5000 receiver to measure TOAs in a future data collection effort, the ECD introduced by the notch filters becomes a critical factor in the quality of the resulting TOA data base.

If a single notch filter is employed during collection of TOA data in an airport approach area and if no receiver calibration is performed to compensate for the notch filter, the TOA data may be biased by as much as ±170 nsec (see Fig. 3.4-5). Of even greater concern than a bias is the potential for variations in ECD from site to site. Site-to-site variations in ECD result if different notch filter center frequencies are selected at different sites, and if a receiver calibration is not performed at each site. For example, the variation in ECD is 340 nsec if the center frequency is changed

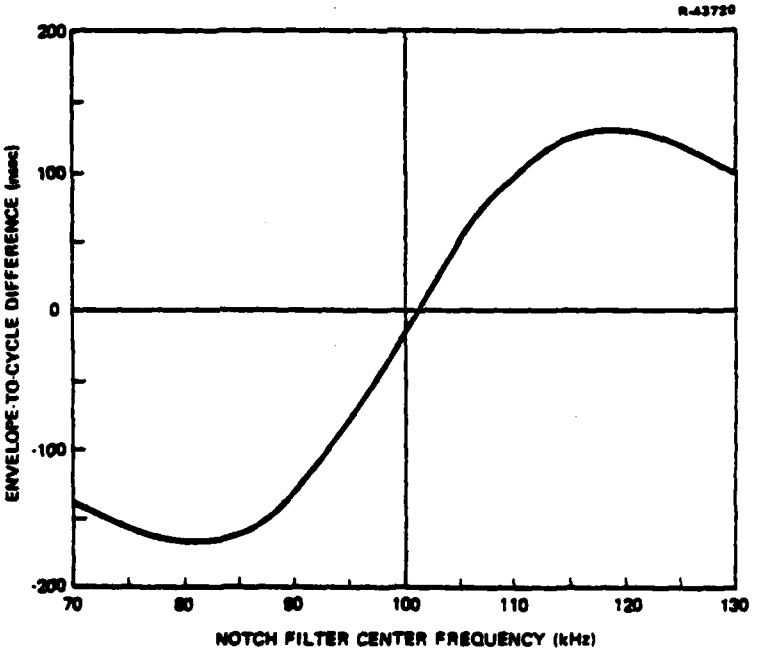

Figure 3.4-5 Effect of a Single Notch Filter on Envelope-to-Cycle Difference

from 80 kHz to 120 kHz. The site-to-site variation in ECD results in an erroneous interpretation as a TOA variation, which may make it difficult or impossible to analyze Loran-C grid warpage in the airport approach area. This effect is compounded if two or three notch filters are employed, as indicated in Table 3.4-1. A TOA bias of -465 nsec results if notch filters are placed at 70, 80, and 90 kHz. A site-to-site TOA variation of 830 nsec results if the notch filters are changed from 70, 80, and 90 kHz to 110, 120, and 130 kHz. If TOA data are collected in the future and are to serve their intended purpose, it is imperative that the Austron 5000 receiver be calibrated after each change in notch filter center frequencies. It would be advantageous to automate the calibration procedure in the Austron 5000 computer software, if possible.

TABLE 3.4-1

EFFECT OF MULTIPLE NOTCH FILTERS ON ENVELOPE-TO-CYCLE DIFFERENCE

NUMBER OF FILTERS	CENTER FREQUENCIES (kHz)	ECD (nsec)
Two	70,80	-306
	80,90	-315
	90,100	-168
	100,110	+103
	110,120	+249
	120,130	+233
Three	70,80,90	-465
	80,90,100	-383
	90,100,110	-58
	100,110,120	+283
	110,120,130	+365

4. DATA ANALYSIS PLAN

4.1 INTRODUCTION

Loran-C data, obtained in accordance with the data collection plan outlined in Chapter 3, will be analyzed to meet the following objectives:

- Preliminary evaluation of the Loran-C system, for possible application to civil aircraft navigation
- Calibration and refinement of proposed Loran-C signal propagation models.

These objectives can not be decoupled, since evaluation of the Loran-C system must include an assessment of model accuracy, and calibration of Loran-C models must account for the requirements of civil aircraft navigation. A data analysis plan is presented in this chapter, which provides for maximum utilization of the Loran-C data for system evaluation and model calibration.

The data analysis plan includes provisions for employing both fixed-site monitor data and mobile-site (test-van) data for the calibration and/or initial assessment of Loran-C signal propagation models. The analyses recommended for the two types of data are listed in Table 4.1-1 and discussed in Section 4.2. The analyses required to properly calibrate the temporal component of the local operational model, using fixed-site monitor TD data, are considerably more involved than the other analyses indicated in Table 4.1-1. Data analysis plan details and implementation considerations are presented for

TABLE 4.1-1

DATA ANALYSES FOR CALIBRATION AND/OR INITIAL ASSESSMENT OF LORAN-C MODELS

T-3533

TYPE OF DATA	APPLICATION	SPECIFIC DATA ANALYSES
Fixed-Site Monitor Data: Two Sites; Four TDs at Each Site; Measured Continuously for One Year	Global Operational Model	Compare TD Time Series to U.S. Coast Guard Constant TD Predictions; Transform to Position Error and Assess the Need for a Temporal Model
	Local Operational Model (Temporal)	Calibrate Model Parameters and Refine Model Structure for Each TD/Monitor Pair; Consider the Possibility of Employing a Common Model for all TD/Monitor Pairs
	Temporal Sensitivity Model	Determine Extent to Which Temporal Variations are Proportional to the Double Range Difference
	Cross-Correlation Analyses	Compute Cross-Correlation Between TDs to Assess Uniformity of Propagation Medium Variations; Compute Cross-Correlation Between TDs and Meteorological Data to Identify Cause/Effect Relationships
Mobile-Site (Test-Van) Data: 10 to 20 Sites in Each of Five Airport Approach Areas; Four TDs at Each Site; Measured Each Season	Local Operational Model (Temporal)	Determine Applicability of the Model Parameters, Estimated With Fixed-Site Data, to the Five Airports
	Local Operational Model (Spatial)	Calibrate Model for Each TD/Airport Pair; Consider the Possibility of Employing a Common Model for all TD/Airport Pairs; Consider the Need for a Seasonal Dependence in the Spatial Model
	Differential Loran-C Analyses	Assess Accuracy of Local Model to Determine Need for Differential Loran-C
Fixed- and Mobile-Site SNR Data	SNR Model*	Compare Model Predictions With Data to Verify Model Utility

*TASC signal amplitude model combined with CCIR noise data.

this case in Section 4.3. The role of the data analyses in the overall evaluation of Loran-C for civil aircraft navigation is discussed in Section 4.4, and the data analysis plan is summarized in Section 4.5.

4.2 RECOMMENDED DATA ANALYSES

4.2.1 Analyses Conducted With Fixed-Site Monitor TD Data

Loran-C TD data are collected with two fixed-site monitors, located at Buffalo, New York and London, Kentucky, every 15 min for one year. The data consist of the eight TD time series associated with the two sites and four Northeast U.S. chain TDs, and are applicable primarily to the investigation of Loran-C temporal variations. The four specific applications indicated in Table 4.1-1 are discussed below.

Global Operational Model - It is recommended in Section 2.4.1 that the global operational model be based on the TD grid predicted using the current U.S. Coast Guard model. It is necessary to compare the U.S. Coast Guard predictions with TD data collected over at least one year to determine whether or not the current model should be augmented to include a temporal component. An initial indication of the need for a temporal model component is provided by comparing the eight TD time series with the corresponding eight constant U.S. Coast Guard TD predictions (obtained from "lattice tables" used in Loran-C chart production). The TD residual* time series are transformed to position error time series, based on the optimal TD pair at each fixed site. The statistical properties of the

*Residuals are the differences between model predictions and data.

position error time series (i.e., mean, standard deviation and sample distribution) are then compared with enroute and terminal navigation accuracy specifications to determine the need for a temporal model. It is expected that these analyses will show that the specifications can be satisfied without a temporal model. In the event that the analyses are inconclusive, it will be necessary to collect additional fixed-site monitor data in regions of maximum temporal variations, during subsequent tests.

The Loran-C data obtained during the 1980-1981 NAFEC data collection effort are not intended for a statistical assessment of the accuracy of the current U.S. Coast Guard spatial model. These analyses require that data be collected at an array of locations in the chain coverage area.

Local Operational Model (Temporal) - The temporal component of the local operational model serves to predict TD variations at the center of the airport approach area -- i.e., the airport itself (see Section 2.4.2). The TD variations observed at the fixed-site monitors are indicative of the TD variations which may occur at an airport in a region of high TD sensitivity. The major data analysis objectives are to calibrate eight temporal models, corresponding to the eight TD/monitor pairs and to compare the eight models to possibly identify common structures and parameter values. Identification of a common model which is applicable to all airports is desirable, because such a model could be calibrated with data from only a few airports. If the data analyses indicate that a common model can not serve the intended purpose, it may be necessary to undertake an expanded data collection effort which includes all airports of interest. The data analysis plan, which is recommended for calibration of the temporal component of the local operational model, is based on extentensive TASC

experience in the calibration of time series models. Implementation of the plan requires the combined application of non-parametric techniques (e.g., spectral analysis) and parametric techniques (e.g., maximum likelihood parameter estimation), in the manner detailed in Section 4.3.

Temporal Sensitivity Model - The temporal sensitivity model presented in Section 2.5.1 is employed to identify regions of the Loran-C chain coverage area where temporal TD variations are largest. The model is based on certain simplifying approximations, including homogeneity of the signal propagation medium and linearity of the secondary phase delay. It is of interest to determine the extent to which propagation medium heterogeneity and secondary phase delay nonlinearity affect the utility of the temporal sensitivity model. This is accomplished by computing the maximum deviation and standard deviation (1σ) of each TD time series from its annual mean. If the temporal sensitivity model is adequate, the maximum and standard deviations for the eight TD time series will be more or less proportional to the respective double range differences (defined in Section 2.5.1). In this case, the model can be applied to the selection of fixed-site monitor locations for future data collection efforts. In the event that the model is found to be an over-approximation of actual TD variation sensitivity, potential refinements are examined. However, sufficient data are not collected during the data collection effort described in Chapter 3 to enable the calibration of a refined model, if required. A data collection effort for this purpose would have to include fixed-site monitors at an array of locations in the chain coverage area.

Cross-Correlation Analyses - In addition to the analyses described above, it is recommended that cross-correlation analyses be performed with the fixed-site monitor TD data in

order to provide general insights into Loran-C signal propagation. In particular, it is recommended that the cross-correlation function and correlation coefficient between each pair of TD time series, and between each TD time series and meteorological data, be computed. If temporal variations in the signal propagation medium are uniform over the chain coverage area, this is manifested in strongly correlated TDs. Strong correlation between certain pairs of TDs and weak correlation between others may indicate that the propagation medium varies uniformly over a certain portion of the chain coverage area. Note that a pair of TDs from the same fixed site are expected to be more strongly correlated than a pair of TDs from different fixed sites, due to the common effect of the master signal. Correlation of TDs with meteorological data is expected to indicate that TD variations are strongly correlated with surface temperature and absolute humidity. If sufficient radiosonde data are available for the vertical gradient of temperature and absolute humidity, it is recommended that these data also be correlated with the TD data. A comparison of results for surface and radiosonde data provide an indication of the relative effects of refractive index and vertical lapse rate variations on TD variations.

4.2.2 Analyses Conducted With Mobile-Site (Test-Van) TD Data

Loran-C TD data are collected with the NAFEC test van at 10 to 20 "mobile sites" in the approach areas of the following airports: NAFEC, Philadelphia, Worcester, Rutland, and Columbus. Data are recorded at each mobile site, every 15 min for two to three hours, and the procedure is repeated four times during the year (each season). The 20 sets of spatially-distributed data, corresponding to four TDs and five airports, enable the investigation of spatial propagation effects in

airport approach areas. Since a different set of data are available for each season, the temporal stability of the spatial effects can also be studied. TD data are recorded at the airport itself, during the same time period that the test van visits the mobile sites. These additional data aid in the proper interpretation of spatial effects, and supplement the data recorded continuously at the fixed-site monitors (see Section 4.2.1). The three applications of mobile-site data, indicated in Table 4.1-1, are discussed below.

Local Operational Model (Temporal) - Analyses of the fixed-site monitor TD data (see Sections 4.2.1 and 4.3) may suggest that the temporal component of the local operational model is the same for the two fixed sites. In this case, a unified model can be calibrated with the fixed-site monitor data and validated with the seasonal data collected at the five airports. Since the airport data do not consist of a continuous yearlong time series, it is not recommended that these data be employed for further model calibration. However, results of the model validation permit recommendations, regarding future data collection requirements, to be made with greater confidence.

Local Operational Model (Spatial) - The spatial component of the local operational model is utilized to extrapolate TDs from the airport, where the temporal model is applicable, to other locations in the airport approach area (see Section 2.4.2). The mobile-site data are employed to calibrate a spatial model for each of the 20 TD/airport pairs, using the following procedure:

- Subtract the TD measured at the airport from the TDs measured in the approach area, in order to remove most of the temporal variation (the differences are referred to as "differential TDs")

- Calibrate the uncertain model parameters with the differential TDs, using a least-squares approach
- Plot the residuals versus range and bearing angle to determine whether or not additional model structure is required, and repeat the calibration if necessary.

The calibrated models for the 20 TD/airport pairs are compared in search of common model structures and parameter values. As in the case of the temporal model, it is advantageous to identify a common spatial model, which is applicable to all airports, because such a model can be calibrated with a minimum amount of data. It is also of interest to calibrate the spatial models with Loran-C data collected in different seasons to assess the need for seasonally-dependent model parameters. If the seasonal dependence is negligible, the collection of mobile-site data can be limited to a single season in future tests.

Differential Loran-C Analyses - The mobile-site data can also be employed to determine the accuracy of differential Loran-C, for comparison with the accuracy of the Loran-C configuration which is proposed for non-precision approach navigation. Differential Loran-C requires the installation of a fixed-site monitor (termed a "pattern monitor") at each airport or group of airports, for use in operations, as opposed to data collection. The TDs measured with the pattern monitor are supplied to the aircraft, typically at a high data rate, and used instead of a temporal model for compensation of temporal TD variations. Extrapolation of the TDs from the airport to locations in the airport approach area is still accomplished with a spatial model. The errors associated with differential Loran-C are simply the residuals of the calibrated spatial model. The errors associated with the proposed non-differential configuration are the sum of the temporal and spatial model residuals. Temporal model residuals are only available for

this comparison in the event that a temporal model is calibrated for the five airports. As discussed previously, such a model may or may not result from analyses of the fixed-site monitor data. Although a temporal model may not be available to permit the comparison of differential and non-differential Loran-C, the accuracy of differential Loran-C can nevertheless be determined. The determination of differential Loran-C accuracy is important, because it provides a best-case performance bound.

4.2.3 Analyses Conducted With Fixed- and Mobile-Site SNR Data

A Loran-C signal amplitude model is presented in Section 2.6, which can be employed with CCIR atmospheric noise data to estimate Signal-to-Noise Ratio (SNR) in the chain coverage area. Application of the signal amplitude model requires knowledge of the ground conductivity. However, the model is expected to provide an estimate, which is within ±5 dB of the actual signal amplitude value, if a nominal conductivity value of 0.005 mho/m is employed. The SNR data collected at the fixed and mobile sites enable an indirect assessment of the signal amplitude model to be made. Specifically, the average daily SNR can be computed for each season and each site (only the airport data need be considered for the mobile sites) and compared with the estimated values provided in Section 2.6. This comparison will indicate whether the assumed conductivity value of 0.005 mho/m is adequate or must be revised to provide a better approximation. However, it should be kept in mind that observed differences between model predictions and SNR data may be partly due to differences between CCIR and actual atmospheric noise levels.

4.3 DETAILED DATA ANALYSIS PLAN FOR CALIBRATION OF TEMPORAL COMPONENT OF LOCAL OPERATIONAL MODEL

4.3.1 Review of Temporal Component of Local Operational Model

The local operational model presented in Section 2.4 is comprised of temporal and spatial components. The temporal model is given by the equation

$$\phi_i(t) = \frac{n_i(t)}{c} R_i + 0.00373 [\alpha_i(t) - 0.75] R_i + [a_i R_i \sin(2\pi f t + \theta_i) + b_i] \qquad (4.3\text{-}1)$$

where $\phi_i(t)$ is the signal propagation delay from transmitter i to the airport, and the remaining parameters are defined in Eq. 2.4-6. The parameters a_i, θ_i, and b_i account for conductivity variations and other uncertain effects which must be modeled empirically. The data analysis plan focuses on the calibration of these parameters with Loran-C data. Prior to the collection of Loran-C data, the temporal model is characterized by a sinusoidal time-dependence. It is also intended that this basic structure be evaluated and refined, as required, during the data analysis effort.

In general, the model parameter values may differ for different transmitters and different airports. Temporal model parameters for 10 different transmitter/airport combinations are relevant to the present study, since fixed-site monitors will be installed at two locations (flight service centers, rather than airports) to continuously track five signals from the Northeast U.S. Loran-C chain. The intention is to calibrate the model parameters for each transmitter/airport

combination,* as well as to determine whether certain parameters are transmitter- and airport-independent. These parameters can be calibrated using data from the Loran-C data collection effort outlined in Chapter 3, thereby minimizing future FAA data collection requirements. Calibration of important parameters which are transmitter- and airport-dependent may require an expanded data collection effort which includes all airports of interest. The need for an expanded data collection effort can only be determined after the data collection and analysis plans have been executed.

4.3.2 Data Analysis Techniques

The data analysis techniques, which are applicable to calibration of the temporal component of the local operational model, may be characterized as follows:

- Non-parametric techniques - Used to characterize the data or model residuals, without making restrictive assumptions; provide information regarding model structure
- Parametric techniques - Used to characterize the data, based on an assumed model structure; applicable to estimation of model parameters.

The role of non-parametric and parametric data analysis techniques, both in the initial model calibration effort and in the overall FAA Loran-C program, is illustrated in Fig. 4.3-1. The relevant techniques in each category are also indicated in the figure.

*Only certain aggregates of the parameters can be calibrated using TD data (see Section 4.3.4).

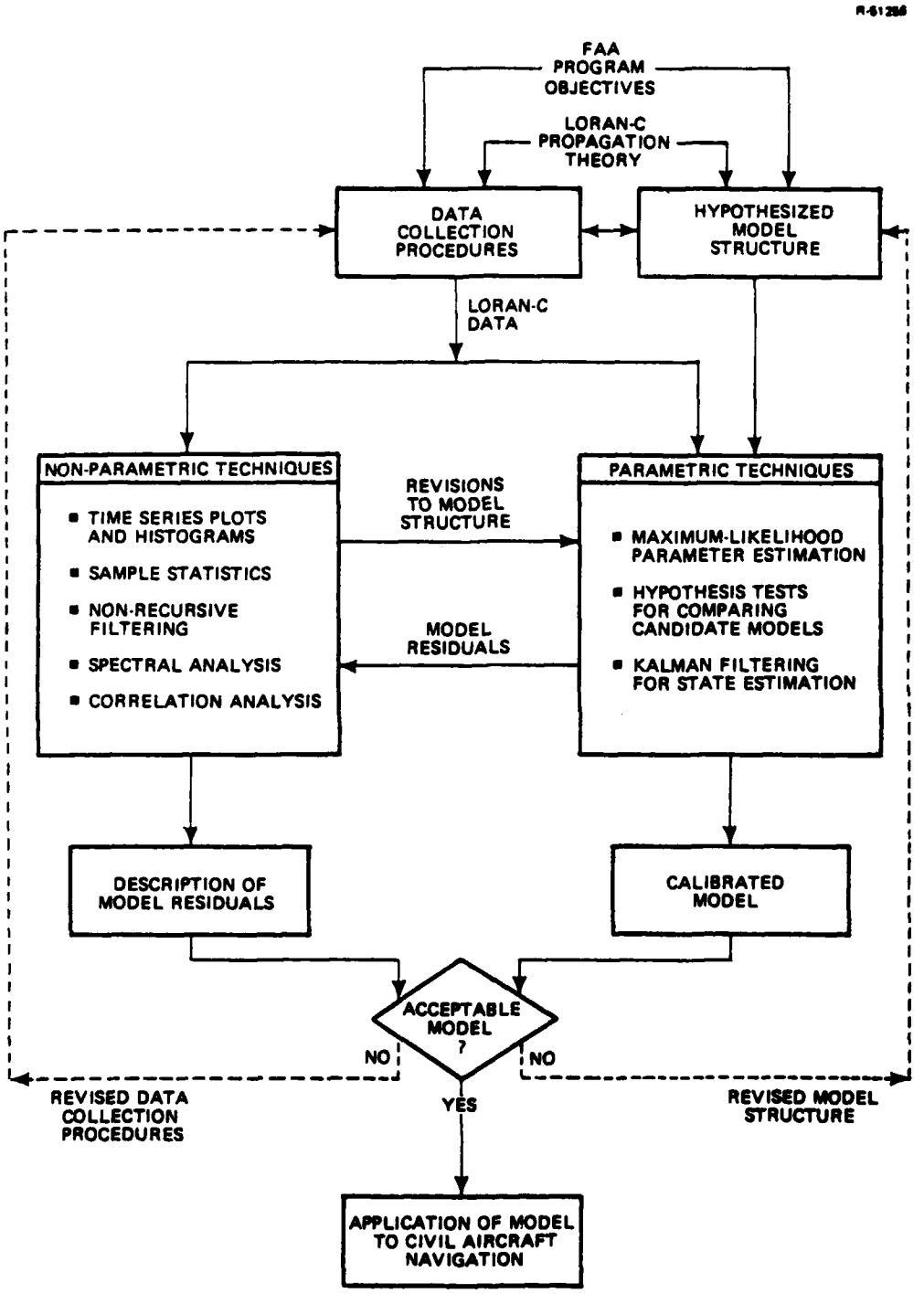

Figure 4.3-1 Role of Non-Parametric and Parametric Data Analysis Techniques

FAA program objectives and Loran-C signal propagation theory have been employed previously in this report to recommend initial data collection procedures and an initial model structure. The first step in analysis of the Loran-C data is to utilize parametric techniques to estimate the uncertain parameters in the recommended model structure (see Fig. 4.3-1).* The model residuals, which result after parameter estimation, are analyzed non-parametrically to extract additional information regarding model structure. The new model parameters are then estimated, and the non-parametric/parametric analysis "loop" is repeated until no additional information can be derived from the residuals.

The resulting calibrated model represents the best model achievable, based on data from the initial data collection effort. Examination of the model residuals (i.e., accuracy), together with an assessment of model complexity and general applicability (e.g., to other airports), reveals whether the model is acceptable for application to civil aircraft navigation, or requires calibration with additional data. In the latter case, accumulated data analysis experience is drawn on to formulate revised data collection procedures and/or a revised model structure, and the procedure is repeated, as illustrated in Fig. 4.3-1.

The following is a brief description of the relevant non-parametric data analysis techniques and their applications:

> Time Series Plots and Histograms - Easily implemented techniques to detect data outliers; also used in selecting a temporal model structure and in assessing the normality† of a residual time series, respectively

---

*Alternatively, non-parametric techniques can be used initially to evaluate the recommended model structure.

†Degree to which the values of the residuals are governed by a normal probability distribution.

Sample Statistics - Including sliding window mean and standard deviation; used in assessing the stationarity* of a residual time series and as figures-of-merit for comparing models

Non-Recursive Filtering - Low-pass filters for removing high-frequency noise, high-pass filters for removing trends, and band-pass filters for isolating significant effects (e.g., diurnal cycle); low-pass filter is implemented as a sliding-window averager with appropriate weighting, and high-pass and band-pass filters are based on combinations of low-pass filters

Spectral Analysis - Based on Power Spectral Density (PSD), as approximated by Fast Fourier Transform; used in identifying frequencies of sinusoidal model components and spectral content of noise

Correlation Analysis - Based on Autocorrelation Function (ACF); used in hypothesizing the stochastic component of the residual time series (e.g., Markov processes); confidence bounds on ACF can be calculated for use in testing for residual whiteness.†

The following is a brief description of the relevant parametric data analysis techniques and their applications:

Maximum Likelihood Parameter Estimation - Technique for estimating the parameters of deterministic and stochastic models; based on maximizing the likelihood function; yields an estimate of the error variance associated with the parameter estimate; embodied in TASC software package, PARAIDE‡

*Degree to which the statistical properties of the residuals are time-invariant.

†Degree to which the residuals can be characterized by white (uncorrelated) noise

‡PARAIDE is a trademark of The Analytic Sciences Corporation.

Hypothesis Tests for Comparing Candidate Models - Based on the generalized likelihood ratio statistic; used to discriminate between statistically significant and insignificant model components

Kalman Filtering for State Estimation - Used in conjunction with stochastic models to estimate the time series characterized by the model, in the presence of noise; best applied after model parameters have been estimated using maximum likelihood technique.

Detailed descriptions of the above techniques can be found in Refs. 35 to 45.

4.3.3 Data Analysis Plan Details

A detailed data analysis plan is presented in Fig. 4.3-2, for calibrating the temporal component of the local operational model. This plan is an expanded version of the non-parametric/ parametric analysis loop, shown in Fig. 4.3-1. Each block is referred to in the discussion below.

Block 1 - Loran-C data are initially processed by the data management system software described in Chapter 5. This software includes editing and subsetting capabilities, which enable a "clean" Loran-C data base to be extracted for analysis purposes. The data management system also provides for subsetting of the meteorological data utilized in computing refractive index (n) and the vertical lapse rate parameter (α), for application to the temporal model (see Eq. 4.3-1).

Block 2 - The structure of the temporal model is initially based on Loran-C signal propagation theory and FAA program objectives. The model structure may be revised based on analyses of model residuals, as detailed in Blocks 5, 6, and 7.

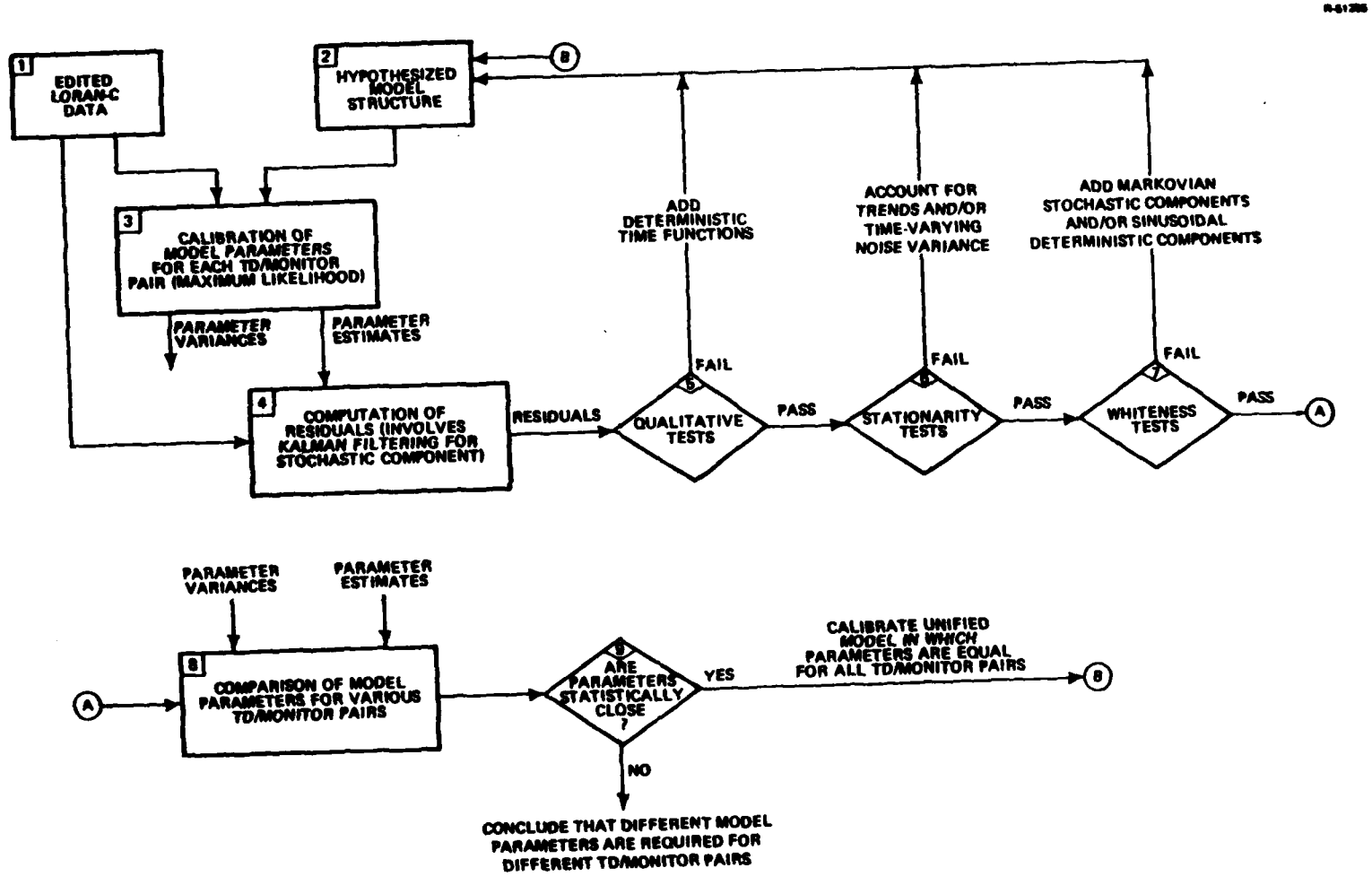

Figure 4.3-2 Data Analysis Plan for Calibration of Temporal Component of Local Operational Model

Block 3 - The Loran-C data are processed, using the maximum likelihood parameter estimation technique, to calibrate the uncertain parameters in the hypothesized model structure (initially, the uncertain parameters are a_i, θ_i, and b_i). The calibration is performed for each TD/monitor pair, thus resulting in eight sets of model parameters, corresponding to the two fixed-site monitors and four TDs. In addition to providing estimates of model parameters, the maximum likelihood approach also provides a measure of confidence in the parameter estimates -- i.e., the estimation error variances. These parameter error variances are most meaningful when the correct model structure is hypothesized. In particular, the model structure must include a correct statistical description of the component of the TD which cannot be modeled deterministically (i.e., the stochastic component). The stochastic model component, although of limited utility in the intended model application, is fundamental to the assessment of the deterministic model component. Initially, the stochastic model component is hypothesized to be white noise with an unknown variance, and the variance is estimated along with the model parameters, using the maximum likelihood technique. The white noise assumption is reasonable if measurement noise is the only factor influencing the ability to model Loran-C signal propagation. In general, however, there is an additional correlated modeling noise (e.g., a Markov random process) which results from approximating the data with a low-order deterministic model. Identification of stochastic models for the correlated modeling noise is addressed in Block 7.

Block 4 - Model residuals are computed as the difference between model predictions and the data. In the case that the stochastic component of the calibrated model includes only white noise, the model prediction is simply the time series associated with the deterministic model component. If the

stochastic component is correlated, however, the model prediction is computed by processing the data in a Kalman filter which includes the calibrated stochastic model. Model residuals are subjected to various tests in Blocks 5, 6, and 7, to assure that the calibrated deterministic/stochastic model is a valid characterization of the data.

Block 5 - The residuals are first examined qualitatively, with the aid of time series plots, to identify deterministic time functions which are omitted in the calibrated model. Examples of deterministic time functions are biases, ramps, parabolas, and sinusoids. If inclusion of additional deterministic model structure is warranted (based on engineering judgement), the parameter estimation procedure is repeated for the new structure (see Fig. 4.3-2).

Block 6 - If no trends in the residuals can be identified from time series plots, the residuals are next subjected to tests for statistical stationarity. These tests may involve the use of non-recursive low-pass filtering to remove high-frequency noise which may disguise trends. The tests may also involve the computation of sliding-window statistics to identify possible time variations in the variance of the residual time series. If trends are detected, they are accounted for via revisions to the deterministic model. If a time-varying noise variance is exhibited by the residuals, the stochastic model component is revised to include this effect.

Block 7 - The ultimate measure of model performance is the degree to which the model residuals are characterized by a white noise process. Whiteness tests are based on the PSD and ACF of the residuals, which are a constant and an impulse, respectively, for an ideal white noise process. The extent of the deviation of the PSD and ACF from their ideal

forms can be evaluated against confidence bounds, to determine whether or not the residuals are white. If a particular frequency is dominant, the deterministic model is augmented to include the corresponding sinusoidal component. If the ACF exhibits a negative exponential behavior, the stochastic model is augmented to include the corresponding Markov component. The statistical significance of the additional model components can be determined, based on hypothesis tests, which employ the generalized likelihood ratio statistic, or on tests which employ the Akaike Information Criterion (Ref. 43). The iterative procedure, consisting of Blocks 2 to 7, is repeated until models are calibrated for all eight TD/ monitor pairs.

Blocks 8 and 9 - The eight models are expected to have the same structure but different parameter values. In this case, it is desirable to compare the parameter estimates for the eight TD/monitor pairs to determine which, if any, parameters are TD- and monitor-independent. These parameters characterize the homogeneous features of the signal propagation medium. The parameter estimates are determined to be statistically "close" if they are within established confidence bounds. The confidence bounds are based on the parameter estimates themselves and on the parameter error variances determined during application of the maximum likelihood procedure (see Block 3). If the parameters are statistically close, the calibration procedure is repeated for a unified model in which the parameters are equal for all TD/monitor pairs. Otherwise, it is concluded that different model parameter values are required for different TD/monitor pairs.

The data analysis plan outlined above is based on extensive TASC experience in the analysis of time series data and the calibration of time series models. It is intended that the plan serve as an initial framework for the data analyses

and be updated, as required, to accommodate the idiosyncrasies of the actual Loran-C data. Two important issues, which must be addressed in implementing the data analysis plan, are highlighted in Sections 4.3.4 and 4.3.5: linear versus nonlinear models and parameter observability.

4.3.4 Linear Versus Nonlinear Models

Linear temporal models* have the following advantages over nonlinear temporal models in the application of maximum likelihood parameter estimation:

- Less computer-processing time is required to maximize the likelihood function
- Parameter estimation errors are normally distributed (assuming the stochastic model component is driven by white noise with a normal distribution).

Therefore, it is desirable to select a linear model structure, even if this results in a greater number of model parameters, or a less intuitive representation, than a nonlinear structure. The temporal model defined by Eq. 4.2-1 includes the nonlinear function

$$f(t) = a_i R_i \sin(2\pi ft + \theta_i) \qquad (4.3\text{-}2)$$

where a_i and θ_i are the unknown parameters. However, the nonlinear function can be written as the following equivalent linear function

*The deterministic component of a linear termporal model consists of the summation of a number of terms, each term being the product of an unknown parameter and a known time function.

$$f(t) = \overbrace{a_i \cos\theta_i}^{A_i} R_i \sin(2\pi ft) + \overbrace{a_i \sin\theta_i}^{B_i} R_i \cos(2\pi ft) \qquad (4.3\text{-}3)$$

where the parameters (A_i, B_i) are the Cartesian representation of the parameters (a_i, θ_i). The parameters A_i and B_i are estimated using the maximum likelihood approach, and the following relationships are employed to estimate the original parameters

$$a_i = \sqrt{A_i^2 + B_i^2}$$

$$\theta_i = \tan^{-1}(B_i/A_i) \qquad (4.3\text{-}4)$$

The parameter estimation errors for a_i and θ_i are characterized by Rayleigh and uniform distributions, respectively, if A_i and B_i are independent and characterized by identical normal distributions (Ref. 45).

4.3.5 Parameter Observability

Another important issue in model calibration is parameter observability -- i.e., the ability to estimate the parameters from the given data. The local operational models presented in this report are formulated on the time-of-arrival level, but only TD data may be available for parameter estimation. For example, there are five parameters A_i in the linear form of the temporal model (see Eq. 4.3-3), corresponding to the five transmitters (i = W, X, Y, Z, and M). Four TDs (TDW, TDX, TDY, and TDZ) are measured every 15 min for one year. If these TD samples are distinguished by subscripts (e.g., TDW_1,

...,TDW_N), the measurement equations can be written in the following vector/matrix form:

$$\begin{bmatrix} TDW_1 \\ \vdots \\ TDW_N \\ \hline TDX_1 \\ \vdots \\ TDX_N \\ \hline TDY_1 \\ \vdots \\ TDY_N \\ \hline TDZ_1 \\ \vdots \\ TDZ_N \end{bmatrix} = \left[\begin{array}{c|c|c|c|c} R_W \sin_1 & & & & -R_M \sin_1 \\ \vdots & 0 & 0 & 0 & \vdots \\ R_W \sin_N & & & & -R_M \sin_N \\ \hline & R_X \sin_1 & & & -R_M \sin_1 \\ 0 & \vdots & 0 & 0 & \vdots \\ & R_X \sin_N & & & -R_M \sin_N \\ \hline & & R_Y \sin_1 & & -R_M \sin_1 \\ 0 & 0 & \vdots & 0 & \vdots \\ & & R_Y \sin_N & & -R_M \sin_N \\ \hline & & & R_Z \sin_1 & -R_M \sin_1 \\ 0 & 0 & 0 & \vdots & \vdots \\ & & & R_Z \sin_N & -R_M \sin_N \end{array}\right] \times \begin{bmatrix} A_W \\ A_X \\ A_Y \\ A_Z \\ A_M \end{bmatrix}$$

+ additional terms

(4.3-5)

where $\sin_1,\ldots,\sin_N$ denote $\sin(2\pi ft_1),\ldots,\sin(2\pi ft_N)$. The matrix in Eq. 4.3-5 is of dimension $4N \times 5$. The matrix has rank 4,* regardless of the number of samples (N), implying that the five parameters, $A_W \ldots A_M$, are not all observable. The non-observability is accounted for in the parameter estimation procedure by dealing with four weighted parameter differences, which are all observable:

$$A_{WM} = (R_W A_W - R_M A_M)/(R_W - R_M)$$

*The matrix is shown to be of rank 4 by multiplying the columns $R_X R_Y R_Z R_M$, $R_X R_Y R_Z R_M$, $R_W R_X R_{ZRM}$, $R_W R_X R_Y R_M$, and $R_W R_X R_Y R_Z$, respectively and adding the resulting columns. This procedure yields a zero column.

$$A_{XM} = (R_X A_X - R_M A_M)/(R_X - R_M)$$

$$A_{YM} = (R_Y A_Y - R_M A_M)/(R_Y - R_M) \qquad (4.3\text{-}6)$$

$$A_{ZM} = (R_Z A_Z - R_M A_M)/(R_Z - R_M)$$

An analogous result holds for the other parameters in the temporal model.

4.4 EVALUATION OF LORAN-C FOR CIVIL AIRCRAFT NAVIGATION

The local operational models calibrated as described in Sections 4.2 and 4.3 provide a framework for evaluating the Loran-C system as a non-precision approach aid for civil aircraft navigation. Although this evaluation is necessarily preliminary, since data are collected at only five airports, it can lead to guidelines for further ground-based data collection and airborne operational testing.

The following procedure is recommended for predicting whether or not a particular receiver model operating in the single-chain hyperbolic mode can meet non-precision approach accuracy requirements at a particular airport.

- Select a Loran-C transmitter triad for analysis; since position accuracy depends on Geometric Dilution of Precision and temporal/spatial TD variations in a non-trivial manner, each possible triad should be analyzed.
- Obtain geodetic coordinates (latitude/longitude) for the waypoints which define the desired approach flight path

- Predict Loran-C TDs for each waypoint based on the receiver's geodetic-to-TD coordinate transformation, including all propagation corrections except those based on real-time calibration

- Compute yearlong TD time series for each waypoint based on the temporal and spatial local operational models applicable to the airport; these time series are assumed to characterize the true TDs

- Subtract the receiver-based TDs from the model-based TD time series to form TD error time series for each waypoint

- Transform two TD error time series to a position error time series for each waypoint by accounting for transmitter/airport geometry; the resulting time series represents the contribution of propagation-related errors to non-precision approach errors for flights at various times of the year

- Compute the sample-rms error over all time and all waypoints, for comparison with non-precision approach accuracy requirements.

The above methodology provides a straightforward means of approximating non-precision approach errors. The methodology can be refined to address the following additional issues:

- Reduction in the effect of temporal TD variations via real-time calibration

- Effect of dead-reckoning navigation and number of waypoints on non-precision approach accuracy

- Sensitivity of accuracy to the direction of approach flight path.

In addition to their utility in the analytic assessment of non-precision approach accuracy, the local operational models

can also be employed in airborne Loran-C tests. Specifically, test flights can be conducted with both manufacturer-provided propagation corrections and model-based corrections to directly ascertain the degree of improvement afforded by the latter. The models also have the potential to be implemented in Loran-C system simulators.

4.5 DATA ANALYSIS PLAN SUMMARY

The Loran-C data analysis plan provides a flexible framework for calibration and/or initial assessment of the proposed Loran-C signal propagation models. The calibrated models which result from implementation of the plan (i.e., temporal and spatial local operational models) are evaluated in the context of FAA Loran-C program goals. The following specific issues must be addressed in this evaluation:

- Model Accuracy - Statistics of the residuals between deterministic model predictions and data
- Model Complexity - Number of model parameters required to achieve the desired accuracy
- Model Robustness - Applicability of the models to other airports
- Calibration-Data Requirements - Data density (in time and space) required to calibrate the model for each airport
- Need for Differential Loran-C - Indicated by the frequency and magnitude of the temporal variations about the deterministic model prediction.

Analysis of the data from the initial NAFEC Loran-C data collection effort is not expected to permit a complete evaluation

of Loran-C. However, the analyses will permit the isolation of critical issues which must be addressed in future data collection and analysis efforts.

5. DATA MANAGEMENT SYSTEM DESCRIPTION

During the Loran-C data collection effort, diverse data will be collected for the analysis of variations in Loran-C propagation characteristics:

- Ground Monitor Data (Fixed and Mobile Monitors)
- Weather Data
- Chain and Monitor Locations and Descriptions
- Anomalous Event Data.

The data management system must provide a general and flexible framework which allows for simple and efficient storage, management, handling and processing of all data. The system should also provide preprocessing and screening of all data as it is entered into the system to insure both quality and integrity of the data. This latter process minimizes manual data handling to avoid errors in the data entry process. In addition to the above functions, the data handling system must maintain and provide easy access to the data for processing in the data analysis system. Various techniques of file storage and accessing were considered given the diverse nature of the data to be collected and the large quantity of measurements to be made. Possible changes and/or additions to the data collected also influenced the design of the system. The result is a data management system designed for maximum flexibility to accommodate changes in data collection procedures.

Specific recommendations concerning functional processing, file structures and implementation of the data management system are discussed in this chapter. Although the data collection effort has not commenced, specific examples of data output graphics and printouts are included based on TASC's previous experience with Loran-C data collection and data management.

5.1 SYSTEM OVERVIEW

The components of the Loran-C data handling system are computer programs and data files accessed by these programs. The data management system description is organized to discuss the computer programs in sequential order consistent with the manner in which Loran-C measurements are processed. Data are described at the point where they are first referenced by a program.

A system-level view of the major components of the data management system and their relationships is shown in Fig. 5.1-1. The output files are shown as input to the software which implements the data analysis techniques described in Chapter 4. The input data consists of:

- Loran-C measurements and supporting data and comments (i.e., signal-to-noise ratios, envelope to cycle differences, operator comments); the input data streams for the Austron 5000 and Micrologic receivers will have different formats
- Loran-C chain status information supplied by the U.S. Coast Guard
- Locations of transmitters and receivers

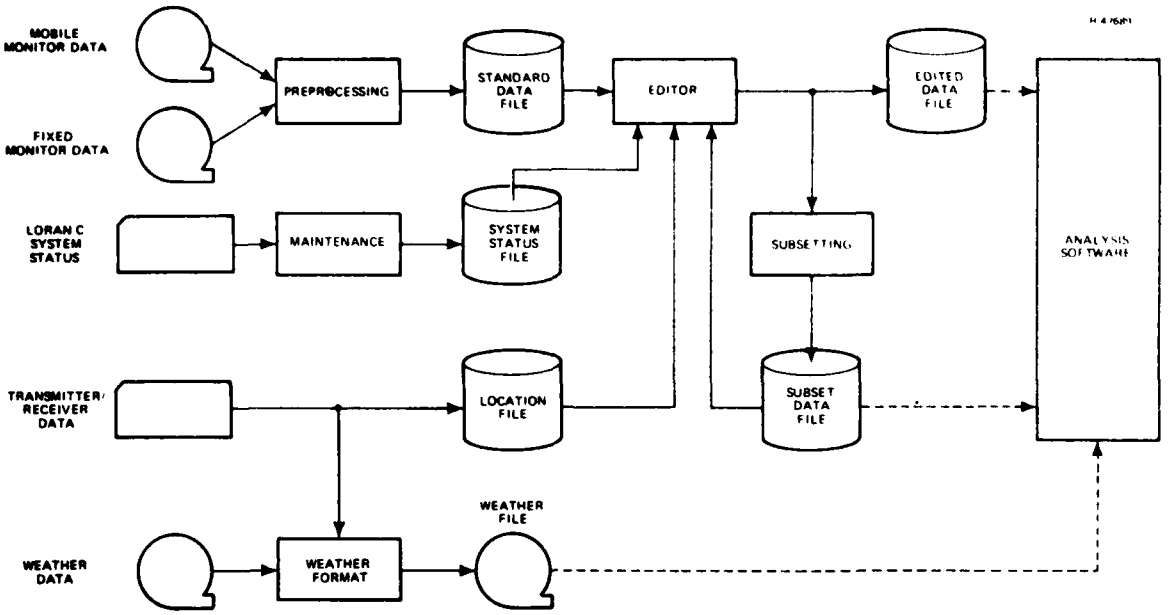

Figure 5.1-1 Data Handling System Overview

- Weather records in the time periods the Loran measurements were taken in a format supplied by the National Oceanic and Atmospheric Administration (NOAA).

Data collected from the Loran-C receivers are initially stored on cassette tapes. The data are then transferred to a magnetic tape which will become the master data tape. No data processing procedures are implemented during the cassette to magnetic tape data transfer. Loran-C chain status and chain operations data are manually recorded by the System Area Monitor (SAM) watchstander on the Loran-C Monitor Log, an example of which is included in Fig. 5.1-2. Arrangements must be made to have the Loran-C Monitor Logs delivered to NAFEC at approximately monthly intervals. Pertinent information

DEPARTMENT OF TRANSPORTATION
U. S. COAST GUARD
CG-3012 (Rev. 6-67)

LORAN-C TRANSMITTING STATION AND/OR MONITOR LOG

SHEET NO 12Ø MONTH

LOCATION OF UNIT: RIVERSIDE

RATE: 493Ø

STATION DESIGNATION: ☐ M ☐ X ☐ Y ☐ Z ☒ MONITOR

DATE (Greenwich): 21 FEB 1979

TIME GCT	MASTER SIGNAL	MASTER BLINK	SLAVE X STANDARD DELAY 11259.7Ø5 SIGNAL	SLAVE X BLINK	SLAVE X READING ENV.	SLAVE X READING CYCLE	SLAVE Y STANDARD DELAY 22363.87Ø SIGNAL	SLAVE Y BLINK	SLAVE Y READING ENV.	SLAVE Y READING CYCLE	SLAVE Z STANDARD DELAY 33200.4Ø5 SIGNAL	SLAVE Z BLINK	SLAVE Z READING ENV.	SLAVE Z READING CYCLE	REMARKS
1311															Y BLK, OOT.
[redacted]															[redacted] Y BOF, III TOL.
[redacted]															[redacted]
[redacted]															[redacted]
1400															STARTED DAILY SYSTEM SAMPLE.
------															TTY: X=-4 Y=-3 Z=-8
1416															MR. MARSHALL AND ET1 MCGUIRE DEPARTED FOR PICKFORD(X-RAY).
1420															SNET POWELL AND SA WATSON DEPARTED FOR GORDON LAKE(MASTER) THEN DENNIS(ZULU).
1500															END OF DAILY SYSTEM SAMPLE.
------															TTY: X=-6 Y=-15 Z=-15
[redacted]															[redacted]
1515															ZEROED Z CUMULATIVE.
1517															MR. MARSHALL AND ET1 MCGIURE ARRIVED AT PICKFORD(X-RAY).

1540															X BLK, OOT. X BOF. III TOL.
[redacted]															[redacted]
[redacted]															[redacted]
1600															TTY: X=+1 Y=-3 Z=-14
1604															Z BLK, OOT.
[redacted]															[redacted]
1606															Z BOF, IN TOL.
1607															SNET POWELL AND SA WATSON RETURNED TO MONITOR.

1613															X BLK, ABN. DUE TO ET'S PERFORMING MAINTANANCE. AWAITING Ø INSTRUCTIONS TO RSM.

1653															ET1 MCGUIRE CALLED TO INSTRUCT A RSM ON X.

REMARKS
(1) Clearly state fault and action taken to correct it or notify authority.
(2) At each significant change, record cycle peak-to-peak variation, signal to noise (S/N), signal to interference (S/I), and atmospherics (X).
(3) Record all WWV frequency and time checks.
(4) Record every change of watch and/or relief. Log shall be properly SIGNED OFF when relieved.
(5) At each change, enter oscillator dial settings (ODS).

STATION PAIR	M-X	M-Y	M-Z	SYSTEM
TOTAL BLINK				
TOTAL OFF AIR				
TOT. UNUSABLE				

EQUIPMENT AND COMPLETED LOG CHECKED BY (Signature of Watch Supervisor):

COMPLETED LOG CHECKED AND APPROV BY (Signature of CO or O-IN-C):

Figure 5.1-2 Example of Loran-C Monitor Log (Times and Values of LPAs are Highlighted)

relative to the status of Loran-C chains are extracted and manually entered into the data base for use in the data editing process. The transmitter and receiver data consists of latitude and longitude of Loran-C transmitter and data collection locations, the former supplied by the U.S. Coast Guard and the latter by FAA conducted surveys. Each data collection location is identified by a site number which is entered by the data collection personnel and automatically transferred to the cassette tape. In this manner, data can be collected at new sites simply by assigning a data collection site number to that location. Exact survey of additional sites can be accomplished at a later date. The frequency and availability of weather data is dependent on the site location; therefore, the weather data file requires a flexible input structure to accommodate various input formats.

The processing software consists of five programs; Preprocessor, Editor, Subsetting, Maintenance and Weather Format. The first three programs reformat the input data into file structures that facilitate future manipulation of the data. The Editor Program combines information concerning the quality of the measurements, as indicated by internal receiver standards calculated at the time measurements are recorded, and chain status information from SAM Loran-C Monitor Logs in order to identify anomalous data points. The results of the editing process are displayed in summary printouts and plots of the data. The Subsetting Program constructs data files from the edited data file to display specific sets of data (e.g., data from a fixed monitor for a specific time difference measurement and time duration).

5.2 MEASUREMENT PREPROCESSING

The purpose of the Preprocessor Program is to convert the variable format character data files written by the Loran-C receivers into standard format files using Honeywell internal representation of numbers for greater processing efficiency. Since the receiver files are potentially variable in format as experiments progress, the isolation of this variability from the rest of the data handling software is a prime goal of the preprocessor. In addition, data tapes from the field may contain a variety of anomalous records not automatically classifiable according to the established standards for the receivers. This may be due to hardware or software problems in the receiver or operator error. The Preprocessor Program detects such anomalous records and prints an exception report.

A flow diagram of the Preprocessor Program is given in Fig. 5.2-1. The input to the preprocessor consists of a 9-track magnetic tape, which is a copy of the tape cassettes produced by the receivers in the field. The input consists of sets of records containing characters in a small number of possible patterns. The preprocessor reads each record and classifies it based on criteria such as:

- Length
- Contents of Key Fields (Character Positions)
- Preceding Records.

The last criteria follows from the existence of groups of records in a fixed sequence such as illustrated by the format of the Micrologic receiver output in Fig. 5.2-2 and the

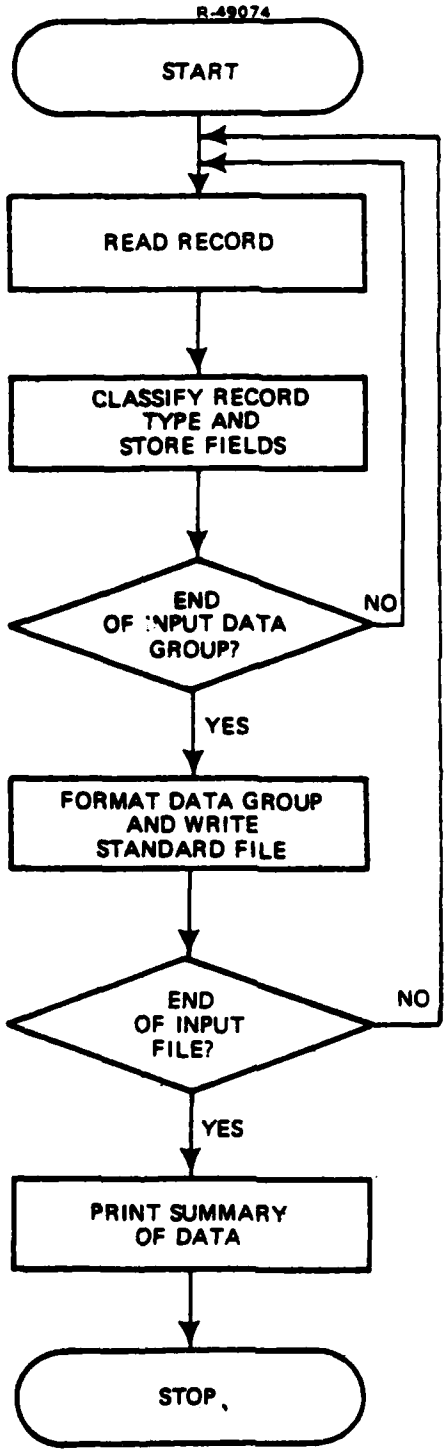

Figure 5.2-1 Preprocessor Program Flow Diagram

T-3483

```
LINE #1 ""RRRRRR//
LINE #2 ""DDDD HH:MM:SS//
LINE #3 "" MASTER AAAAA.AA BBBBB.BB CCCCC.CC DDDDD.DD EEEEE.EE //
LINE #4 ""     MMM       AAA       BBB       CCC       DDD       EEE //
LINE #5 ""     MMM       AAA       BBB       CCC       DDD       EEE //
LINE #6 ""       M         A         B         C         D         E //
LINE #7 ""       M         A         B         C         D         E //

WHERE  // = CARRIAGE RETURN AND LINE FEED
       R = OPERATION RECORD COUNT ("MANUAL" FOR MANUAL OPERATION RECORD,
           "######" FOR TIMED OPERATION RECORD)
       D = DAY
       HH:MM:SS = TIME OF DAY, HOURS:MINUTES:SECONDS
       M = INFORMATION FOR MASTER TRANSMITTER
       A = INFORMATION FOR SLAVE TRANSMITTER WITH SMALLEST TIME DELAY
       B = INFORMATION FOR SLAVE TRANSMITTER WITH NEXT LARGEST TIME DELAY
       C = INFORMATION FOR SLAVE TRANSMITTER WITH NEXT LARGEST TIME DELAY
       D = INFORMATION FOR SLAVE TRANSMITTER WITH NEXT LARGEST TIME DELAY
       E = INFORMATION FOR SLAVE TRANSMITTER WITH NEXT LARGEST TIME DELAY

LINE #3 IS THE TIME DELAYS OF THE TRANSMITTERS ("MASTER" IS OUTPUT FOR
THE MASTER), LINE #4 THE SNRS, LINE #5 THE ENVELOPES, LINE #6 THE MODES,
LINE #7 THE BLINK INDICATION (SPACE FOR NO BLINK, "*" FOR BLINK).
```

Figure 5.2-2 Micrologic Receiver Output File Format

Austron 5000 receiver output in Fig. 5.2-3. As an example, when the "line 1" record is recognized in the input tape, the subsequent records should conform to the patterns shown. The preprocessor classification criteria depends on the set of possible valid input records, as determined by the receivers. Because this set of records may change with time, dictated by new receivers or experimental modifications, the preprocessor logic should be implemented in a manner so as to be easily modifiable.

The existence of groups of records in a fixed format is critical for the Austron 5000 receiver since data recorded on the Austron 5000 tape casette includes information in addition to that indicated in Fig. 5.2-3. In particular, any operator keyboard inputs or status reports automatically generated by the receiver are transferred to the tape cassette. The Preprocessor Program must discriminate between valid data

T-3473

```
LINE #1   DDD HH:MM:SS  CHAIN 1
LINE #2  M AA  BBB CCCC DD.DD EEEEE.EE
LINE #3  W AA  BBB CCCC DD.DD EEEEE.EE FFFFF.FF
LINE #4  X AA  BBB CCCC DD.DD EEEEE.EE FFFFF.FF
LINE #5  Y AA  BBB CCCC DD.DD EEEEE.EE FFFFF.FF
LINE #6  Z AA  BBB CCCC DD.DD EEEEE.EE FFFFF.FF

WHERE  D = DAY
       HH:MM:SS = TIME OF DAY, HOURS:MINUTES:SECONDS
         CHAIN 1 = CHAIN DESIGNATOR
      M,W,X,Y,Z = STATION DESIGNATOR
             AA = INDICATOR OF RECEIVER MODE (ALPHABETIC OUTPUT)
            BBB = GAIN NUMBER
           CCCC = AVERAGE OF NOISE-DIFFERENCE NUMBERS
          DD.DD = CYCLE NUMBER
       EEEEE.EE = TIME OF ARRIVAL RELATIVE TO INTERNAL OSCILLATOR
       FFFFF.FF = TIME DIFFERENCE MEASUREMENT

LINE #2 IS INFORMATION FOR THE MASTER, LINE #3 CONTAINS INFORMA-
TION FOR STATION W, LINE #4 IS INFORMATION FOR STATION X, LINE
#5 IS INFORMATION FOR STATION Y AND LINE #6 IN INFORMATION FOR
STATION Z
```

Figure 5.2-3 Austron 5000 Receiver Output File Format

records, operator inputs and status reports. Operator inputs can be isolated from data records because operator input records start in the first column of the record field while valid data records start in either the second or third column. Status reports not only have to be differentiated from operator inputs on valid data records, the status message must be identified because they contain useful information concerning the operating conditions of the Loran-C system.

The general format of the status report is:

_DDD_HH:MM:SS_ _1,Y_ _MESSAGE_BGN(or END)

where

_ = Space
D = Day

HH:MM:SS = Time of day, Hours:Minutes:Seconds
1,Y = Chain designation, station designator
MESSAGE = Status report
BGN(or EDN) = Indicates condition has just begun (or ended)

An example of a status report is:

```
298 16:51:14  1,M  HIGH NOISE BGN
298 16:51:21  1,M  HIGH NOISE END
```

In addition to recognizing the HIGH NOISE status report, which actually indicates a poor signal-to-noise ratio, status reports for BLINK and SKYWAVE ERROR must also be discriminated. The data management system must also match the start and completion of status reports since, for example, a status report for the initiation of BLINK condition for station X can be followed by a status message for the initiation of HIGH NOISE for station Y before the issue of a status report for the end of the BLINK condition for station X.

Comparison of the Austron and Micrologic receiver outputs indicate a significant difference in the type of data, representation of the data and the data format. Differences which must be considered in designing the data management system include:

- The Austron 5000 output includes TOA measurements relative to an internal quartz-crystal oscillator, in addition to TD measurements. (These TOA measurements are subject to oscillator frequency variations.)
- The receiver mode indicator, which indicates receiver function at the time of the measurement, is an alphabetic representation for the Austron 5000 and numeric representation for the Micrologic receiver. To maintain files with numeric representation and maintain

consistency between receivers, Table 5.2-1 defines and converts the Austron representation to a numeric representation

- Austron 5000 chain and station designators (i.e., chain 1,M,W,X,Y in Fig. 5.2-3) are operator defined inputs, and the Preprocessor Program must accept the various designators

- A gain value is output for the Austron 5000 receiver only.

The output file of the preprocessor contains all input measurements which can be interpreted by the preprocessor labeled in a standard fashion. All output measurement data is classified into four groups and each group consists of up to five output files. The four groups are divided based on data from fixed site monitor #1, fixed site monitor #2, the Micro-logic mobile monitor and the Austron 5000 mobile monitor. This grouping is partially motivated to isolate differences in the data structure output from two receivers. Each output file within a group contains information related to a specific time difference measurement and supporting data (e.g., signal-to-noise ratio). In this manner, each group will have files for up to four time-differences and a supporting data file for the master transmitter for a maximum of five files for each group. The output file structures for each group should contain the following information:

Site Number - Numeric designation to identify the location where data are collected; approximately 50 to 60 sites will be utilized during the data collection period

Receiver Type - Numeric designation to identify either the Micrologic or Austron receiver

TABLE 5.2-1

RECEIVER MODE INDICATOR

T-3472

RECEIVER CONDITION	AUSTRON DESIGNATOR	MICROLOGIC DESIGNATOR	DATA BASE DESIGNATOR
Cycle Search	AC	1*	0*
Verify Cycle Search	AV	1*	1
Front-of-Pulse Search	AF	2	2
Verify Front of Pulse (Narrowband)	-	3	3
Verify Front of Pulse (Wideband)	-	4	4
Wait For Settling	AW	-	9
Verify Tracking Point	AS	5	5
Normal Tracking	AT	6	6
Low SNR - Cycle Not Verified	-	7	7
Low SNR - Cycle Verified	-	8	8
Not Searching	K	-	10

*Micrologic does not distinguish between cycle search and cycle verify. Micrologic mode designator of 1 will correspond to data-base designator of 1.

Record Count* - Numeric designator that each receiver outputs to identify the beginning of a new data record and automatically increments by one

Time - Time, expressed in days, hours, minutes and seconds, that the data was recorded

Time Difference - Loran-C time difference measurement

*Unique to the Micrologic receiver.

Signal-to-Noise Ratio - Receiver-generated estimate of signal-to-noise ratio

Gain* - Indication of the numeric gain utilized in third cycle crossing determination process

Mode - Numeric designator indicating receiver function (e.g., search, acquisition or tracking) at the time data is recorded

Envelope Number - Indication of where, relative to the third cycle, the determination of the third cycle crossing process initiates

Blink - Receiver indication, based on the blink indicator from the Loran-C transmissions, that a transmitted signal exceeds timing tolerances

Editing Marks - Numeric designators that indicate the "quality" of the time difference measurement; editing marks are assigned during the data editing process and are not part of the receiver data record.

The capability to process possible future TOA measurements can be included in the data-base management system by augmenting the file records with the TOA and associated editing marks.

The initial emphasis on designing a detailed record layout must be on both simplicity and flexibility. Records must be constructed in a fashion that makes them easier to interpret by both the data handling system and the analysis software. It is also important to use standard FORTRAN representations for each item within a record even if more compact representations are possible. For example, the BLINK indication

*Unique to the Austron 5000 receiver

is recommended as an integer value even though it could be represented by a single bit. Table 5.2-2 shows a recommended record layout for the measurement file. All files should be formatted identically and the appropriate quantities set to zero which are not applicable to a particular receiver. For a full year of data, sampled every 15 minutes, a file with this layout will require about 1/20 of a 2400-ft 1600 BPI magnetic tape.

TABLE 5.2-2
MEASUREMENT RECORD LAYOUT

T-3474

QUANTITY	FORTRAN TYPE	COMMENTS
Site Number	Integer	Numeric Designator for Receiver Location
Receiver Type	Integer	Numeric Code for Receiver Type
Record Number	Integer	
Day	Integer	Day Since 1 January 1980
Time	Integer	Time of Day in Hours, Minutes, and Seconds
Time Difference	Real	μsec
Gain	Integer	Receiver Function
Signal to Noise	Real	Receiver Function
Envelope Number	Integer	Receiver Function
Mode	Integer	Receiver Function
Blink	Integer	Receiver Indication
Range Mark*	Integer	Measurement Out of Reasonable Range
Outlier*	Integer	Number of Standard Deviations From Trend Line
Signal Quality*	Integer	Adequate/Inadequate Flag
Manual*	Integer	Operator-Supplied Flag

*Editing marks assigned during the data-editing process (See Section 5.3).

5.3 MEASUREMENT DATA EDITING

The procedure used to edit the Loran-C measurements should not eliminate any data. Rather than removing erroneous measurements, these data are flagged by editing marks which are an integral part of the edited data file. The editing criteria are discussed in detail in Appendix A. All flags, except a manual editing flag, are set by the Editor Program which reads the standard file output from the preprocessor and writes an edited file. The formats of the two files are the same, only the editing mark field values in the records are changed. Initially, the editing mark flags are set to some value indicating "unedited." Several runs of the editing program may be required to effectively set all editing marks, especially in the early months of operation when some engineering judgement must be applied in setting parameter bounds. Eventually, however, a "manual" editing mark should be the only non-automatic aspect of the editing program. Figure 5.3-1 depicts the Editor Program flow diagram.

Recommended editing marks are:

- Range - Measurement value is within expected upper and lower bounds
- Outlier - Measurement value is more than "n" standard deviations from the time series trend line
- Signal Quality - Signal "quality" is adequate
- Manual - Measurement is rejected, based on operator inspection of printout and plots

The signal quality indicator will include flags for poor signal-to-noise ratio, presence of "blink" in the signal (indicating

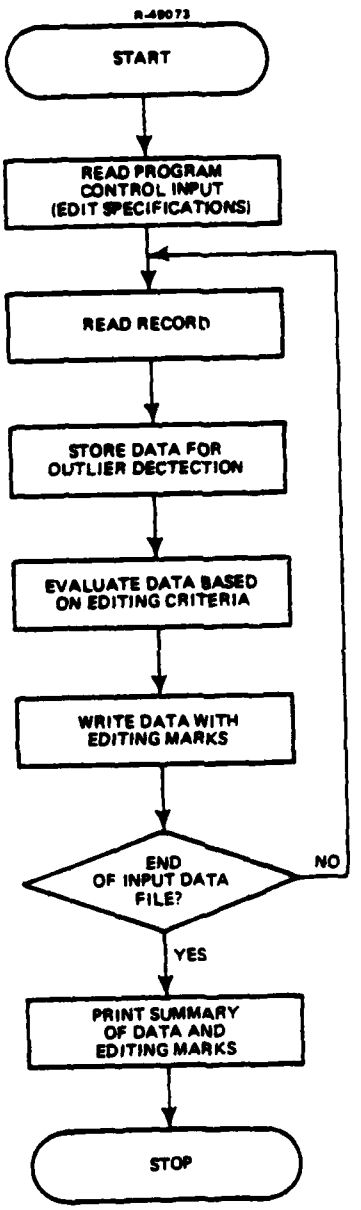

Figure 5.3-1 Editor Program Flow Diagram

that the chain is out of tolerance) and operator indication of poor signal quality recorded on the tape (through control settings or standard format comments).

The editing program processes all measurements on the standard input data file, or utilizes the Subsetting Program to prepare a subset data file if different editing criteria are needed for different classes of measurements (e.g., during certain time periods, certain transmitters, etc). The control input to the editor specifies, using Fortran NAMELIST input, which editing marks are to be applied and what criteria are to be used, if changed from the default (e.g., signal-to-noise ratio threshold). The manual rejection flagging is accomplished by a subroutine which is called to examine each record and transfer a flag to the program. Groups of consecutive data records spanning a time period are maintained in the program to enable outlier flagging to be accomplished. When a new record is read, it is added to its group (i.e., time difference measurement, receiver type) and the oldest record in the group is deleted.

The editing program prints summaries of all edited data points and corresponding editing marks of any editing performed, as well as plots of the data not assigned an editing mark. Operator inspection of the output, especially plots, is valuable for rapidly detecting anomalies in the data collection process, unanticipated signal behavior, or suspect data values not automatically flagged by the software. In the latter case, the editing program should be run to set the manual editing mark. Summary and graphical outputs of the Data Management System are discussed in Section 5.6.

5.4 SUBSET PROCESSING

It is frequently desirable to examine a subset of the available data set. This may be dictated by processing efficiency, for the purpose of a detailed analysis of an unusual phenomenon limited in extent in time and/or space or for graphical display. It is therefore useful to have a Subsetting Program, as shown in Fig. 5.1-1, which accepts a simple command language input to specify criteria for selection of a data subset. The Subsetting Program also interfaces with the standard data file shown in Fig. 5.1-1. The subset processor writes an output file in the same format as the standard (or edited) file which it reads. The output of the subset processor may then be run through the editing program if further manual editing is required or simply to verify data quality by means of the editing plots and printout.

The Subsetting Program flow diagram, Fig. 5.4-1, is controlled by card image input prepared by the user in a flexible format. The subsetting capability can be achieved by a combination of SELECT and REJECT criteria. The SELECT criteria can be used to establish broad collections of data. The REJECT criteria can be used to eliminate a few specific areas of data that may meet the selection criteria but are not acceptable in the subset being created. Thus, a data record is written to the subset if it is included in one of SELECT sets but is not included in one of REJECT sets. Table 5.4-1 shows recommended criteria to be used to define SELECT or REJECT sets. To illustrate the interaction of these sets, consider a simple system where the only subsetting criteria are YEAR and MONTH. An input stream such as the following might be used.

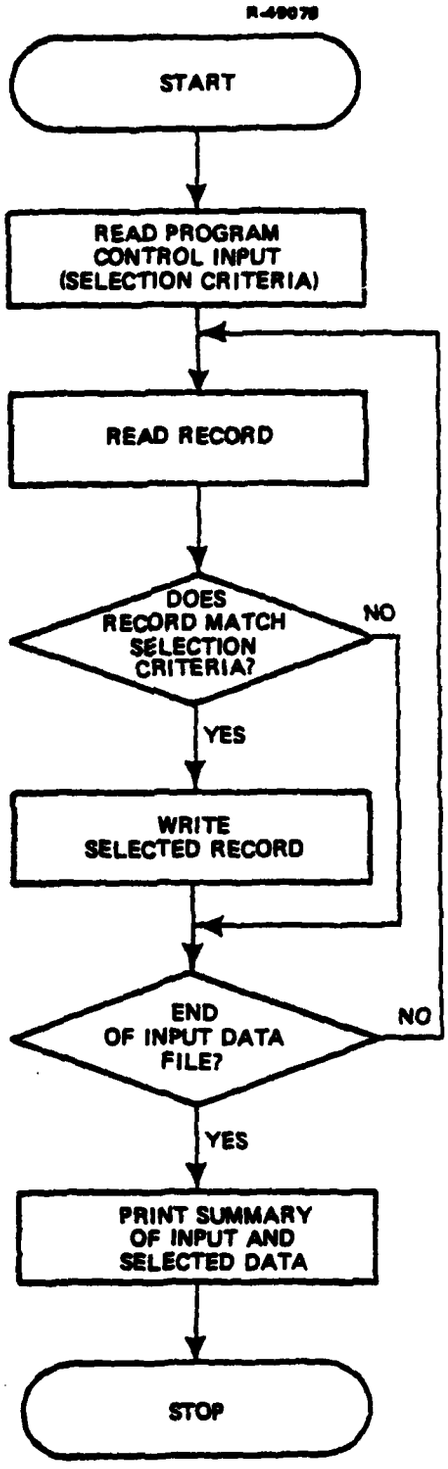

Figure 5.4-1 Subsetting Program Flow Diagram

TABLE 5.4-1

SUBSETTING PROGRAM CONTROL INPUT

T-3823

KEYWORD AND SAMPLE OPERANDS	EXPLANATION
YEAR 80 82	Year selection keyword. Year selection criteria will be years 1980 and 1982. Ten or less year operands may follow a 'YEAR' keyword.
MONTH 1 12	Month selection keyword. In this example only months 1 (January) and 12 (December) will be selected. Limit on the number of month operands is 12.
SITE 1	Site selection keyword. Receiver site selection criterion will correspond to site numerically designated '1'. 50 site operands may follow a 'site' keyword.
TD X Y	Time difference selection keyword. Time difference measurements of MX and MY are accepted. Four operands may follow a TD keyword.
CHAIN NE	Chain selection keyword. Chain name of 'NE' is accepted. Five operands may follow a CHAIN keyword.
SNR 0 20	Signal-to-noise ratio selection keyword. Measurements with SNR in the range of 0 to 20 dB are accepted. Two operands must follow a SNR keyword.
RECVR AUST	Receiver type selection keyword. Data taken with receivers of the indicated type are selected. Four or less operands may follow the RECVR keyword.
EDIT M2	Editing mark selection keyword. Data with marks of M (manual editing) are selected if they are greater than severity level 2 (see Appendix A). Five or less operands may follow the EDIT keyword.
EVERY 10	Data sampling selection keyword. Every 10th measurement time in the input data file is selected. One operand must follow the EVERY keyword.
DAY 3	Day of month selection keyword. Data taken on the third day of the month are selected. Up to 30 operands may follow the DAY keyword.
HOUR 7	Hour of day selection keyword. Data taken between 0700 and 0800 GMT are selected. Up to 24 operands may follow the HOUR keyword.

```
SELECT    YEAR    80
SELECT    YEAR    81    MONTH    1  2  3  4
REJECT    YEAR    80    MONTH    11
END
```

This input stream would lead to a subset of data that contains all records between January 1980 and April 1981 with the exception of data recorded during November 1980.

The operation of the Subsetting Program requires first processing the control input to build an internal table of selection criteria. The input data file is then read sequentially, the fields in each measurement record being checked against the selection criteria table. Records which are acceptable are written to an output file in the same format as the standard input data file. Appendix B contains suggestions on implementing this type of subsetting capability.

5.5 SUPPORT FILES AND PROCESSORS

This section describes the minor data handling system operations in support of the measurement processing described above. The file relationships are illustrated in Fig. 5.1-1. The location file contains information about the configuration of a chain and all data collection sites. Data stored in this file include station or site number and location (i.e., latitude and longitude). File manipulation on the location file is performed in order to:

- Add a data collection site to list of valid data collection sites
- Modify information about a data collection site
- Delete a data collection site.

Due to the small volume of data contained in this file, it is maintained in card image format via the system editor.

The system status file consists of records describing anomalous conditions for the Northeast U.S. Chain as specified by chain operations data manually recorded by the SAM watchstander (illustrated in Fig. 5.1-2) or receiver problems as recorded by FAA personnel performing the tests. These data are manually transferred from logs to create a chain and receiver status file which indicates when problems with chain or receiver operations are causing erroneous data to be collected. In this manner, the system status file indicates the reliability of the chain and receivers during the data collection period. A file containing the events to be added is generated via the system editor and submitted to the file update program. Separate designators are required to distinguish between transmitter and receiver problems. Input fields are checked for valid chain identifiers, transmitter identifiers, reasonable dates, reasonable times, and valid event identifiers, and an exception report is generated to list all invalid records. Optionally, reports of the history of individual transmitter or receiver reliability can be generated.

The weather data file contains weather data as received from the National Climatic Center for various weather stations. Because weather data are available in both tape and chart formats, the data management system must have the capability to interface with both types of input data. An example of climatic data in a chart format is depicted in Fig. 5.5-1. The weather data file contains a subset of this data, including the following information:

- Data Collection Site (Latitude/Longitude)
- Data Collection Time

- Data Averaging Time
- Temperature
- Relative Humidity
- Pressure.

Climatological data from the National Weather Service for ground conditions and if available at an altitude of 1.0 km is entered into the file. The latter data allows an estimate of vertical lapse rate to be derived. The averaging time indicates whether the data characterizes an instantaneous reading or an average over a previous time period.

5.6 SUMMARY AND GRAPHIC OUTPUTS

To check the validity of the data or isolate possible equipment problems, summary printouts of the data are required. Summary printouts are divided into detailed and quicklook printouts. The detailed printouts are a listing of all data contained in a file or a subset of the data in a file. These printouts are formed by the Subsetting Program described in Section 5.4. The quicklook printouts are part of the preprocessing and editing programs. These printouts are intended to provide an overview of the type of new data being entered into the system and an indication of the overall quality of the new data. The quicklook printout associated with the Preprocessor Program indicates the quantity of time difference measurement at each site associated with data being input to the system. For each time difference measurement, the site number, type of recorder, data collection time period and the number of measurements is printed. The quicklook summary associated with the Editor Program has the same information as the Preprocessor quicklook but specifies the number of data

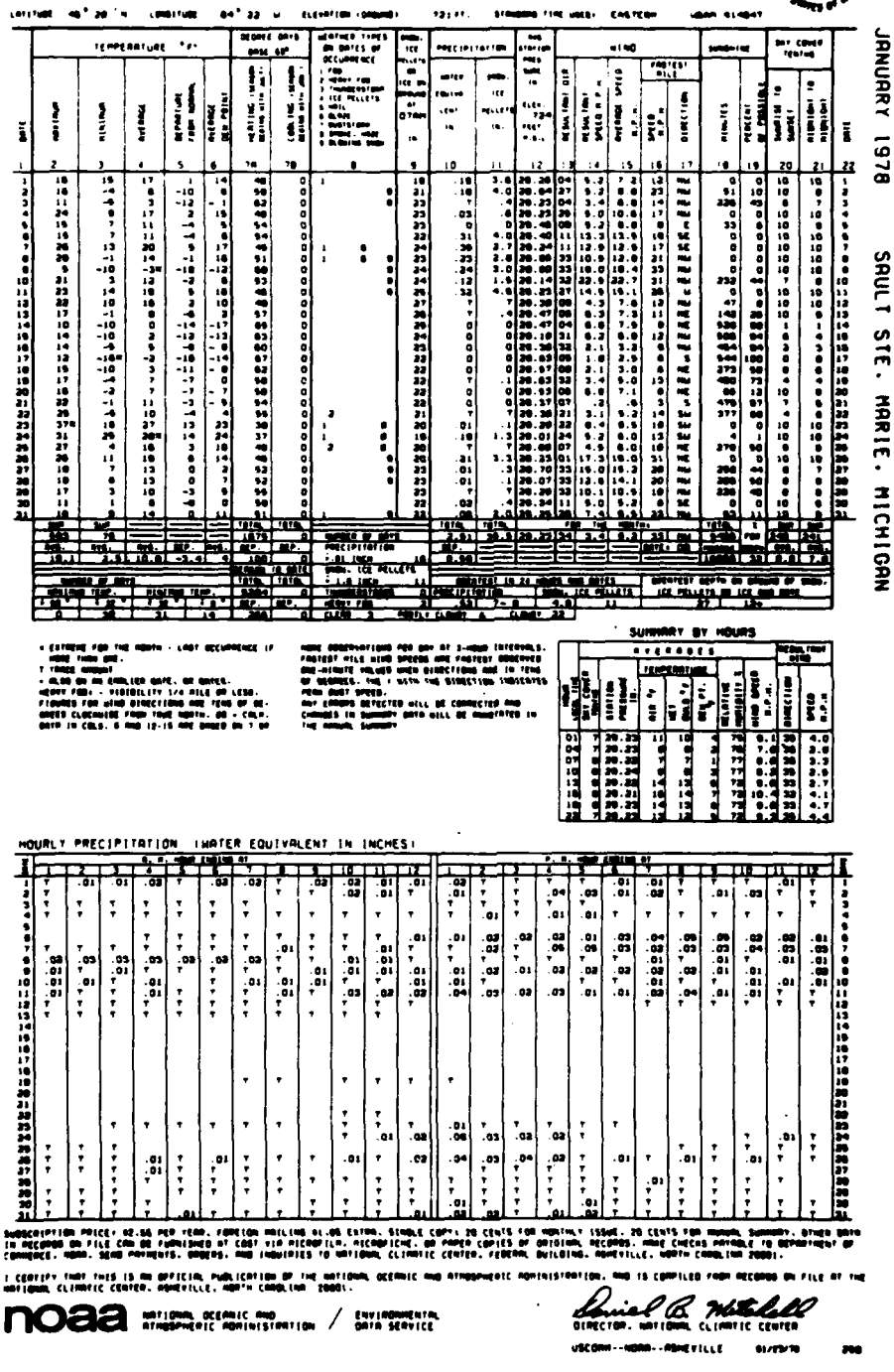

JANUARY 1978

SAULT STE. MARIE, MICHIGAN

NATIONAL WEATHER SERVICE OFC

CITY-COUNTY AIRPORT

Local Climatological Data

MONTHLY SUMMARY

JANUARY 1978 SAULT STE. MARIE, MICHIGAN

Figure 5.5-1 Example of Weather Data Supplied by National Weather Service

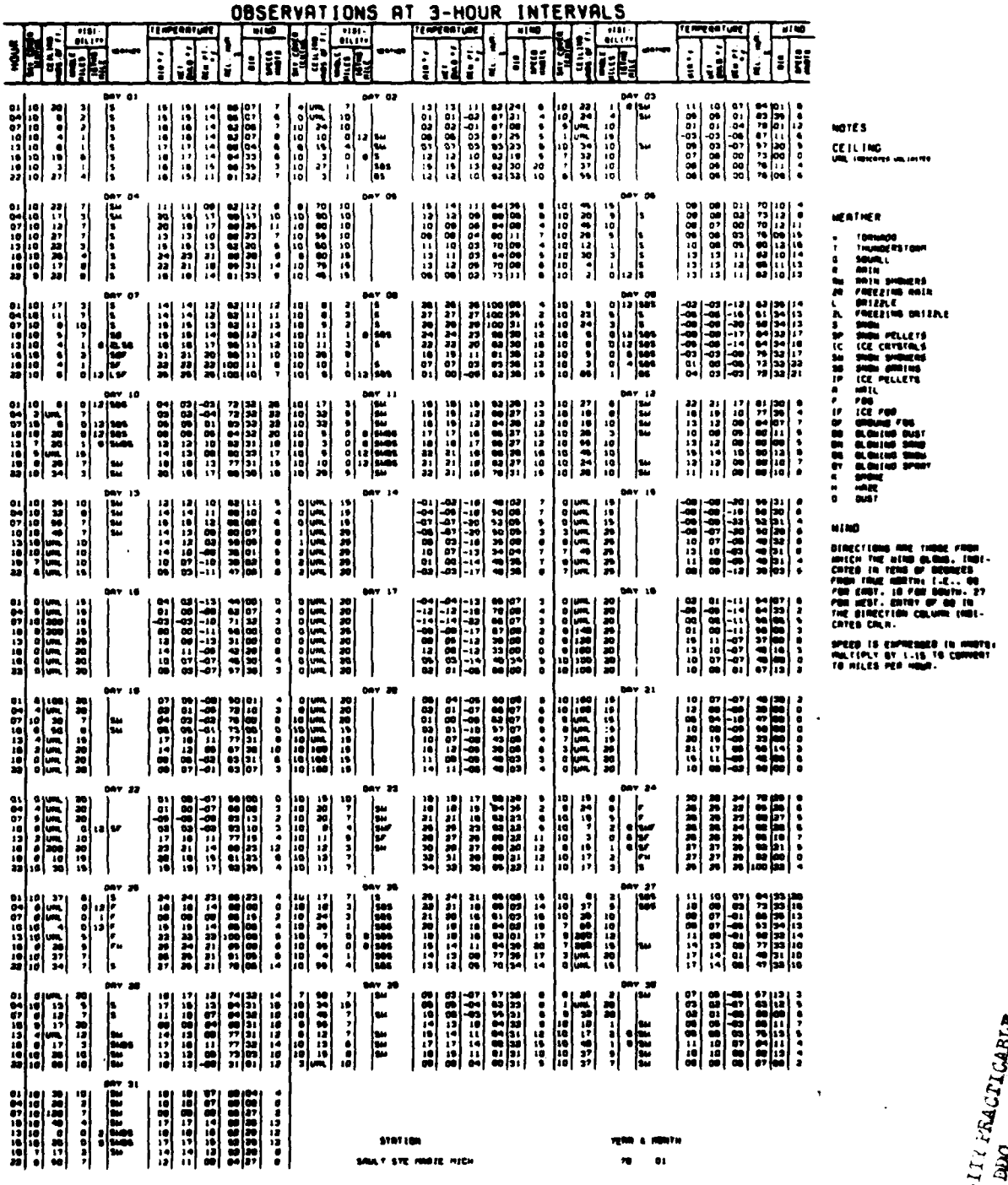

Figure 5.5-1 Example of Weather Data Supplied by National Weather Service (Cont'd)

points that were flagged for each of the four general editing marks specified in Section 5.3.

The most efficient manner to review data is with graphic outputs. A separate graphics package should be developed to interface with the Subsetting Program. Plots which have been useful in TASC analyses of St. Marys River Loran-C data are shown in Fig. 5.6-1 through Fig. 5.6-4 and are recommended as part of the data collection system. Figure 5.6-1 is a plot of an edited TD time series, together with the mean and $\pm 1\sigma$ levels associated with these data. Sliding-window (2 hr) smoothing has been employed to produce a statistical summary of the same TD time series, which is presented in Fig. 5.6-2. The $\pm 1\sigma$ levels associated with data in the sliding window are included on the plot so that the smoothed time series can be interpreted in the context of the variability of the actual time series. In Fig. 5.6-3, the mean diurnal cycle and associated $\pm 1\sigma$ levels are plotted for sample TD data. The diurnal cycle is computed by a sliding-window (2 hr) smoothing after sorting the time series by time of day. In addition to time-series plots, histograms of the TD data can aid in the manual detection of outliers and the statistical description of short-term behavior. An example of a histogram is presented in Fig. 5.6-4 for TD data. A flow diagram of the Plot and Print Program is illustrated in Fig. 5.6-5.

5.7 IMPLEMENTATION CONSIDERATIONS

This section discusses the following implementation issues:

- System Hardware
- Computer Languages
- File Accessing
- Program Design.

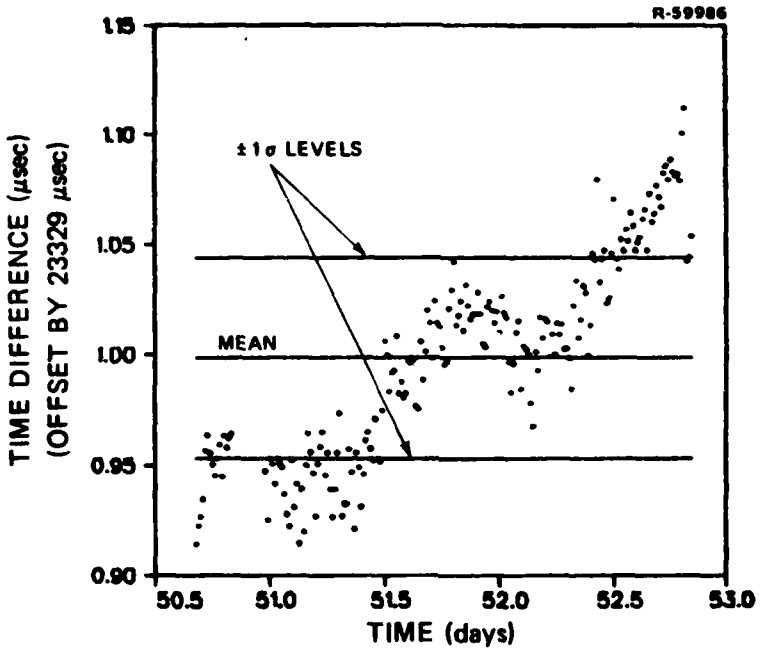

Figure 5.6-1 Example TD Time Series Data Plot

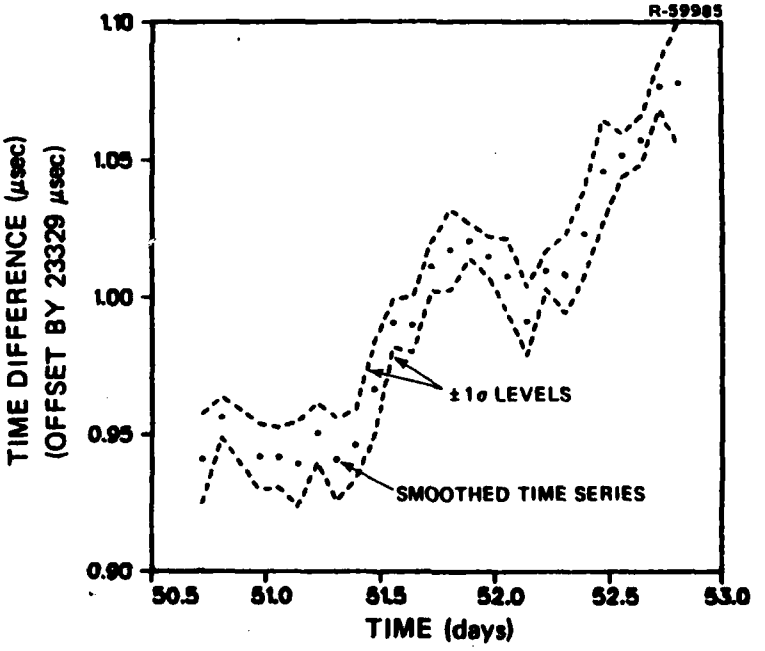

Figure 5.6-2 Example Smoothed TD Time Series Data Plot

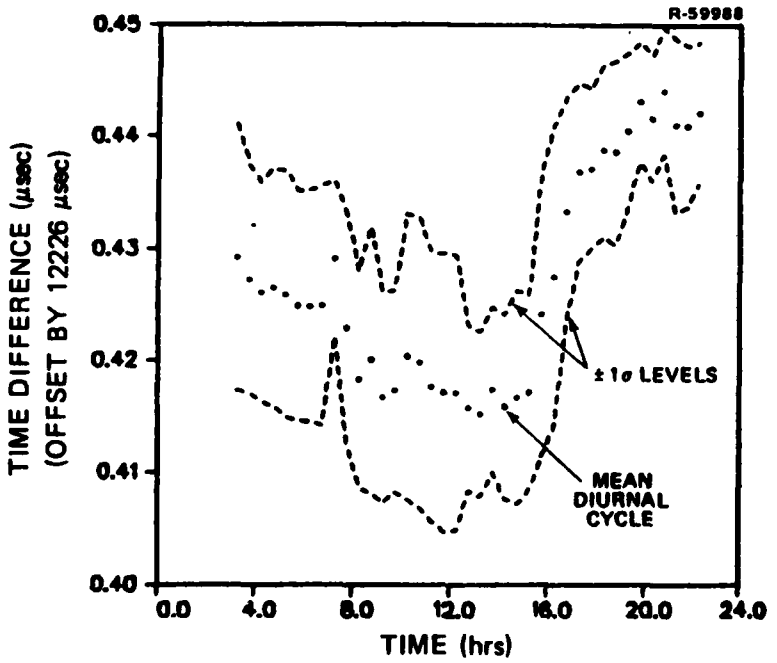

Figure 5.6-3 Example Diurnal Cycle Plot for TD Data

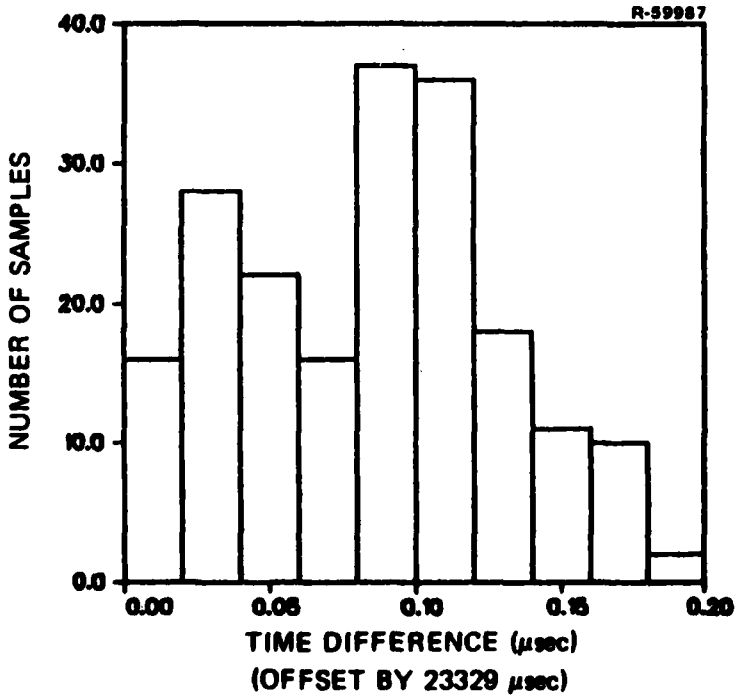

Figure 5.6-4 Example Histogram for TD Data

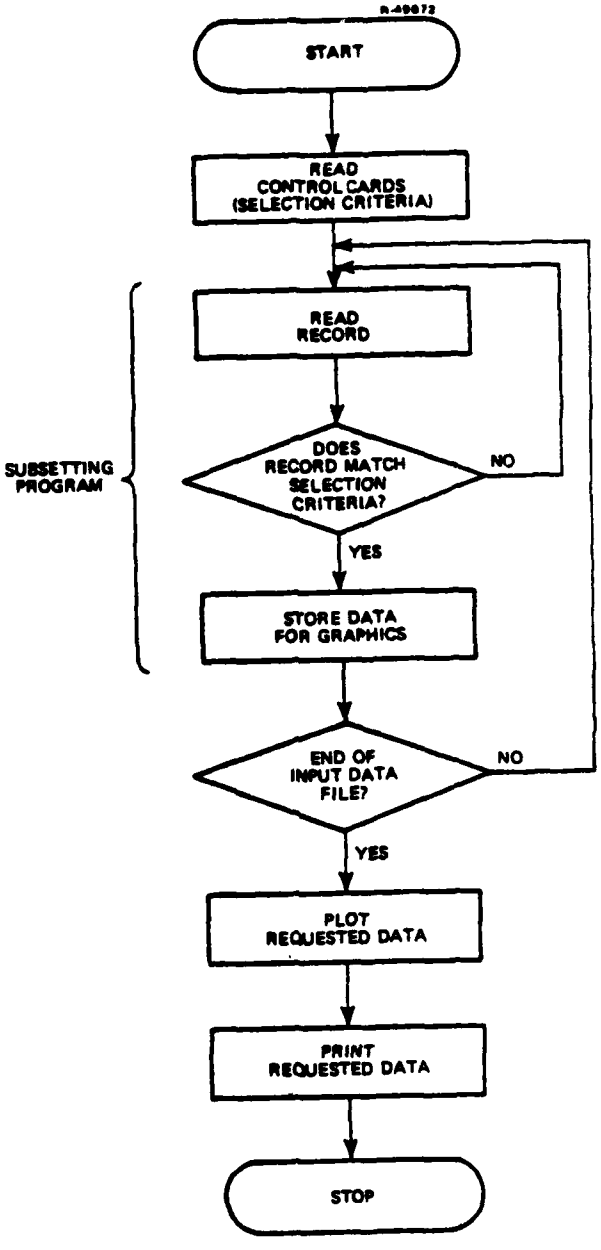

Figure 5.6-5 Plot and Print Program Flow Diagram

These items have been considered in order to maximize the utility of the data management system on the FAA Honeywell 6070 computer and to allow for potential implementation on TASC's IBM 3031. Implementation on both machines will provide data base development support during the data collection and data analysis phases and provide an alternative processing site in the case of a system failure. To reduce development time and maximize compatibility with both hardware configurations, it is recommended that the system be coded in ANSII FORTRAN. This will also simplify maintenance and future enhancement of the data management system.

After careful investigation of available data management and file accessing systems, it is recommended that the data management system utilize sequential files. Sequential organization will allow data to be stored on either disk or tape. A direct (random) access organization could be used to reduce the time required to access a few data items. The problems with direct access, however, include: no ANSII standard, data files must be on disk, and difficulty in modifying the structure. The file structure for the measurement data (Section 5.2) provides for a relatively small number of moderate sized files. At most there will be 20 files with 35,000 records each. The data within each file should be organized chronologically, and the software should be designed to ensure requests for data are made in chronological order. Also, sequential organization will speed development time and simplify modification which will be required if the system is required to process new or changed record formats.

It is important that state-of-the-art design and programming techniques, including top-down design and structured programming, be followed in implementing the data management

system. These concepts are particularly important for the data management system since it is a research support system, and possible new requirements could require substantial software and file changes. A good design for each individual program will minimize the cost of required changes. In particular, the design should allow for the straightforward accommodation of the types of changes indicated in Table 5.7-1. All non-ANSII-standard Fortran code should be isolated in subroutines. To minimize the time and expense associated with any future transfer of data between different computer systems. Modularized code increases testability and reliability of the software, and simplifies modifications and enhancements which may be required as the data management system is utilized.

TABLE 5.7-1
POSSIBLE SYSTEM CHANGES

T-3475

SITUATION	DESIGN APPROACH
File changes due to - receiver equipment changes - new editing marks - need to compress the data files	Localize file access to a single subroutine. Pass each subroutine only those data items related to its function. Avoid compressing files until the system is "stable".
New subsetting requirements	Define a separate routine for each type of subsetting; include a stub where "one time" subsetting requests can be implemented.
More complex editing specifications	Define a separate routine for each type of editing mark. Define a data structure to hold all the data within the window used for the trend line.
Interactive execution	Isolate control input processing so that it can be enhanced later; isolate processing routines so they will remain unchanged even if the control structure changes.
Simultaneous access to several measurement files	Code the FORTRAN logical unit number as a variable so it can be changed during execution.
Substantial change in data volume	Insure tapes and disks can be easily interchanged.

6. SUMMARY

Efforts have been devoted to developing a unified data collection and analysis plan to support NAFEC and the FAA in the assessment of Loran-C as either a replacement for or supplement to the current network of VOR/DMEs. This effort has focused on four specific areas:

- Developing mathematical models of temporal and spatial variations in Loran-C signal phase
- Developing data collection procedures to enable an assessment of the accuracy and adequacy of proposed models
- Defining a data analysis plan that will enable maximum utilization of the data collected in identifying parameters of the proposed models and cause and effect relationships of Loran-C temporal variations
- Defining a plan for the design of a data management system for the storage and maintainance of collected data and an efficient interface for data analysis programs.

Two specific model structures have been developed; the first is referred to as an operational model and the second a sensitivity model. The operational model is intended to characterize spatial and temporal variations in Loran-C signals so as to provide a reference for use in certifying airborne equipment and conducting analytic system-level Loran-C studies, and for implementation in Loran-C system simulators. Because of the diverse accuracy requirements between the

non-precision approach and enroute/terminal flight, the operational model is a two-tier model consisting of a global and local model. The global model is intended to meet the enroute and terminal Area Navigation requirements. It is recommended that the global model be based on the U.S. Coast Guard TD grid. The local model is intended for the non-precision approach phase of flight and is divided into a temporal component for the airport and a spatial component to account for variations in the approach area. Model structures for the local model have been developed and will be assessed as data are collected.

The sensitivity models have been developed to enable identification of areas where significant temporal variations might occur or to define directions relative to selected test sites where significant spatial variations might occur. An advantage of the sensitivity models is that they are a function of geometric parameters (i.e., range and bearing) and not propagation-related parameters. This is possible since only sensitivity of TDs to variation in propagation parameters are desired and not the absolute TD variation. This structure allows the sensitivity models to be used before data are collected to aid in defining data collection sites which will maximize the observability of Loran-C signal variations.

The data collection plan, designed to support the assessment of the specified models, is divided into two portions. The first is a continuous collection of Loran-C data at two sites - Buffalo, NY and London, KY. The second is local site data collection at five airports. Continuous data collection will allow further evaluation of cause and effect relationships of Loran-C temporal variations, provide data which will be used to determine if the global model must be augmented with a temporal model, allow for an assessment of the temporal portion of the local model, and to examine correlations between

various TD measurements. The local site data is intended primarily to identify the magnitude of spatial variations in the approach area of five airports and, in turn, to determine how adequate the local site spatial model is in compensating these variations. A second use of the local site data, since two receivers will be at each site, is the assessment of the utility differential Loran-C.

Another aspect of the local site data collection is to provide for an assessment of the operational adequacy of Loran-C, in terms of susceptibility to noise and interference effects, in the ground environment of the five local site airports. This will be accomplished through monitoring RFI, with a spectrum analyzer, at various airport facilities (e.g., VORTAC, ILS, airport surveillance radars, etc) and recording of signal-to-noise ratios with and without notch filters.

In summary, mathematical models have been defined and data collection procedures recommended to enable subsequent evaluation of proposed models. A data management and data analysis plan have been formulated which will allow this model evaluation process to be accomplished in an efficient manner once data are collected.

APPENDIX A
LORAN-C MEASUREMENT DATA EDITING

This appendix discusses the algorithms used by the Editor Program of the Loran-C data management system, as discussed in Section 5.3. Four editing marks - Range, Outlier, Signal Quality and Manual are set based on TD measurement values.

A.1 RANGE EDITING

The range editing mark indicates whether or not the value of a TD falls between expected lower and upper bounds (thresholds); e.g., the editing mark is set to the value "0" if the TD is within the expected bounds and to the value "1", otherwise. Because the purpose of the range editing mark is to isolate TDs which are clearly in error, the lower and upper bounds are chosen to bracket any physically reasonable temporal variations.

TASC experience with Loran-C data indicates that bounds set by a priori theoretical consideration may poorly reflect actual signal behavior. A normal value should be established by inspection of early data taken at a data collection site, and the lower and upper bounds will be established relative to these nominal TDs. A result of choosing the bounds in this manner is that the range editing mark flags cycle jumps as well as any gross TD errors resulting low SNR, lost signals, or malfunctions in receiver equipment and chain

operations. If the deviation of a TD from the nominal TD is less than the established tolerance at a particular sampling time, but is clearly abnormal with respect to adjacent samples on the TD time series, it is detected as an outlier and flagged by the outlier editing mark.

A.2 OUTLIER EDITING MARK

The outlier editing mark is employed to flag TD data which are inconsistent with the short-term behavior of the TD time series, but which are not flagged by other editing marks. Such outlying data in a TD time series are not likely to be caused by temporal variations in the Loran-C signal propagation medium, but rather by unusual atmospheric noise or transmitter/receiver anomalies. Therefore, it is reasonable to edit outliers prior to performing detailed analyses of temporal grid instability. Nevertheless, an attempt should be made to isolate the cause of the outliers by carefully examining signal quality indicators such as SNR, ECD and weather data recorded by the National Weather Service.

It is more difficult to design a technique which automatically detects outliers in a time series than it is to design a similar technique for a data set collected at a single time. For example, care must be taken not to interpret trends as outliers or outliers as trends. A useful outlier detection method is illustrated in Fig. A.2-1, where three samples (at times t_1, t_2 and t_3) in a TD time series are examined by the outlier test. A time window is defined which is centered on the test data point. Since a time window is constructed for each sample of the TD time series, the window is referred to as a sliding window. All data which are contained in the window and are not erroneous according to other

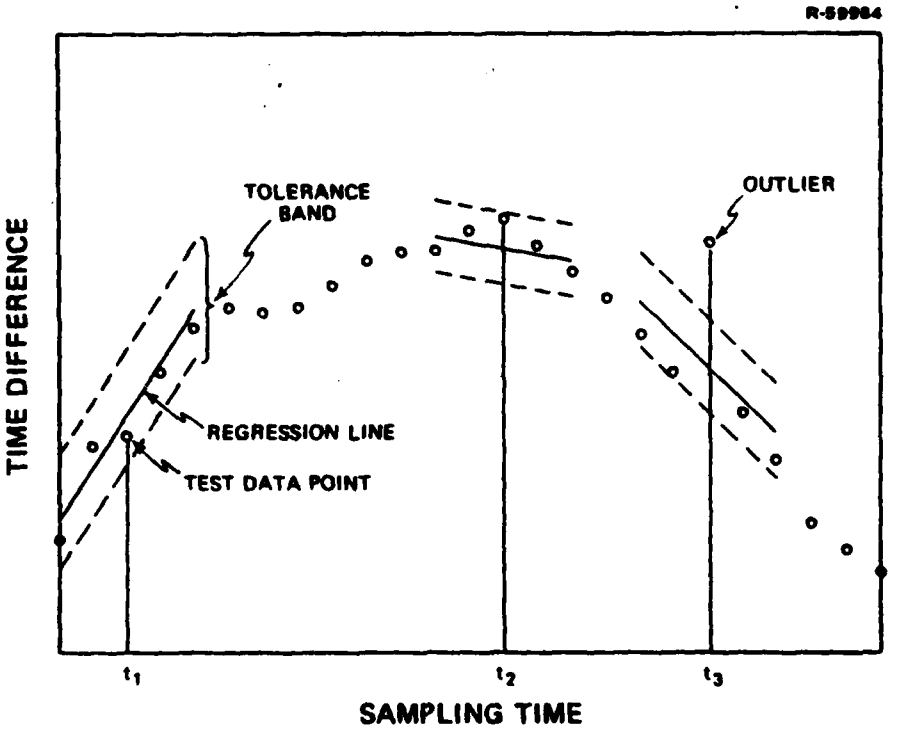

Figure A.2-1 Illustration of Outlier-Detection Procedure

flags or editing marks are least-squares fit by a regression (or trend) line. The test data point is then checked against a tolerance band of width σ, centered on the regression line. If the test data point is within tolerance, the outlier editing mark is set to "0". Otherwise, the outlier editing mark is set to "1", "2" or "3" to indicate that the test data point differs from the regression line by 1σ to 2σ, 2σ to 3σ, or more than 3σ, respectively. If a test data point does not qualify for the outlier test because it is erroneous according to other flags or editing marks, the outlier editing mark may be set to "4" (not usable). If the time window contains too few samples to permit accurate estimation of the time series trend, the outlier editing mark may be set to "5" (too few samples).

Application of the outlier detection method described above requires the specification of the time-window width, the minimum number of samples permitted in a window, and the tolerance σ. These parameters will be chosen based on analyses of data collected during the first month of the data collection effort. The following factors will be considered in the choice:

- The time window must be wide enough to show outliers in perspective to the rest of the time series, and thus depends on the frequency and duration of outlying data
- The time window must be narrow enough so that high-frequency components of grid instability are not interpreted as outliers
- Enough samples must be included in the window to decrease the effect of outliers on the calculation of the regression line
- The tolerance σ should be large enough to accommodate high-frequency grid instability.

Reasonable initial parameter choices may be a tolerance of 50 nsec and a window of 2 hrs containing at least five samples. However, these parameter values should be adjusted based on real data processing.

It must be emphasized that the detection of outliers can be accomplished quite efficiently by eye but an automatic procedure has the advantage of objectivity and minimal data handling. If outliers (determined by eye) remain after the automatic outlier detection procedure is applied, they are flagged manually by the manual editing mark.

A.3 SIGNAL QUALITY EDITING MARK

The signal quality editing mark is composed of a number of criteria related to the quality of the received signal. These will consists of:

- Receiver indicated signal-to-noise ratios below a certain prespecified threshold
- Receiver indication of blink
- Any anomalous condition as specified in the System Status File.

Since the receiver generated SNR estimate is based on a measure that differs for each receiver, a separate threshold is required for the Austron and Micrologic receivers. The signal quality editing mark is summarized by one of the following values: good signal quality (0), poor signal-to-noise (1), blink (2) or anomalous condition (3).

A.4 MANUAL EDITING MARK

The manual editing mark is employed to manually flag suspect data which are not flagged automatically by other editing marks. Data are selected for manual editing based on the following information:

- Signal related indicators which may not be examined automatically in the pre-processing program (see Section 5.2)
- Plots of the edited TD time series and the associated histogram which may reveal outliers which are not detected by the outlier test (see Section 5.2).

This information is summarized in a value of the manual editing mark; for example: no manual editing (0), poor signal conditions (1), or outlier data (2).

If there is more than one reason for signal quality or manual editing of the TD data, the most important reason is indicated by the editing mark. For example, if transmitter problems and poor signal-to-noise conditions are encountered simultaneously, the manual editing mark would be assigned the value "3" to indicate a transmitter malfunction.

APPENDIX B
DESIGN OF SUBSETTING PROGRAM

This appendix describes a design approach that TASC has used to implement data subsetting capabilities similar to those required by the data management system. The purpose here is not to specify all the details for this particular system, but to show an approach that could be used.

There are three primary components to the subsetting system:

- Software to compare each record on the input file to the selection/rejection criteria
- Software to read and interpret the subset specifications
- A data structure that provides a compact, efficient representation of the selection/rejection specifications.

B.1 DATA STRUCTURE

The first step is to design a data structure that will hold the information that is described in Section 5.4. Since the implementation of this structure will be in FORTRAN, it is necessary to specify a maximum size - for example, no more than ten selection and rejection criteria. The number ten is arbitrary, but it is perhaps a reasonable tradeoff between user flexibility and program memory requirements. For each type of criteria there is a two-dimensional array of

either logical or real variables. If there is a reasonably short list of possible values, the array should be logical. For criteria where a maximum/minimum range of values is appropriate, the array should be real. Each row of the array corresponds to a selection or rejection criterion. For logical arrays, each column corresponds to a possible discrete value. For real arrays there are two columns; the first holds minimum values and the second holds maximum values. There is also a need to keep a single dimension array of integers that describes whether a given row in the two-dimensional arrays is a selection criteria, a rejection criteria or unused.

For example, the input stream

```
SELECT    MONTH  11  12  YEAR  80
REJECT    SNR  -1000  5
SELECT    MONTH  1  2  3  YEAR  81
END
```

selects data from the winter of 1980/1981 but will only accept data if the signal-to-noise ratio is high. The resulting data structure would be as shown in Fig. B-1. The arrays for other criteria such as TD, DAY, etc would have the default values.

B.2 CONTROL INPUT PROCESSING

The inputs to the control input processing are the SELECT and REJECT statements and the output is the data structure. There is a clear tradeoff here between the amount of flexibility for the user and time required to develop this portion of the subsetting capability. If the design is carefully thought out, the development costs can be kept within reasonable limits and the user interface can be quite friendly.

T-3484

```
INTEGER  IROW  (10)  /10 * 0/
LOGICAL  LMONTH  (10,12)/120*.T./, LYEAR (10,5)/50*.T./
REAL  SNR (10,2)/10*-1000.,10*10000./
```

		LMONTH												LYEAR					SNR	
ROW#	IROW	1	2	3	4	5	6	7	8	9	10	11	12	1	2	3	4	5		
1	1	F	F	F	F	F	F	F	F	F	F	T	T	T	F	F	F	F	-1000.	10000.
2	2	T	T	T	T	T	T	T	T	T	T	T	T	T	T	T	T	T	-1000.	10.
3	1	T	T	T	F	F	F	F	F	F	F	F	F	F	T	F	F	F	-1000.	10000.
4	0	T	T	T	T	T	T	T	T	T	T	T	T	T	T	T	T	T	-1000.	10000.
.	.	.											.	.	.	.	.	.		
.	.	.											.	.	.	.	.	.		
.	.	.											.	.	.	.	.	.		
10	0	T	T	T	T	T	T	T	T	T	T	T	T	T	T	T	T	T	-1000.	10000.

Notes:

1) The values in elements of IROW are 1 - selection criteria; 2 - rejection criteria, 0 - unused.
2) The columns in LYEAR have been chosen as column 1 - 1980, column 2 - 1981, etc.

Figure B-1 Sample Data Structure

In particular, restrictions such as column alignment of fields in the input record or order of the specifications should be avoided. Also, the user should have to specify a minimal description of the desired subset.

To achieve these goals, it will be necessary to examine the input stream carefully and interpret the contents. To simplify the discussion, the following definitions will be used:

TOKEN - any TYPE, KEYWORD, VALUE, or TERMINATOR specification in the input stream. TOKENS are preceded and followed by blanks

TYPE - specification of SELECT or REJECT in the input stream

KEYWORD - a category for subsetting such as TD, YEAR, SNR, etc (Table 5.4-1)

VALUE - a specific item or limit to be used to determine a subset

TERMINATOR - the word END.

Figure B-2 gives an overview of the logic necessary to process the input stream. The flow shown here is only for elements in the data structure that hold true/false values. For arrays that hold maximum and minimum values some slight extensions are needed. Also, there is a need to test for invalid conditions. Since these conditions should be handled by a printed message and program termination, there is no need to show them on the overview flow chart. The boxes on the flow chart that should be implemented as separate subroutines are:

- Get Next/First TOKEN - read a card image, examine it a character at a time until a token is found, remember how much of the card has been examined, read the next card (if necessary), return the value of the TOKEN
- Classify TOKEN - compare the value of the token with a table of types, then keywords, if it is neither, assume it is a value, return an integer code indicating the kind of TOKEN
- Convert to integer - the value is in character form and must be converted to integer.

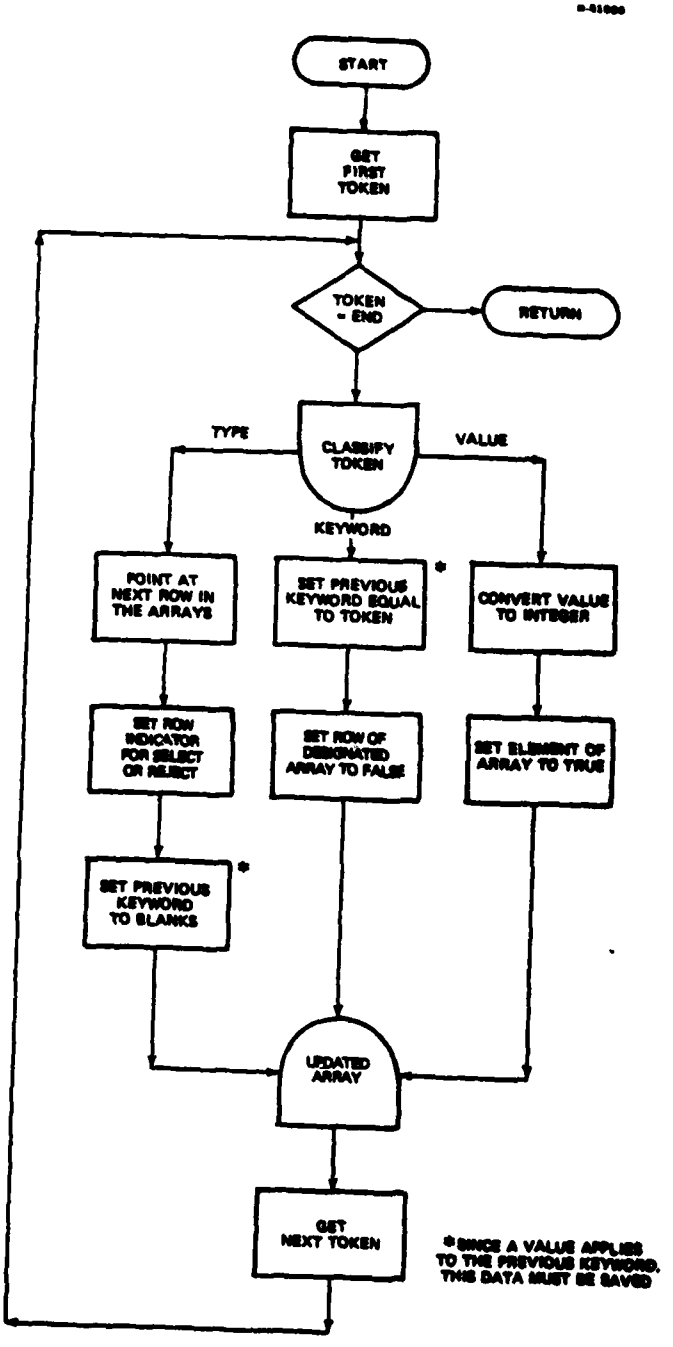

Figure B-2 Control Input Processing

REFERENCES

1. Quinn, G., "Loran-C and Omega in Aviation," Conference Proceedings Navigation in Transportation, U.S. Department of Transportation, Report No. DOT-TSC-RSPA-78-22, November 1978.

2. "Approval of Area Navigation Systems For Use in the U.S. National Airspace System," Federal Aviation Administration, Advisory Circular AC-90-45A, 21 February 1975.

3. DePalma, L.M., and Schoen, E.A., "Review of NAFEC Loran-C Signal Monitor Test Plan," The Analytic Sciences Corporation, Technical Information Memorandum TIM-1021-1, May 1979.

4. "Specification of the Loran-C Transmitted Signal," U.S. Coast Guard, Draft Report, August 1979.

5. Johler, J.R., Keller, W.J., and Walters, L.C., "Phase of the Low Radio Frequency Groundwave," National Bureau of Standards Circular 573, June 1956.

6. Fine, H., "An Effective Ground Conductivity Map for Continental United States," Proc. IRE, Vol. 42, September 1954, pp. 1405-1408.

7. Wait, J.R., and Walters, L.C., "Curves for Ground Wave Propagation over Mixed Land and Sea Paths," IEEE Transactions on Antennas and Propagation, Vol. AP-11, January 1963.

8. Millington, G., "Ground Wave Propagation over an Inhomogeneous Smooth Earth," Proceedings of the Institute of Electrical Engineers, Vol. 96, Pt. III, January 1949.

9. Johler, J.R., and Berry, L.A., "Loran-D Phase Corrections over Inhomogeneous, Irregular Terrain," ESSA Technical Report IER-59 ITSA-56, November 1967.

10. Doherty, R.H., Campbell, L.W., Samaddar, S.N., and Johler, J.R., "A Meteorological Prediction Technique for Loran-C Temporal Variations," Presented at the Wild Goose Association Annual Convention, (Williamsburg, VA), October 1979.

REFERENCES (Continued)

11. Warren, R.S., Gupta, R.R., and Shubbuck, T.J., "Design and Calibration of a Grid Prediction Algorithm for the St. Marys River Loran-C Chain," Proc. of Seventh Annual Technical Symposium of the Wild Goose Association (New Orleans, LA), October 1978.

12. Gupta, R.R., and Anderson, E., "Application of Semi-Empirical TD Grid Calibration to the West Coast Loran-C Chain," Presented at Eighth Annual Technical Symposium of the Wild Goose Association (Williamsburg, VA), October 1979.

13. Gressang, R.V., "Estimating Bias in Loran Lines of Position," IEEE Transactions on Aerospace and Electronic Systems, Vol. AES-6, No. 3, May 1970, pp. 400-404.

14. Foltz, J.M., and DePalma, L.M., "Analytic Evaluation of Loran-Based Buoy Position Auditing Systems," The Analytic Sciences Corporation, Technical Report TR-1923-1, November 1979.

15. DePalma, L.M., "Observability and Control of Grid Instability in the St. Marys River Loran-C Chain," The Analytic Sciences Corporation, Technical Information Memorandum TIM-1119-4, October 1978.

16. Uttam, B.J., and D'Appolito, J.A., "Direct-Ranging Loran Model Identification and Performance Predictions," IEEE Trans. Aerospace and Electronic Systems, Vol. AES-11, No. 3, May 1975, pp. 380-385.

17. Gelb, A., (Editor), Applied Optimal Estimation, MIT Press, Cambridge, MA, 1974.

18. Adams, R.J., and McKinley, J.B., "Airborne Evaluation of the Production AN/ARN-133 Loran-C Navigator," Systems Control, Inc. (VT), Report No. CG-D-32-79, July 1979.

19. Doherty, R.H., and Johler, J.H., "Interpretation of West Coast Loran-C Spatial Errors Using Programmable Calculator Analysis Techniques," Proc. of the Seventh Annual Technical Symposium of the Wild Goose Association (New Orleans, LA), October 1978.

20. Uttam, B.J., "Loran-C Additional Secondary Phase Factor and Skywave Correction Study," The Analytic Sciences Corporation, Technical Report TR-585, June 1975.

REFERENCES (Continued)

21. LoVecchio, J.A., "Developments in Terrestrial and Airborne Applications of Loran-C," Proc. Seventh Annual Technical Symposium of the Wild Goose Association (New Orleans, LA), October 1978, pp. 118-128.

22. Dean, W.N., "Diurnal Variations in Loran-C Ground Wave Propagation," Magnavox Government and Industrial Electronics Co., unpublished report, 1978.

23. "Final Report on Loran-C Propagation Study," Sperry Systems Management Division, Report No. GJ-2232-1892, April 1971.

24. Goddard, R.B., "Differential Loran-C Time Stability Study," U.S. Coast Guard, Report No. DOT-CG-31146-A, November 1973.

25. Bean, B.R., and Dutton, E.J., Radio Meteorology, Dover Publications Inc., New York, 1968.

26. Bean, B.R., Horn, J.D., and Ozanich, A.M., Jr., Climatic Charts and Data of the Radio Refractive Index for the United States and the World, National Bureau of Standards Monograph 22, Washington, D.C., 1960.

27. Bean, B.R., and Thayer, G.D., "On Models of the Atmospheric Refractive Index," Proc. IRE, Vol. 47, May 1959, pp. 740-755.

28. Biggs, A.W., "Terrain Influences on Effective Ground Conductivity," IEEE Transactions on Geoscience Electronics, Vol. GE-8, No. 2, April 1970, pp. 106-114.

29. "Electrical Characteristics of the Surface of the Earth," Proc. of the Thirteenth Plenary Assembly of the International Radio Consultative Committee (Geneva, Switzerland), 1974, Vol. V, pp. 39-65.

30. "World Distribution and Characteristics of Atmospheric Radio Noise," Proc. of the Tenth Plenary Assembly of the International Radio Consultative Committee (Geneva, Switzerland), Report No. 322, 1963.

31. "Loran-C Signal Monitor Test Plan," Systems Control, Inc. (VT), Report for Task VII A of Contract No. DOT-FA75WA-3662, December 1977.

32. Mauro, P.G., and Gakis, J.D., "The Effects of Primary Power Transmission Lines on the Performance of Loran-C Receivers in Experimental Terrestrial Applications," Transportation Systems Center, Report No. DOT-TSC-RSPA-79-8, July 1979.

33. Ryan, R., "RF Response of Austron 5000 Notch Filter," U.S. Coast Guard (EECEN), Letter to Mr. E. Schoen, 7 February 1979.

34. Watt, A.D., V.L.F. Radio Engineering, Pergamon Press, New York, 1967.

35. Box, G.P., and Jenkins, G.M., Time Series Analysis: Forecasting and Control, Holden-Day, San Francisco, CA, 1976.

36. Jenkins, G.M., and Watts, D.G., Spectral Analysis, Holden-Day, San Francisco, CA, 1968.

37. Van Trees, H.L., Detection, Estimation and Modulation Theory, Part I, John Wiley and Sons, Inc., New York, 1968.

38. Johnson, N.L., and Leone, F.C., Statistics and Experimental Design, John Wiley and Sons, Inc., New York, 1964.

39. Scheffé, H., The Analysis of Variance, John Wiley and Sons, Inc., New York, 1959.

40. Schweppe, F.C., Uncertain Dynamic Systems, Prentice Hall, Inc., New Jersey, 1973.

41. Hogg, R.V., and Craig, A.T., Introduction to Mathematical Statistics, Macmillan, New York, 1965.

42. Mood, A.M., and Graybill, F.Q., Introduction to the Theory of Statistics, McGraw-Hill Book Company, New York, 1963.

43. Akaike, H., "A New Look at the Statistical Model Identification," IEEE Trans. Automat. Contr., Vol. AC-19, No. 6, December 1974.

REFERENCES (Continued)

44. Massey, F.J., Jr., "Kolmogorov-Smirnov Test for Goodness of Fit," American Statistical Association Journal, Vol. 47, September 1952.

45. Papoulis, A., Probability, Random Variables, and Stochastic Processes, McGraw-Hill, New York, 1965.

46. Goldsmith, A., ed, "National Plan for Navigation," Department of Transportation, Report No. DOT-TST-78-4, November 1977.

47. Illgen, J.D., and Feldman, D.A., "Loran-C Signal Analysis Experiments - 'An Overview'," Proc. of Seventh Annual Technical Symposium of the Wild Goose Association (New Orleans, LA), October 1978.

48. Stein, K.J., "Loran-C-Based R-Nav System Gains," Aviation Week and Space Technology, Vol. 112, No. 12, March 1980, pp. 51-58.

END

DATE
FILMED

8-80

DTIC